IMPROVING HEMODIALYSIS TREATMENT: MODELING, EXPERIMENTAL DESIGN, AND CLINICAL STUDIES

VAIBHAV MAHESHWARI

NATIONAL UNIVERSITY OF SINGAPORE

2013

IMPROVING HEMODIALYSIS TREATMENT: MODELING, EXPERIMENTAL DESIGN, AND CLINICAL STUDIES	**VAIBHAV MAHESHWARI**	**2013**

IMPROVING HEMODIALYSIS TREATMENT:

MODELING, EXPERIMENTAL DESIGN, AND

CLINICAL STUDIES

VAIBHAV MAHESHWARI

(*B.Tech., NIT Durgapur, India*)

A THESIS SUBMITTED
FOR THE DEGREE OF DOCTOR OF PHILOSOPHY
DEPARTMENT OF CHEMICAL AND BIOMOLECULAR ENGINEERING

NATIONAL UNIVERSITY OF SINGAPORE
2013

DECLARATION

I hereby declare that the thesis is my original work and it has been written by me in its entirety. I have duly acknowledged all the sources of information which have been used in the thesis.

This thesis has not been submitted for any degree in any university previously.

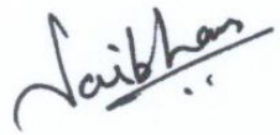

Vaibhav Maheshwari

29 July 2013

To my teachers

Acknowledgements

I used to believe that PhD is a solo journey. You have to define your research problem; you have to articulate your thoughts; and you have to communicate it with scientific community. Now when I have completed my PhD research work and introspect into last few years, I can firmly say that PhD is not a solo journey. Without help of many people, I could not have completed this. Here, I take the opportunity to say THANK YOU ALL.

First and foremost, I sincerely thank my supervisors Prof Laksh and Prof Rangaiah for their guidance throughout this memorable journey. I will remain eternally grateful to both of them for giving me ample freedom to pursue this research. Nevertheless, I sought their guidance time and again. Prof Laksh enlightened me about teaching & education, writing skills, and many facets of both personal and professional life. At the same time, I learnt to be systematic, organized, and transparent in all activities from Prof Rangaiah. I also thank Dr. Titus Lau for his support and guidance in clinical research.

I extend my heartfelt gratitude to my lab-mates and friends with whom I have shared my frustration and joy, success and failures, highs and lows of PhD. I thank Naviyn with whom I spent perhaps the maximum time in this journey. If I want to emulate the humbleness of anyone then it would be Naviyn. I thank Shruti who has been very helpful. She is one of those many people who helped me whenever I asked for. Her jokes always uplifted the mood in the E5-B-02 (my sitting place). I will remain indebted to many NUS friends: Manoj, Krishna, Shivom, Karthik Raja, KMG, Ashwini, Sumit, Vamsi, Wendou, Bhargava, Susarla Naresh, Shailesh, Deepti & Anupam, who have been part of this journey. They not only made this journey enjoyable but also memorable. Without friends, this journey would only be a dream. My seniors Lakshmi Kiran and Loganathan guided me in my early days of research and also helped me improving my presentation skills.

Technical help from Sridharan Srinath immensely helped me at important junctures of my research.

I thank NUS for financial support and NKF for providing the research grant to conduct clinical research. I also thank research collaborators for their help in clinical research – NUH dialysis center nurses (Aafiah, Eve, Farrah, Frances, George, Karen, Rajani, Sister Soriani), Yijun Loy and Serene Lim (physiotherapists), Dr. Ling Lieng Hsi. I thank all the patients who have been part of clinical study. I thank Mr. Boey and Samantha for lab related issues, Steffen for resolving finance queries in NKF grants, Doris and Vanessa for providing administrative support. I thank NUS library which has played an important role in providing the required reference materials.

Then, there are persons whom I have never met personally but who have been of great help – the first person is Dr. Richard Ward (University of Louisville) who provided the confidential patient data which eventually directed my research, and second is Joanna (from NKF) who unfailingly resolved my queries and acceded to all grant related queries.

I find myself very lucky to have a group of friends from Self Realization Fellowship whom I have been meeting on Sundays. I thank them for many things which cannot be expressed in words. In the later part of this PhD journey when my research took upswing, I married to Anchal. She is one of those who suffered the most because of this research, and I thank her for understanding heart. This work is the result of many prayers and well wishes of my parents who are always worried about me. I thank my brother who has always been an inspiration for me. Last but not the least, I thank the reader for taking time to read this thesis.

I thank God for his unconditional love and everything.

SUMMARY xiii

LIST OF TABLES xv

LIST OF FIGURES xvii

ABBREVIATIONS & NOTATIONS xxi

1. Introduction 1

1.1 Engineering and Medicine 1

1.2 Kidneys and Kidney Failure 2

1.3 Dialysis 3

1.3.1 Peritoneal dialysis 3

1.3.2 Hemodialysis 4

1.4 Statistics 6

1.5 Motivation and Objectives 9

1.6 Thesis Organization 11

Part 1 Toxin Kinetic Modeling and Clinical Study 13

2. Literature Review: Toxin Kinetic Modeling 15

2.1 Toxins 15

2.2 Uremic Toxicity and Marker Toxin(s) 17

2.3 Toxin Kinetic Modeling 20

2.3.1 Single-pool Model 21

2.3.2 Two-pool Model 24

2.3.3 Multi-compartment Model 27

2.3.4 Regional Blood Flow Model 29

2.4 Kinetics of other toxins 31

2.4.1 Phosphate Kinetics 32

2.4.2 Sodium Kinetics and Profiling 33

2.4.3 Kinetics of Guanidino Compounds 35

2.5 Summary 37

3. Diffusion-adjusted Regional Blood Flow Model for β_2-Microglobulin 39

3.1 β_2-microglobulin and Kinetic Studies 40

3.2 Model Description 42

3.3 Model Parameter Reduction and Estimation 47

3.4 Interpretation of Parameter Estimates 53

3.5 Model Applications 58

3.5.1 Estimation of Removed Toxin Mass 58

3.5.2 Simulating Effect of Exercise 59

3.6 Summary 64

4. Clinical Study to Compare Toxin Removal in Hemodialysis, Hemodiafiltration, and Hemodialysis with Exercise 65

4.1 Hemodiafiltration 66

4.1.1 Clinical Evidences for HDF 68

4.2 Exercise during Dialysis 71

4.2.1 Exercise and Temperature....72

4.3 Clinical Trial Design....73

4.3.1 Study Design and Ethics Approval....74

4.3.2 Patient Recruitment and Inclusion-Exclusion Criteria....75

4.3.3 Study Interventions....77

4.3.4 Data collection....78

4.4 Patient and Dialysis Information....80

4.5 Results from the Clinical Study....83

4.6 Discussion....87

4.7 Summary....92

Part 2 Model-based Design of Experiments....95

5. Multi-Objective Framework for Model-based Design of Experiment Techniques....97

5.1 Mathematical Models and Experiment....98

5.2 Mathematics of MBDOE....102

5.3 Parameter correlation....105

5.4 Multi-Objective Optimization based DOE framework....108

5.5 Solution Approach (Genetic algorithm)....110

5.6 Case Studies....111

5.6.1 Modified Bergman minimal model for Type 1 diabetes subjects....114

5.6.2 Baker's Yeast Fermentation Reactor Model....127

5.7 Discussion....135

5.8 Summary 137

6. Optimal Sampling Protocol for Toxin Kinetic Modeling 139

6.1 Sampling protocols in TKM 139

6.2 Materials and Methods 142

6.3 Results 146

6.4 Discussion and Sampling Recommendation 151

6.5 Summary 155

7. Conclusions and Recommendations for Future Works 157

7.1 Contributions 158

7.1.1 Toxin Kinetic Modeling and Clinical Study 158

7.1.2 Model-based Design of Experiments 162

7.2 Recommendations for Future Works 164

7.2.1 One TKM for All Marker Toxins 164

7.2.2 Clinical Study: HDF vs. HD-Ex 165

7.2.3 Clinical Study: Cool vs. Warm Dialysate 166

7.2.4 Model Predictive Controller and Dialysate Temperature 168

7.2.5 Exploring Synergies between Exercise Regimen and Dialysate Temperature 168

7.2.6 MOO based DOE for Larger Systems 169

REFERENCES 171

SUMMARY

Hemodialysis (HD) is a life-saving treatment option for end stage kidney disease patients. It removes excess fluid and toxins which are normally removed by healthy kidneys. During HD, blood is passed through hollow fiber membranes, which remove accumulated toxins and fluid via diffusion and convection. This makes HD a perfect example of synergy between chemical engineering principles and medical care. Although HD sustains patients' lives, poor patients' outcome is a major concern. Hence, the broad focus of this research work is to improve HD care such that it will result in better patient outcome. One potential way to achieve this is to enhance the toxin removal, the mainstay of HD since its inception in 1950's. One effective way to accomplish this is via process systems engineering (PSE) principles, especially mathematical modeling.

In HD, compartmental toxin kinetic modeling continues to play an important role in understanding the toxin removal behavior. The present work proposes a comprehensive kinetic model for middle-sized marker toxin (β_2-microglobulin) in HD patients. One of the major advantages of mathematical models is that, they are not restricted to explain the underlying phenomena only, but also can be extrapolated to simulate other relevant scenarios. Guided by this, the proposed model is expanded to explain the enhanced toxin removal due to exercise during dialysis. Simulation results suggest that the increased toxin removal can only be explained by a decrease in inter-compartmental resistance, the major barrier for toxin removal. In order to verify the simulation results, a pilot scale clinical study was conducted in the National University Hospital, Singapore. Results indicate that exercise can lead to improved toxin removal. It is also found that the exercise during dialysis increases the body core temperature and cardiac output resulting in decreased compartmental resistance i.e. enhanced toxin removal. This is the first

clinical study which thoroughly investigated the exercise induced physiological changes in HD care.

However, the clinical experiment did not quantify the decrease in inter-compartmental resistance, which can provide better understanding of exercise induced physiological changes and pave way for personalized prescription of intra-dialytic exercise. The inter-compartmental resistance cannot be measured, but it can be inferred from one of the parameters in the proposed toxin kinetic model. To estimate the model parameters, good data should be collected. In this context, model based design of experiments (MBDoE) techniques would be effective. However, the existing MBDoE techniques increase the correlation among parameters, which may lead to inaccurate estimates. Therefore, they are improved by proposing a multi-objective framework. The proposed framework is first tested for example case studies and then for the developed toxin kinetic model. This is the first study to investigate the optimal sampling for improving the HD model.

Overall, the thesis combines the *in silico* approach (of model development and improvement via better estimation of model parameters) with the *in vivo* approach (of clinical study to test the model generated hypothesis in HD care), and provides useful results and improved techniques for improving the HD care.

LIST OF TABLES

Table 3.1: Constant model parameters for all patients 51

Table 3.2: Estimated model parameters for β_2-microglobulin kinetics 52

Table 3.3: Estimates of removed toxin mass (mean±s.e.m.) 59

Table 3.4: Simulating effect of intra-dialytic exercise – Decrease in rebound % (a) for 100% increase in cardiac output (CO) and (b) for 15% increase in inter-compartmental mass transfer coefficient (K_{ip}) 63

Table 4.1: Patient demographics at the time of consent 81

Table 4.2: Percentage rebound for each uremic toxin in different dialysis protocols 83

Table 5.1: Design variables, their bounds, and initial guess for the proposed clinical test for Type 1 diabetes subjects 117

Table 5.2: Transformation of constraints into bounds 119

Table 5.3: Parameter estimates and statistics for D-optimal and DMOO design 122

Table 5.4: Parameter estimates and statistics for A-optimal and AMOO design 124

Table 5.5: Parameter estimates and statistics for E-optimal and EMOO design 125

Table 5.6: Percentage normalized Euclidean distance for alphabetical and MOO based designs for Type 1 diabetes model 126

Table 5.7: Design variables, their bounds, and initial guess values for Baker's yeast fermentation reactor system 128

Table 5.8: Parameter estimates and statistics for D-optimal design and DMOO design. 131

Table 5.9: Parameter estimates and statistics for A-optimal design and AMOO design. 132

Table 5.10: Parameter estimates and statistics for E-optimal design and EMOO design 134

Table 5.11: Percentage normalized Euclidean distance for alphabetical and MOO based designs for Baker's yeast fermentation reactor model 135

Table 6.1: Existing sampling protocols for various uremic toxins 141

Table 6.2: Model parameters with their known true values and initial guesses used for model-based design of experiment techniques 144

Table 6.3: Two factors – Experiment duration and number of decision variables, each at 4 levels 145

Table 6.4: Decision variables (d.v.) or optimal sampling instances in different experiment duration (during dialysis + post-dialysis). Sampling instances during dialysis (normal text) and post-dialysis (bold text), respectively. 149

Table 6.5: Point estimates (θ), *t*-value, and Percentage normalized Euclidean distance (δ) from true parameter for each scenario 150

LIST OF FIGURES

Figure 1.1 Schematics of (A) peritoneal dialysis[6] and (B) hemodialysis [7] 5

Figure 1.2: Block representation of Hemodialysis, Hemofiltration, and Hemodiafiltration6

Figure 1.3: Adjusted (for race and gender) all-cause mortality in US population [11]. 7

Figure 1.4: Yearly total Medicare expenditure in US by modality [11]. 9

Figure 2.1: (A) Patient (single-pool model) attached to hemodialyzer; (B) Constant volume single-pool model; and (C) Variable volume single-pool model. V_d and C_s are urea distribution volume and urea concentration in body, respectively. G is urea generation rate; K_D is dialyzer urea clearance; K_r is residual renal clearance; α is fluid intake; and Q_{uf} is ultrafiltration rate. 22

Figure 2.2: Two-pool model representation of physiology. Intracellular fluid volume is greater than extracellular fluid. Toxin generation is assumed to occur in intracellular compartment. 25

Figure 2.3: Urea kinetics modeling by single- and two-pool models. Sharp post-dialytic increase of urea concentration disproves the single-pool hypothesis for UKM 27

Figure 2.4: Multi-compartmental representation of physiology. C and V denote concentration and toxin distribution volume. The suffix ‘i’ denotes intracellular compartment, ‘ei’ denote interstitial-extracellular and ‘ep’ is plasma-extracellular compartment. 28

Figure 2.5: Blood flow/tissue water volume and water content of different organs under baseline condition [48].....30

Figure 2.6: Regional blood flow representation of physiology. The flow line thickness is approximately proportional to the amount of cardiac output received. Q_H and Q_L represent the amount of blood flow received by HFR and LFR, respectively; Q_B is the blood flow to dialyzer; Q_{uf} is ultrafiltration rate; CO is cardiac output; k_H and k_L are fluid fraction of HFR and LFR, respectively. 31

Figure 2.7: Phosphate kinetics model comprising four pools [56]. 33

Figure 2.8: Dialysate sodium profile to control the serum sodium concentration.....35

Figure 3.1: Compartmental representation of physiology. Toxins are distributed in intracellular (IC) and extracellular compartments (EC). Urea is distributed in both IC and EC, and β_2M is distributed in EC. The hollow arrows between IC and interstitium denote fluid movement, while solid arrows between interstitium and plasma represent the fluid as well as β_2M movement. 40

Figure 3.2: Diffusion-adjusted regional blood flow model (parallel-cum-series representation of physiology) for explaining β_2M kinetics. Toxin transfer is due to diffusion across capillary endothelium, and blood/plasma circulation causes convective transport. Q_h/Q_{hp}, Q_l/Q_{lp}, and Q_b/Q_{bp} are blood/plasma flows to HFR, LFR, and dialyzer, respectively. Q_{cr} and Q_{ar} are cardiopulmonary and access recirculation, respectively. Shaded compartments represent contact with blood (A – arterial node and V – venous node). Here, IC is not presented because β_2M distribution is restricted to EC alone. 43

Figure 3.3: Plasma β_2M concentrations during 240 min dialysis treatment and for 4 hours following the treatment. Data is presented as mean± standard error of mean (s.e.m.) [74]. 47

Figure 3.4: Arterial plasma concentration profile (model fit) and measured concentration of β_2-microglobulin for Patient 1 (top) and Patient 10 (bottom) 56

Figure 3.5: β_2-microglobulin concentration profile in different body compartments for Patient 1 (top) and Patient 10 (bottom).....57

Figure 3.6: Simulation of effect of intra-dialytic exercise for Patient 1 (top) and Patient 10 (bottom) – Decrease in post-dialysis rebound due to 100% increase in cardiac output. ...61

Figure 4.1: Blood and dialysate flow along dialyzer length. Horizontal arrows represent transfer of accumulated toxins and excess fluid from blood to dialysate stream 67

Figure 4.2: Pre- and post-dilution modes of hemodiafiltration. The given blood and dialysate flow rate are usual numbers practiced in routine dialysis settings. The replacement fluid rate is assumed to be 80 mL/min. 68

Figure 4.3 Blood temperature snapshot during HD session for two sample patients. In panel A, the kink in dialysate and venous temperatures is due to the measurement of access recirculation. 80

Figure 4.4: Schematic flow-chart of clinical trial 82

Figure 4.5: Arterial (red - -) and Venous (blue - -) blood temperature during HD-Ex session 85

Figure 4.6: Patients' cardiac output and peripheral vascular resistance index during the first bout of exercise. In bottom panel, cardiac output and resistance index are presented as mean ± standard deviation. 86

Figure 5.1: Schematic of model development following the principles of model-based design of experiments techniques 100

Figure 5.2: Geometrical interpretation of the D-, A-, and E-optimal design for two parameters 105

Figure 5.3: Schematic representation of trade-off between information measure and correlation measure. Between the two extremes of alphabetical (D-, A-, E-) design criterion and Pritchard and Bacon criterion, experimenter has freedom to select appropriate optimal experiment design from the Pareto-optimal front. Star is one chosen design for illustration. 112

Figure 5.4: Schematic of the design procedure followed in the case studies 113

Figure 5.5: Transformation of exact time-instants into delta-time instants 118

Figure 5.6: Pareto-optimal front for DMOO design 121

Figure 5.7: Time profiles of basal insulin infusion and blood glucose sampling instances (●) for D-optimal and DMOO design vectors and resulting glucose concentration profiles 122

Figure 5.8: Pareto-optimal front for AMOO design 123

Figure 5.9: Time profiles of basal insulin infusion and blood glucose sampling instances (●) for A-optimal and AMOO design vectors and resulting glucose concentration profiles 123

Figure 5.10: Pareto-optimal front for EMOO design 124

Figure 5.11: Time profiles of basal insulin infusion and blood glucose sampling instances (●) for E-optimal and EMOO design vectors and resulting glucose concentration profiles 125

Figure 5.12: Pareto-optimal front for DMOO design 130

Figure 5.13: Time-profile of manipulated vairables (u_1 and u_2) and sampling instances (●) for D-optimal and DMOO design 130

Figure 5.14: Pareto-optimal front for AMOO design 131

Figure 5.15: Time-profile of manipulated vairables (u_1 and u_2) and sampling instances (●) for A-optimal and AMOO design. 132

Figure 5.16: Pareto-optimal front for EMOO design 133

Figure 5.17: Time-profile of manipulated vairables (u_1 and u_2) and sampling instances (●) for E-optimal and EMOO design. 133

Figure 6.1: Pareto-optimal front for 240 min experiment duration and 8 decision variables 146

Figure 6.2: Pareto-optimal front for 300 min experiment duration and 8 decision variables 147

Figure 6.3: Pareto-optimal front for 360 min experiment duration and 8 decision variables 147

Figure 6.4: Pareto-optimal front for 480 min experiment duration and 8 decision variables 148

ABBREVIATIONS & NOTATIONS

6 MWT	6-min walk test
AC	Anti-correlation
ADMA	Asymmetric dimethylarginine
AGE	Advanced glycation end-product
ALE	Advanced lipoxidation end-product
AMOO	MOO based A-optimal design
β_2M	β_2-microglobulin
BTM	Blood Temperature Monitor
BUN	Blood Urea Nitrogen
C	Toxin concentration
C_0	Pre-dialysis serum urea concentration
$C_{art/ven}$	Arterial/Venous concentration
C_{end}	End-dialysis serum urea concentration
CO	Cardiac Output
CHD	Conventional Hemodialysis
CHO	Carbohydrates
CKD	Chronic Kidney Disease
COPD	Chronic Obstructive Pulmonary Disease
CRF	Chronic Renal Failure

C_s	Solute Concentration
DAE	Differential-Algebraic Equations
DA-RBF	Diffusion-adjusted Regional Blood Flow
DBP	Diastolic Blood Pressure
DMOO	MOO based D-optimal design
DOE	Design of Experiments
e	Extracellular fluid volume fraction
EC	Extracellular Compartment
EMOO	MOO based E-optimal design
ESRD	End Stage Renal Disease
FIM	Fisher Information Matrix
$f_{h/l}$	Blood flow fraction to HFR/LFR
f_P	Plasma fraction in EC
FMC	Fresenius Medical Care
G	Toxin Generation Rate (Urea, Creatinine, β2M …)
GA	Genetic Algorithm
GC	Guanidino Compounds
GCP	Good Clinical Practices
HCT	Hematocrit
HD	Hemodialysis

HDF	Hemodiafiltration
HD-Ex	Exercise during HD
HF	Hemofiltration
HFR	High Flow Region
HIV	Human Immunodeficiency Virus
HR	Heart Rate
HRR	Heart Rate Recovery
IC	Intracellular Compartment
IDH	Intra-dialytic Hypotension
K_D	Dialyzer Clearance
$k_{h/l}$	Fluid volume fraction of HFR/LFR
K_{ie}	Inter-compartmental (IC-EC) Mass Transfer Coefficient
K_{ip}	Inter-compartmental (interstitium-plasma) Mass Transfer Coefficient
K_{NR}	Non-renal Clearance
K_r	Residual Renal Clearance
LFR	Low Flow Region
MBDOE	Model-based Design of Experiments
MOO	Multi-objective Optimization
MPC	Model Predictive Controller
MR	Removed toxin mass

NHG	National Healthcare Group
NKF	National Kidney Foundation
nPCR	Normalized Protein Catabolism Rate
NSGA	Non-dominated Sorting Genetic Algorithm
NUH	National University Hospital
ODE	Ordinary Differential Equation
OGTT	Oral Glucose Tolerance Test
PCR	Protein Catabolism Rate
PD	Peritoneal Dialysis
PSE	Process System Engineering
Q_{ar}	Access recirculation
$Q_{B/H/L}$	Blood Flow to Dialyzer/HFR/LFR
Q_{cr}	Cardiopulmonary recirculation
Q_{F}	Filtration rate in HDF
$Q_{hp/lp}$	Plasma flow to HFR/LFR
Q_{uf}	Ultrafiltration Rate
RBF	Regional Blood Flow
RPE	Rate of Perceived Exertion
RRT	Renal Replacement Therapy
SBP	Systolic Blood Pressure

SST	Serum Separator Tubes
UF	Ultrafiltration
UKM	Urea Kinetic Modeling
US	United States
USRDS	United States Renal Data System
T / t	Dialysis Duration
TKM	Toxin Kinetic Modeling
V_d	Toxin distribution volume
V_{urea}	Urea Distribution Volume
Z	Sensitivity Matrix

Greek Symbols

α	Fluid Intake
δ	Percentage normalized Euclidean distance
ϕ	Design vector
θ	Parameters

1. Introduction

"The dialysis lets the patient live a close to normal life

so they can be a grandparent or go to work."

- *Nora Daludado*

1.1 Engineering and Medicine

Engineering and medicine have been working synergistically for a long time. An engineer's hand is visible in the ubiquitous stethoscope often seen as the symbol of doctor's profession, prosthetics (artificial limbs), pacemaker, advanced imaging devices for diagnosis of diseases, artificial blood purification system, etc. Accordingly, the role of engineers in medicine has always been appreciated in invention of new devices, equipment, medical peripherals, and ensuring their optimal function, i.e. pre-dominantly in the hardware segment of medical care. It will not be a mistake to say that *if doctors save life, then engineers sustain it* (via medical equipment). Lately, with increasing collaboration among doctors and engineers, the medical field is being rapidly revolutionized, and process system engineers are playing a pivotal role in this revolution. Process system engineering (PSE) has changed the way we think about various diseases conditions such as tumor growth modeling in cancer diagnosis and treatment, organs and tissue level modeling in diabetes care, electrical equivalent of cerebral and cardiovascular system, population based modeling of pandemic spread, modeling of circadian rhythm to understand the aging process, and HIV modeling, to name a few. Biomedical engineering bridging medicine and technology has emerged as a new branch of engineering [1]. "Medicine by numbers" is a new buzzword [2].

The PSE approach deals with the analysis and design of complex systems, resulting in mathematical models of underlying system. Modeling is the soul of PSE, and provides a

wealth of information, which cannot be assessed by direct human perception. Presently, a disease can be modeled on the computer platform and the cause-effect relationship can be established for exogenous and endogenous inputs. A disease model allows testing of novel interventions before their trial and subsequent deployment in physical world. The present thesis employs these strengths of PSE to suggest ways of improving the hemodialysis care for kidney patients. This chapter comprises a brief overview of kidney and its failure (Section 1.2), available treatment options (Section 1.3), disease statistics (Section 1.4), research motivation (Section 1.5), and finally concludes with a description of how this thesis is organized (Section 1.6).

1.2 Kidneys and Kidney Failure

Human body constitutes several organs working in harmony to ensure healthy living. Of these organs, kidneys are a pair of vital organs responsible for homeostatic functions: (i) salt and water balance; and (ii) electrolytes and acid-base balance. More importantly, kidneys serve as natural filter of blood removing waste products and excess water via urine. Kidneys are medically termed as renal, which is derived from Latin *renalis* means kidneys. Although Mother Nature endowed the human body with two kidneys, only one of them is sufficient to sustain the necessary physiological functions. This is nature's way of building reliability by design such that an individual can survive on 50% renal capacity alone, should one of the kidneys dysfunction. However, if both kidneys malfunction, then waste products and fluid starts accumulating and their levels may well go beyond physiologically acceptable limits. Increased fluid levels and high concentrations of toxins cause myriad of complications, and eventually death.

Traditionally, kidney failure is classified as acute and chronic. Acute renal failure refers to a sudden decline in renal function that is generally reversible, while chronic renal

failure (CRF) is a slow progressive decline of kidney function over a period of months or years. It can occur due to reasons like diabetes, hypertension, glomerulonephritis, polycystic kidney disease, family history of kidney disease, kidney stones, urinary tract infection, etc. [3]. The advanced stage of CRF is known as stage five CRF or end stage renal disease (ESRD), where patient's daily urine output is negligibly small. At this stage, available treatment options are renal transplant or dialysis. Renal transplant is the best known treatment option because it has the potential to function as the native kidney, but renal graft (i.e. kidney transplant) compatibility is a serious issue and is subject to a high probability of rejection. Unavailability of donor graft and patient-donor graft mismatch prohibits widespread use of transplant, and the patient has to resort to an artificial blood purification system, known as artificial kidney or dialysis.

1.3 Dialysis

Dialysis is defined as the diffusion of molecules in solution across a semi-permeable membrane along an electrochemical concentration gradient [4]. For ESRD patients, the primary functions of dialysis are to remove accumulated toxins and excess fluid. Two modes of dialysis known as peritoneal dialysis (PD) and hemodialysis (HD) are universally employed renal replacement therapies (RRTs).

1.3.1 Peritoneal dialysis

PD uses body's own peritoneum membrane surrounding the abdomen i.e. blood is cleaned inside the body. Fluid exchange and toxin removal occurs between the capillary blood and dialysate solution in peritoneal cavity. Dialysate is usually concentrated glucose solution with desired concentration of solutes such as sodium, potassium, calcium, magnesium, chloride, and bicarbonate. High concentration of glucose in dialysate solution causes osmotic fluid movement through peritoneum membrane to

cavity, and solutes are transferred due to concentration gradient i.e. by diffusion [3]. A catheter is surgically placed inside the peritoneal cavity through the abdominal wall. Dialysate enters the abdominal cavity through the catheter, where it remains in contact with peritoneum membrane for 24 hours except for the short periods of time when dialysate exchange is performed. Schematic of PD is shown in Figure 1.1A.

1.3.2 Hemodialysis

Hemodialysis ('*hemo*' means blood) is an RRT where blood is taken out from the patient's body at a constant rate and purified in a dialyzer (Figure 1.1B). Dialyzer is a hollow fiber membrane module through which blood and dialysate flow in the counter-current direction to maximize the toxin mass transfer. In ESRD patients, both small- and large-sized toxins co-exist. The blood is taken out from the patient's body at constant rate and passed through the hollow fibers in the dialyzer while dialysate flows in the shell side. The clean blood is then returned to the patient's body and the cycle continues. The dialysate composition in HD differs from that in PD. In HD, dialysate is essentially ultrapure water with solutes: sodium, potassium, bicarbonate, magnesium, chloride, calcium, and glucose [5]. Dialysate composition can be altered based on patient's disease condition; for example, in HD patients with diabetes, dialysate with less glucose is prescribed. Standard HD prescription is for 4 hours × 3 times per week, and generally performed at dialysis centers. A patient either follows Monday, Wednesday, Friday or Tuesday, Thursday, Saturday dialysis schedule. Before a patient can be initiated on HD, an artificial blood access is created. This allows repeated puncturing and sufficiently high blood flow for dialysis. The access is a surgically created connection of artery and vein in patient's hand (Figure 1.1B).

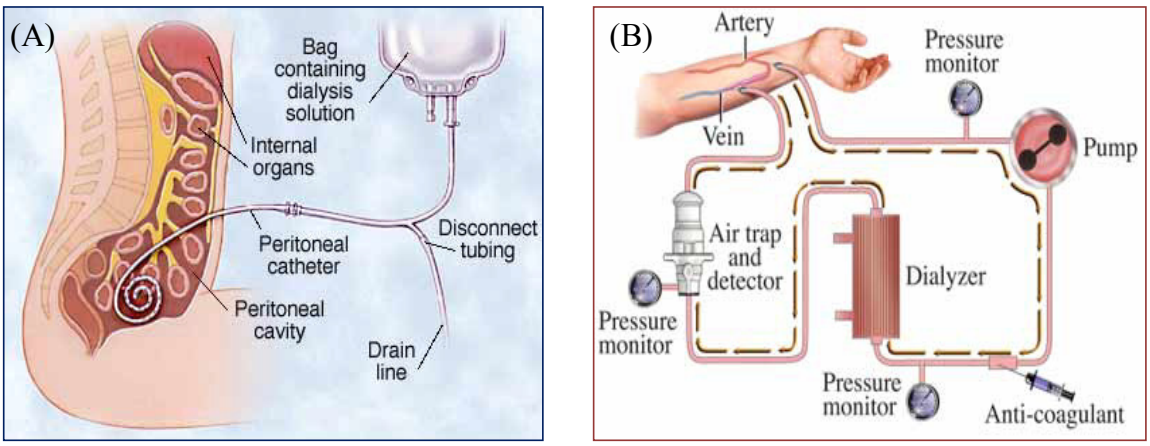

Figure 1.1 Schematics of (A) peritoneal dialysis [6] and (B) hemodialysis [7]

Based on the toxin exchange mechanism across dialyzer membrane, HD is classified into three sub-categories, namely, conventional hemodialysis (CHD), hemofiltration (HF), and hemodiafiltration (HDF). HD is an umbrella term for all extracorporeal RRTs, where extracorporeal means that the procedure is performed outside body.

1) *Conventional hemodialysis* is primarily based on diffusion of toxins across dialyzer membrane. Diffusion is more efficient for small-sized toxins, and CHD is therefore inefficient for removal of large-sized toxins.
2) *Hemofiltration* is the convection based RRT where large amount of fluid is removed from blood stream along the dialyzer length. To compensate for the removed fluid volume, the output stream is replenished by ultrapure replacement fluid. The excessive fluid movement from blood to dialysate drags large-sized molecules; however, diffusion-based toxin removal is inhibited. There is no dialysate stream in HF.
3) *Hemodiafiltration* combines both diffusion and convection in a single system, and removes both large-sized toxins (via convection) and small-sized toxins (via diffusion). All three modalities are schematically presented in Figure 1.2.

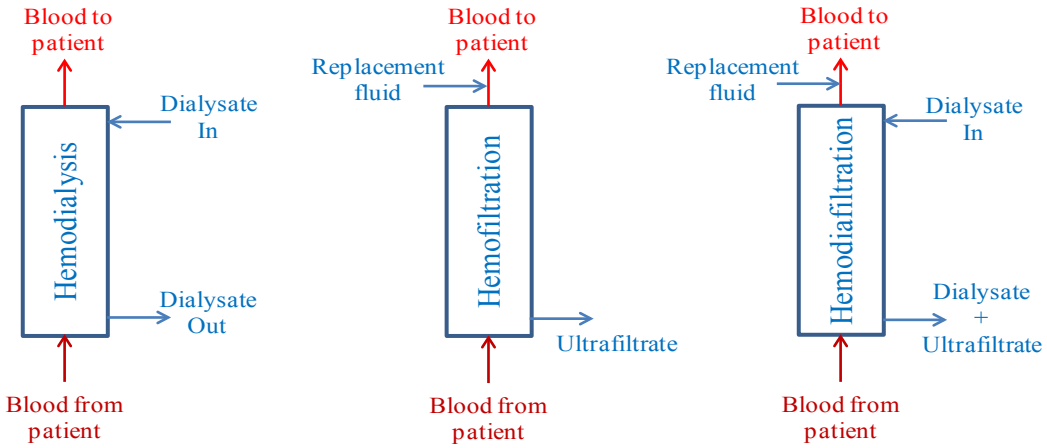

Figure 1.2: Block representation of Hemodialysis, Hemofiltration, and Hemodiafiltration

PD has a distinct advantage over HD, as the former is a continuous process where patient need not come to the dialysis center regularly, but only has to exchange the dialysate several times a day. It has been found that PD may be advantageous initially but is associated with poor patient outcomes after 12 months from the start of PD [8]. The foremost reason is the high possibility of PD site infection, especially during dialysate exchange. Also, the long term use of dialysate in peritoneum cavity reduces the functional efficiency of peritoneal membrane [9]. Long-term outcomes for PD patients are not desirable, and are worse than HD patients [10]. According to the recent USRDS (United States Renal Data System) report, the December 2010 prevalent population included 383,992 patients on HD and 29,733 on PD [11]. According to Fresenius Medical Care (FMC), leading provider of dialysis products and medical care for patients with chronic kidney disease (CKD), only 8% ESRD patients were on PD in 2012 [12]. HD allows patients to be fully rehabilitated and to have a satisfactory nutritional intake. Owing to these reasons, the focus of this thesis is on HD.

1.4 Statistics

According to FMC, the number of patients being treated for ESRD globally was estimated to be 3 million at the end of 2012. Note that the numbers correspond to only

150 out of 230 countries where FMC has market share, and so more ESRD patients can be expected. With a ~7% growth rate, the ESRD patients continue to increase at a significantly higher rate than the 1.1% growth rate of world population [12]. According to recent USRDS report, a total of 116,946 new patients began ESRD therapy in 2010, of which 97.5% patients were initiated on dialysis.

Despite the advantages of HD over PD, mortality and morbidity rates of HD patients are still high. Mortality can be defined as the condition of being subjected to death due to disease or treatment condition, while morbidity is anything that is exceptional or abnormal, and usually occurs as a result of treatment side-effects, when prescribed treatment is inappropriate or inadequate. Mortality among dialysis remains 10 times greater than the patients of similar age without kidney diseases. Despite decades of HD practice and innovations, only 1 out of 2 dialysis patients is still alive 3 years after start of dialysis therapy. The annual mortality rate exceeds 20% in chronic HD patients. All-cause mortality adjusted for age, gender, race, and co-morbidity is 6.3–8.2 times greater for dialysis patients than for individuals in the general population [11]. Notably, mortality among dialysis patients is significantly higher than the patients in the general population who have diabetes, cancer, congestive heart failure, stroke, or acute myocardial infarction (Figure 1.3).

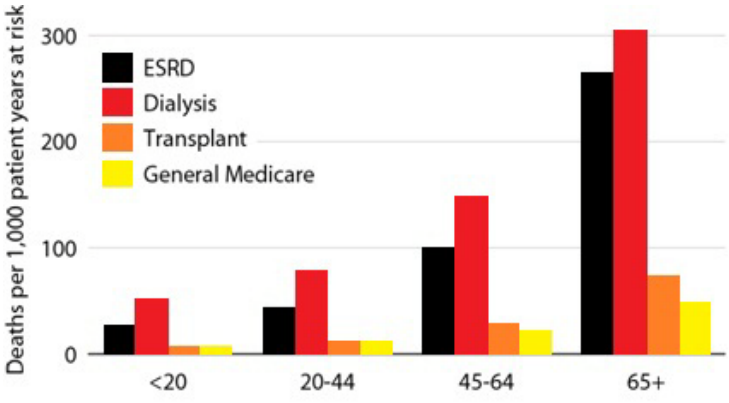

Figure 1.3: Adjusted (for race and gender) all-cause mortality in US population [11].

Certainly, the dialysis population is at relatively high risk of death, and plausible reason for this is the high prevalence of co-morbid factors such as diabetes and hypertension [13]. With the current dialysis regimen, patients with ESRD exhibit the retention of large variety of uremic toxins [14]. Accumulated toxins result in a wide range of undesired biological functions, such as chronic inflammatory state, mineral metabolism disorders, etc. which contribute towards cardiovascular disease [15]. Though cardiovascular mortality is the single largest cause of mortality in general population, the cardiac mortality of dialysis patients aged 45 years or younger is 100-folds greater than that in the general population [16]. Other important co-morbid factors are anemia (reduced hemoglobin levels or red blood cell concentration), dyslipidemia (very high lipid levels), inadequate nutrition, abnormalities in bones, etc. Complications during dialysis such as cramps, giddiness, nausea, etc. also add to the mortality and morbidity numbers. These intra-dialytic episodes are commonly described as incidence of intra-dialytic hypotension (IDH), and occur in as much as 30-35% of HD patients [4].

Though dialysis patients are small in number compared to the patients on modern age epidemics such as diabetes, cancer, or hypertension, the cost involved for dialysis care is enormous. In US, the total expenditure for ESRD patients alone was $47.5 billion in the year 2010, where $33 billion came from Medicare. This ESRD expenditure combines transplant, HD, and PD. But, as mentioned earlier, HD is the most prevalent renal replacement therapy for ESRD patients; thus the major contribution to expenditure is by HD alone (Figure 1.4). The total expenditure per HD patient per month is $7,300. This number corresponds to Medicare payment alone [11]. Additional expenditure by non-Medicare patients and out-of-pocket payment by all HD patients will further inflate these numbers.

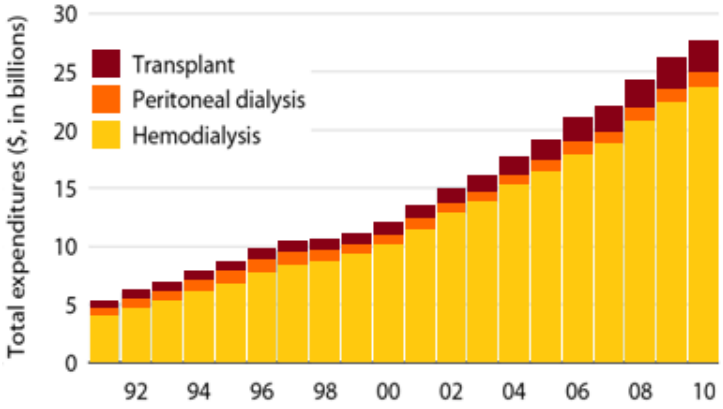

Figure 1.4: Yearly total Medicare expenditure in US by modality [11].

1.5 Motivation and Objectives

Following the opening quote of this chapter, the focal point of this research is to move the performance of HD from *close to normal life* to *closer to normal life*. Improving the performance of any process can have numerous facets. In the context of improving HD care, numerous aspects such as control of inter-dialysis fluid retention, optimal fluid removal during dialysis, prevention of IDH episodes, maintaining optimal hemoglobin level, sodium control, precise electrolyte balance etc. can be considered; however, increasing the toxin removal can possibly have the greatest impact [17]. Current HD process is far from decreasing the toxin concentration as found in healthy subjects of age-matched group, and the ultimate goal is to achieve similar toxin removal as achieved by 24 × 7 functioning of healthy kidney. It is impossible to completely replace the native healthy kidney function with artificial kidney i.e. HD, but improving the efficiency of HD process can significantly decrease the existing co-morbidities and bring down the mortality. Thus, increasing toxin removal is the central theme of the current clinical research.

A number of clinicians and researchers have advocated increasing the frequency or increasing the duration of dialysis, and both modalities have been found to increase the

toxin removal. These modalities include short daily HD and long nocturnal HD, referred as intensive HD [18]. Nevertheless, these modalities are (i) logistically expensive, (ii) inconvenient to patients, and (iii) have not been tested in randomized controlled clinical trials for studying the hard outcomes like decrease in mortality or hospitalization rate. Hence, interventions which can work during routine dialysis settings are necessary. HDF is proclaimed as one such solution for enhancing the toxin removal [19]. HDF's long-term toxin removal outcomes are comparable to CHD [20] and the process is costlier than CHD. Hence, the immediate question is how to improve toxin removal without disturbing the existing dialysis operation mode and without incurring additional cost.

Identifying the major resistances to toxin removal and ways to overcome them can pave way for enhanced toxin removal. This demands a very good understanding of patient-dialysis system. PSE tools and techniques have potential to guide research efforts in this direction. These can be loosely categorized into four areas, namely experimentation, modeling, control, and optimization. Understanding a system and representing that understanding into the form of a mathematical model is an important step to solve a problem. Model simulations can provide new insights and hypotheses which need to be tested in real setting, or a model can be refined further so that better prediction of system behavior can be obtained. This refinement requires new experiments and collection of data. This thesis work primarily addresses *in silico* modeling and the *in vivo* testing of hypotheses in clinical setting, and further improvement of models using intelligent experimental designs. The important objectives of thesis are highlighted below.

- Mathematical modeling (Chapter 3): The PSE approach to understand the patient-dialysis system starts with modeling. Hence, the first focus is on modeling the toxin removal, which is at the heart of HD process. In this thesis, a comprehensive

toxin kinetic model will be developed, which will be followed by model calibration aspects.

- Model applications (Chapter 3): The model should not be limited to explain the underlying phenomenon only. A model can be used to simulate the system behavior under certain conditions before observing the system response in real settings. In this direction, the developed HD model will be employed to study the toxin removal due to exercise during dialysis. Exercise during dialysis is known to improve toxin removal. How exercise augments the toxin removal will be explored in greater detail, and new inferences and hypotheses will be elucidated.
- Clinical trial design (Chapter 4): Testing the model-generated hypothesis in real-time settings completes the loop of any investigation. Hence, to test/substantiate the hypotheses, a prospective clinical trial is necessary. In this clinical research, the effect of exercise on physiological changes will be explored. Also, the toxin removal aspects for HD, HDF, and HD with exercise will be explored.
- Model-based design of experiments (Chapters 5 and 6): Developing a model is the first step to understand the system. To further improve the model, more experiments are required. Experimenters often ensure data quantity, but overlook the data quality aspects. Experiments should be designed beforehand because fixing the data quality later is more expensive. In this context, concepts of model-based design of experiments (MBDOE) will be explored.

1.6 Thesis Organization

The thesis is divided into two parts. In Part 1, the modeling aspects in hemodialysis, originated hypotheses, clinical trial design, and clinical testing of hypotheses are presented. The aspects related to experimental design are detailed in Part 2 of the thesis. In Part 1, Chapter 2 describes the existing modeling paradigms in the context of toxin

kinetic modeling (TKM) and emphasizes the utility of TKM in HD literature. Also, the challenges that can be addressed by PSE methodologies are highlighted. In Chapter 3, a comprehensive diffusion-adjusted regional blood flow model for toxin β_2-microglobulin (β_2M) is proposed (β_2M is one of the many toxins present in excess in dialysis patients). The developed model is also validated with clinical data. The model is further employed to explain the effect of exercise during dialysis, and new hypotheses are proposed. To test the proposed hypotheses, a prospective clinical trial is designed. The clinical trial not only aims to study physiological changes associated with exercise during CHD, but also intends to compare the toxin removal outcomes with the most efficient and clinically employed renal replacement therapy, HDF. The clinical trial design aspects and obtained results are presented in Chapter 4.

In Part 2, MBDOE aspects are explored. It is observed that traditional alphabetical design techniques suffer from increased correlation among parameters, which can be detrimental to parameter estimation and their precision. To overcome these drawbacks, a novel multi-objective optimization (MOO) based design of experiments framework is proposed and first tested on two example case studies. The MBDOE description, existing drawbacks, proposed solution, and results from two example case studies are presented in Chapter 5. In Chapter 6, the proposed MOO based DOE framework is applied to the developed toxin kinetic model (presented in Chapter 3) and important insights are developed. Finally, Chapter 7 summarizes important conclusions of the thesis and provides recommendations for future work.

Part 1

Toxin Kinetic Modeling and Clinical Study

2. Literature Review: Toxin Kinetic Modeling

"*Literature always anticipates life.*
It does not copy it, but moulds it to its purpose."

- *Oscar Wilde*

As Sir Isaac Newton prophesied "*To explain all nature is too difficult a task for any one man or even for any one age*", the review in this chapter does not intend to provide *the complete* picture of toxins and their kinetics, rather it highlights the importance of TKM in HD research; consequently, existing nephrology literature is molded accordingly. After an introduction to toxin environment, classification, pathology of various toxins (Section 2.1), choice of marker toxin(s) (Section 2.2), TKM paradigm in HD, and concept of dialysis adequacy (Section 2.3), existing modeling studies for a number of toxins are presented (Section 2.4).

2.1 Toxins

Dialysis patients are often loaded with a number of uremic toxins, which have known biological effects leading to malfunction of cells or organ systems. When these biological effects are clinically visible, the patient is said to be in the state of uremia meaning urine in the blood [21]. A solute is characterized as uremic toxin based on the following criteria, commonly known as Massry/Koch postulates [22].

1. Toxin must be identified and characterized as a unique chemical entity.
2. Quantitative analysis of the toxin in bodily fluids must be possible.
3. The level of the presumed toxin must be elevated in bodily fluids of subjects with uremia.
4. The level of presumed toxin in bodily fluids should correlate with one of the manifestations of uremia.

5. Decreasing the levels of presumed toxin in the bodily fluids must improve the associated symptoms.
6. Adding the presumed toxin to achieve levels similar to those in uremia should reproduce the associated symptoms.

Based on the above criteria, more than 115 uremic toxins have been identified which correlate with pathological dysfunction [23, 24]. It is good to identify and characterize all the uremic toxins so that non-dialytic ways of toxin removal can be discovered or ways to curb their generation can be identified. However, unlike kidneys, dialysis is a non-selective way of toxin removal and primarily depends on size of concerned toxin. Hence, all the identified toxins are classified in 4 major classes. These four classes are based on physiochemical characteristics namely, molecular mass, protein binding, and polarity [25].

1. Small-sized toxins (polar, water soluble, non-protein bound, molecular weight < 500 Da)
2. Small-sized protein-bound solutes (polar, water soluble, molecular weight < 500 Da)
3. Middle-sized toxins (non-protein bound, molecular weight between 500 – 12000 Da)
4. Large-sized toxins (molecular weight > 12000 Da)

The two classes of middle-sized and large-sized toxins are often combined into a single class referred as middle-large-sized toxins. In uremia, molecular weight of toxin can range from 60 Da (Urea) to 32,000 Da (Interleukin-1β), and serum concentrations order can range from g/L for urea to ng/L for methionine enkephalin [24]. However, high concentration does not imply equally large biologic toxicity e.g. urea is a time-honored marker of toxin milieu, but high concentration of urea have limited biologic activity [24].

Johnson *et al*. proved it by adding urea in dialysate stream thus inhibiting urea removal, and it did not impact the clinical status of ESRD patients [26]. Protein bound solutes are difficult to remove due to increased combined size of toxin-protein. These solutes also alter the protein binding characteristics such as reduced drug-binding capacity owing to unavailability of protein molecules for binding with drug molecules.

2.2 Uremic Toxicity and Marker Toxin(s)

Retention of myriad uremic toxins that under normal conditions are excreted by healthy kidney exerts toxicity. The condition is also referred as uremic syndrome, which is a complex mixture of organ dysfunction [27]. It is impractical to recount the biological effect of all known uremic toxins; hence, some of the extensively studied uremic toxins with their toxicity are presented below.

Among the non-protein bound small-sized toxins such as urea, guanidino compounds (GCs), reactive carbonyl compounds, polyamines have shown to induce deleterious effect on organ systems. Increased levels of urea alone may not induce clinically significant symptoms, but its increased levels does denote the increased levels of other uremic toxins [26]. The GCs comprise guanidinosuccinic acid, creatine, guanidinovaleric acid, guanidinoacetic acid, creatinine, arginine, methylguanidine, asymmetric dimethylarginine (ADMA) etc. These compounds are found in high concentration in cerebrospinal fluid as well as in serum [28, 29], and proposed as candidate neurotoxins. Reactive carbonyl compounds, derived from metabolism of carbohydrates and polyunsaturated fatty acids can exert their toxicity directly or indirectly i.e. via increased formation of advanced glycation end-products (AGEs) or advanced lipoxidation end-products (ALEs). Both AGE and ALE group of toxins are associated with poor cardiovascular outcomes. Polyamines are suggested to play role in dis-coordinated muscle movement, convulsion,

abnormally low body core temperature, vomiting, immune deficiency, etc. [30]. It is impractical to measure all the toxins in routine dialysis, and urea is considered as representative of small-sized non-protein bound toxins.

The second class of uremic toxins with protein-binding characteristics behaves like large-sized uremic toxins. Removal of such toxins with CHD remain abysmally low, because only the small fraction of the solute is available for diffusion [31]. Important toxins in this category, namely, *p*-cresol, indoxyl sulphate, and AGEs, have been studied extensively [32]. *p*-cresol, a representative from this group of molecules, has been shown to associate with uremic immunodeficiency and endothelial (interior of blood vessels) dysfunction, conceivably linking its serum levels to mortality [33]. Indoxyl sulphate is associated with vascular calcification (calcium deposition), vascular stiffness, progression of glomerular sclerosis (tissue hardening), and mortality in CKD patients [34]. AGEs are believed to contribute towards inflammatory response in dialysis patients. They also play a role in atherosclerosis (thickening of arterial wall) and worsening of renal failure [35]. Homocysteine is another protein bound toxins and is associated with increased risk of cardiovascular disease in CRF patients [36], and may also relate with irregular intracellular metabolism [27]. Briefly, protein bound uremic solutes contribute to a number of functional disturbances in uremia, but at present, no effective extracorporeal renal replacement therapy is available for removal of such toxins.

The last category of uremic toxins i.e. middle/large-sized toxins has increasingly been recognized to contribute towards uremic syndrome. Some of the toxins in this class are β_2M, leptins, proinflammatory cytokines, etc. [14, 24], of which, β_2M is recognized as a marker [37, 38]. In ESRD patients, β_2M levels can increase up to 60 folds or more. Increased levels of β_2M have been associated with amyloid deposits leading to bone related complications in maintenance HD patients. Leptin is a 16,000 Da protein; it is

speculated to mediate anorexia (poor appetite) and muscle wasting [39]. Large-sized toxins are also associated with cardiovascular damage [40].

There is yet another small and water soluble toxin – phosphate, whose removal characteristics are completely different from any other toxin mentioned above. High phosphate levels are associated with pruritus (itching) and hyperparathyroidism (excess of parathyroid hormone), which is related to osteodystrophy (dystrophic or imperfect bone development), cardiovascular disease including calcification. Phosphate is also engaged in intestinal dysfunction. ESRD patients are often in the state of hyperphosphatemia, and are advised to restrict their phosphate intake.

In summary, uremic syndrome is a multifaceted state due to retention of numerous toxins. These toxins result in chronic inflammatory state, oxidative stress, endothelial dysfunction, vascular stiffness or calcification, oxidative stress responsible for cardiovascular disease, etc. Some of the protein bound uremic toxins modify proteins, act on receptors, and (de)activate cell signaling pathways. Uremic toxins and associated toxicity have received unique attention among dialysis research community, which is evident from the number of scholarly contributions. A monograph devoted to uremic toxins and toxicity was published in scientific journal *Seminars in Dialysis* in 2002 [21]. A recent book *Uremic Toxins* from Wiley & Sons [25] further expounds about uremic toxins, their toxicity, and known biological pathways through which these toxins damage the organ system. To increase the toxin removal via artificial kidney i.e. via HD requires an understanding of toxin build up and their subsequent removal, information about major resistance for toxin removal, etc. TKM has been a major contribution in this direction.

2.3 Toxin Kinetic Modeling

It is now understood that dialysis is associated with a number of co-morbid factors and uremia is purportedly the major contributor for poor outcomes in patients [17]. It is also understood that conventional dialysis is always inadequate when compared with the native kidney function. Hence, increasing the toxin removal is the mainstay of present dialysis research. Before we aim for increasing the toxin removal, it is important to understand the toxin removal characteristics, known as TKM in HD literature.

Kinetics is the study of motion and its cause. In the context of TKM, it refers to movement of toxins from patient to the dialysate. From the chemical engineering point of view, reaction kinetics is the study of rate of chemical reactions whereby substrate depletion or product formation occurs at certain rate. In dialysis, there is no chemical reaction involved but toxins are removed through dialyzer and their concentration in patients depletes with time. Hence, toxin kinetics during dialysis describes the rate of change of toxin mass. The driving force governing the toxin removal is concentration gradient between blood and dialysate stream, with dialyzer membrane offering resistance. In order to mathematically represent the toxin removal process, a control volume is considered first. Control volume, also referred as compartment or pool in TKM literature, is a region where the physical entity of interest (here toxin concentration) assumes the same value over the entire compartment [2]. The control volume assumption can be extrapolated to each organ and tissue level, but, in the context of TKM, limited number of compartments is sufficient to describe underlying toxin removal kinetics. Based on the control volume assumption and body fluid distribution, existing TKM paradigms are reviewed here.

It is impossible to study each and every toxin in uremia; hence, generally marker toxins are studied, and it is assumed that the removal kinetics of other toxins will follow suit. Urea is a traditional choice of marker. It is not due to pathophysiological reasons, but due to the fact that several decades ago when concept of uremic toxicity was developed, not many uremic toxins were known and urea was found in significantly higher concentration in ESRD patients. Also, the cost of analysis for urea is relatively low when compared to that of other uremic toxins [25].

2.3.1 Single-pool Model

In human body, approximately 60% of body weight is due to fluid where urea is distributed; e.g. in a 70 kg male, the fluid volume will be ~42 L. In the single-pool modeling assumption, the whole bodily fluid is assumed as single pool (Figure 2.1A). Blood is taken out at constant rate from patient's body and flows through the dialyzer, where dialysate flows in counter-current direction. Gotch and co-workers started with concept of constant volume urea kinetic modeling (UKM), illustrated in Figure 2.1B [41]. However, during dialysis, excess fluid is also removed or body fluid volume continuously decreases. Typical fluid removal can range from 2.5–3.5L, which depends on the inter-dialytic fluid gain, obtained from the difference between pre-dialysis weight and post-dialysis weight at the end of previous HD session. To account for intra- and inter-dialytic fluid gains, constant volume UKM was further modified to variable volume UKM [42], which is shown in Figure 2.1C.

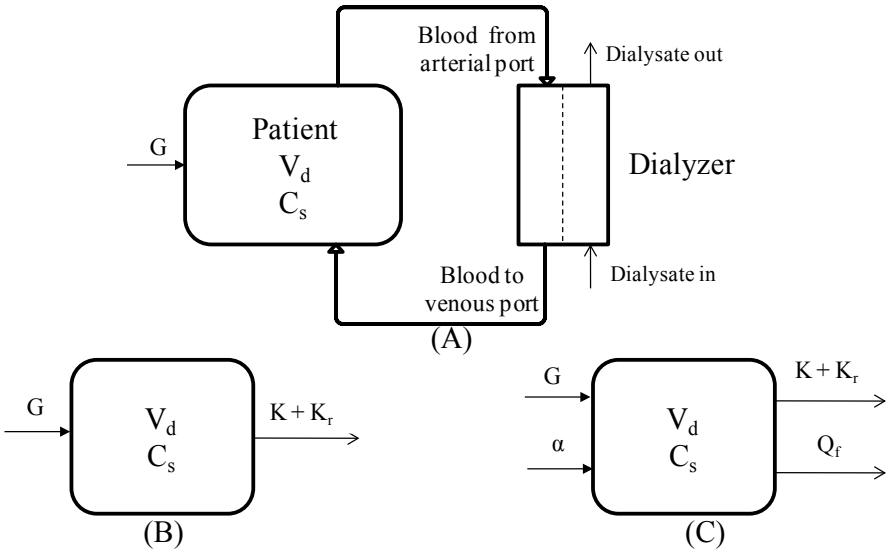

Figure 2.1: (A) Patient (single-pool model) attached to hemodialyzer; (B) Constant volume single-pool model; and (C) Variable volume single-pool model. V_d and C_s are urea distribution volume and urea concentration in body, respectively. G is urea generation rate; K_D is dialyzer urea clearance; K_r is residual renal clearance; α is fluid intake; and Q_{uf} is ultrafiltration rate.

Variable volume single-pool UKM resulted in more realistic values of urea distribution volume (V_d). The rate of change of urea mass is equal to urea generation rate (G) minus removal rate via dialyzer and residual renal clearance (= $(K_D + K_r)\ C_s$, where C_s is the toxin concentration). In variable volume single-pool model, distribution volume decreases continuously at constant ultrafiltration rate (Q_{uf}). The relevant equations are provided below.

Constant volume single-pool model:

$$V_d \frac{dC_s}{dt} = G - (K_D + K_r)C_s \tag{2.1}$$

Variable volume single-pool model:

$$\frac{d(V_d C_s)}{dt} = G - (K_D + K_r)C_s \tag{2.2}$$

$$\left.\begin{aligned} \frac{dV_d}{dt} &= -Q_{uf}, && \text{(during dialysis)} \\ \frac{dV_d}{dt} &= \alpha, && \text{(between dialysis)} \end{aligned}\right\} \tag{2.3}$$

In equation 2.1, one can safely assume that toxin generation during dialysis period will be much smaller when compared to the removal. Also, the K_r is negligibly small in dialysis patients, thus neglecting both G and K_r, the simplified version of equation 2.1 will result in,

$$\frac{dC_s}{dt} = -\frac{K_D C_s}{V_d} \Rightarrow C_{end} = C_0 e^{-\frac{K_D t}{V_d}} \quad (2.4)$$

where C_0 and C_{end} are pre-dialysis and post-dialysis serum urea concentration, 't' is the dialysis duration, V_d is urea distribution volume and requires prior estimation. In equation 2.4, increasing K_D and/or 't' will result in smaller post-dialysis serum urea concentration. Based on this, the time on dialysis required to control the blood urea nitrogen (BUN) at desired levels was calculated [43].

Importance of UKM: Urea and other nitrogenous compounds are products of protein catabolism, thus knowledge of protein catabolism rate (PCR) can help dietitians to prescribe nutrition intake. Inadequate protein intake may lead to malnutrition, while excessive protein intake may be associated with high inorganic phosphate intake; so, optimal protein intake is important for dialysis patients. Gotch and co-workers [41] observed a wide range of pre-dialysis BUN levels in patients despite the same dialysis dose, which suggested that their dietary protein intake must vary widely. Since other toxic protein catabolites, such as H^+ and inorganic phosphate were expected to correlate with urea generation [44], UKM was found to be a suitable method to measure the normalized PCR (nPCR, g/kg/day) in individual patients. As nPCR can assist in deciding protein intake, UKM also helped in assessing compliance with dietary protein prescription.

Dialysis adequacy: Increasing the $K_D t / V_{urea}$ will result in lower end-dialysis concentration i.e. more toxin removal according to single-pool model. According to this

formula, increasing the dialyzer clearance (K_D) and/or dialysis duration (t) will culminate in increased toxin removal. V_{urea} is urea distribution volume and needs prior estimation using patient data. It was observed that $K_D t / V_{urea}$ correlates with nPCR [45]. Thus, dialysis dose was quantified using $K_D t / V_{urea}$, which is a dimensionless parameter and describes the prescribed fractional clearance of body water. Though dialysis adequacy refers to urea, it was assumed that urea clearance will provide the proportional fractional clearance of other low molecular weight uremic toxins. This was the first step in quantifying the dose of dialysis, and used in clinical setting till date. Nevertheless, a number of researchers have proven the inadequacy of $K_D t / V_{urea}$; this aspect is discussed in Section 2.4.

2.3.2 Two-pool Model

The single-pool assumption is too simple to describe the post-dialytic as well as intra-dialytic characteristics of toxin concentration. Urea concentration or concentration of any toxin for that matter increases sharply immediately after dialysis. During dialysis also, the observed decline in urea concentration is much steeper than that predicted by the single-pool model. This led to a theory that urea is distributed in intracellular (IC) and extracellular compartments (EC), with inter-compartmental membrane offering resistance to toxin transfer, and eventually resulted in the two-pool UKM [42], comprising two control volumes (Figure 2.2).

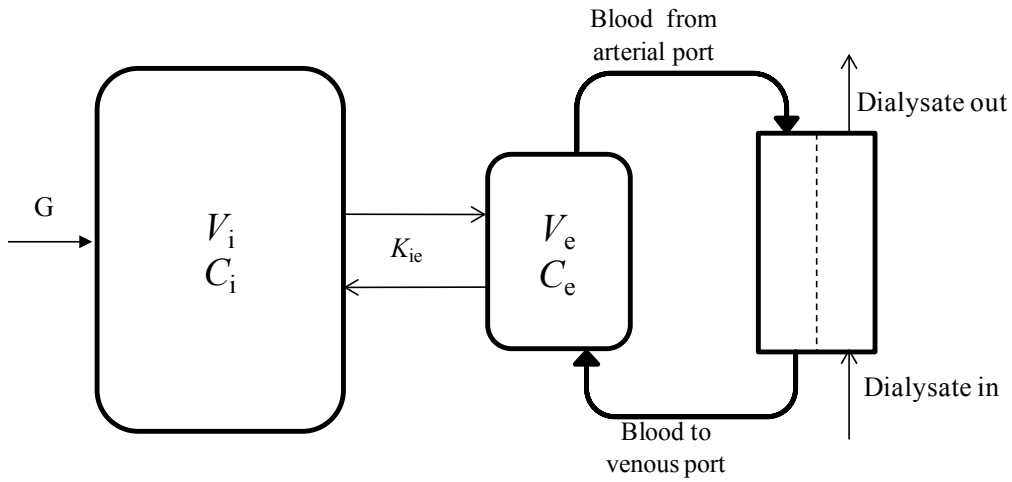

Figure 2.2: Two-pool model representation of physiology. Intracellular fluid volume is greater than extracellular fluid. Toxin generation is assumed to occur in intracellular compartment.

During dialysis, only blood from EC comes in contact with dialyzer. Due to high dialyzer clearance, fluid and mass transfer between blood and dialyzer is rapid i.e. concentration in EC drops significantly faster than that of IC. When dialysis ends, toxin transfer from IC to EC, results in sharp increase in toxin concentration. This phenomenon is characterized as *rebound,* and any good TKM must reflect this physiological behavior.

The model equations for two-pool model during dialysis are described below.

$$\frac{\mathrm{d}(V_\mathrm{e}C_\mathrm{e})}{\mathrm{dt}} = K_{\mathrm{ie}}(C_\mathrm{i} - C_\mathrm{e}) - (K_\mathrm{D} + K_\mathrm{r})C_\mathrm{e} - Q_{\mathrm{uf}}C_\mathrm{e} + \frac{2}{3}Q_{\mathrm{uf}}C_\mathrm{i} \tag{2.5}$$

$$\frac{\mathrm{d}(V_\mathrm{i}C_\mathrm{i})}{\mathrm{dt}} = \mathrm{G} - K_{\mathrm{ie}}(C_\mathrm{i} - C_\mathrm{e}) - \frac{2}{3}Q_{\mathrm{uf}}C_\mathrm{i} \tag{2.6}$$

$$\frac{\mathrm{d}V_\mathrm{e}}{\mathrm{dt}} = -\frac{1}{3}Q_{\mathrm{uf}} \tag{2.7}$$

$$\frac{\mathrm{d}V_\mathrm{i}}{\mathrm{dt}} = -\frac{2}{3}Q_{\mathrm{uf}} \tag{2.8}$$

where V and C are toxin distribution volume and toxin concentrations in the compartments, respectively. Subscript 'i' and 'e' represent IC and EC respectively; K_{ie} is inter-compartmental mass transfer coefficient or inter-compartmental clearance; Q_{uf} is the

constant ultrafiltration rate. Physiologically, the typical fluid distribution is such that approximately 66% of body fluid resides in IC and remaining 33% in EC. Following the early example of a 70 kg male, out of 42 L of fluid, 28 L will be in IC and the rest 14 L in EC. During dialysis, fluid is removed from both compartments, and cellular membrane presumably offers no resistance to fluid movement. The inter-compartmental fluid exchange occurs through water channels known as *aquaporins*, present on the cell wall. In the model equations 2.5–2.8, it is assumed that fluid removal from IC and EC occurs in proportion of their physiological fluid volume. Similar assumption is valid for fluid ingested during inter-dialytic period. The toxin mass balance for EC (equation 2.5) comprises inter-compartmental diffusive mass exchange, dialyzer and residual renal clearance, convective removal with ultrafiltered fluid, and convective mass transfer from IC to EC. The toxin generation is assumed to be intracellular because majority of toxins are byproducts of cellular metabolism.

The model simulation for single-pool clearly shows its inability to capture the rebound phenomenon (Figure 2.3). Unlike the single-pool model simulation, the two-pool model predicts that the toxin concentration sharply decreases during the initial phase of dialysis, because the blood compartment is rapidly cleared of toxins.

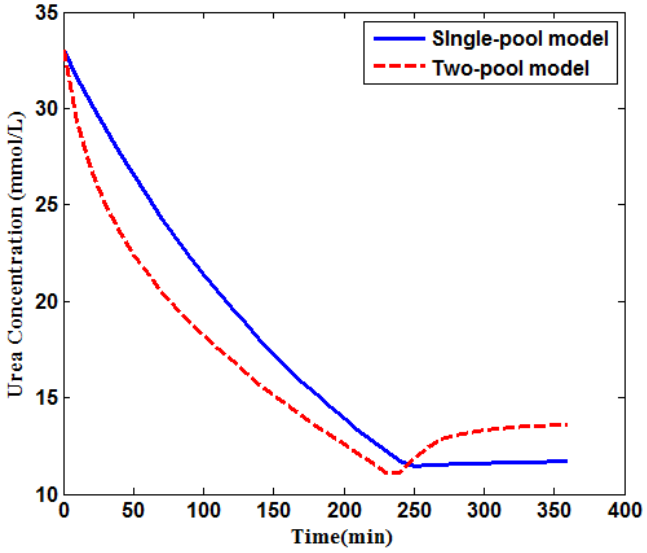

Figure 2.3: Urea kinetics modeling by single- and two-pool models. Sharp post-dialytic increase of urea concentration disproves the single-pool hypothesis for UKM

The rebound for small-sized toxins lasts from 40 min to 1 hour, after which the toxin concentration equilibrates. For middle-sized toxins, the diffusive flux is much smaller because diffusion is inversely proportional to molecular size. Hence, the rebound for middle-sized toxins can be more pronounced than that of small-sized toxins, and persists for a longer period. Single-pool model does not consider this physiological behavior and over-estimates the delivered dose. On the other hand, the two-pool model enables calculation of the correct dialysis dose defined as $eK_D t / V_{urea}$ or equilibrated Kt/V. The presence of rebound discounts the actual delivered dose of dialysis. The two-pool model has two model parameters, K_{ie} and V_d whose estimation is necessary before it can be used for calculation of dialysis adequacy. The parameter estimation aspects will be discussed later in Part 2 of the thesis.

2.3.3 Multi-compartment Model

The preceding model segregates physiology into two-pools, and explains the toxin rebound. However, the EC comprises interstitial and blood compartment separated by

capillary endothelium, resulting in three-compartmental representation of physiology (Figure 2.4). The interstitial compartment comprises ~75% of extracellular fluid volume and remaining 25% belongs to blood plasma. Using the earlier example of a 70 kg male with 42 L of total fluid volume, the blood plasma will constitute ~3.5 L from 14 L of EC fluid volume. Typical blood volume in humans is 5 L, which also includes the contribution from red blood cells, white blood cells, and platelets.

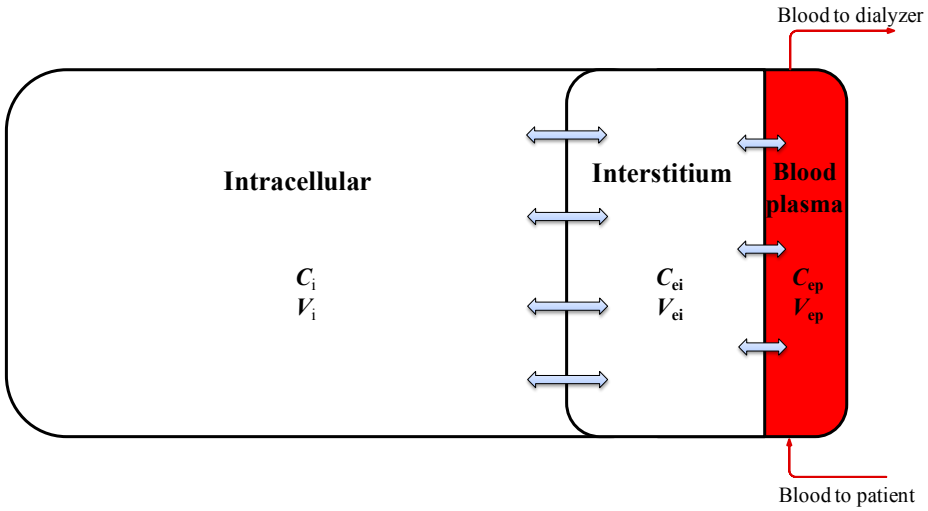

Figure 2.4: Multi-compartmental representation of physiology. C and V denote concentration and toxin distribution volume. The suffix 'i' denotes intracellular compartment, 'ei' denote interstitial-extracellular and 'ep' is plasma-extracellular compartment.

Writing the model equations based on these assumptions will result in additional mass transfer coefficient between interstitium and plasma compartments. The capillary endothelium might offer additional resistance to large-sized toxins, but it has been observed that transcapillary mass transfer coefficient for urea (60 Da), creatinine (113 Da), and vitamin B-12 (1355 Da) are at least 10 folds larger than the transcellular mass transfer coefficient [46]. This suggests that transcellular resistance will be the major impediment for toxin removal. Also, estimating transcapillary mass transfer coefficient will require additional concentration measurement either from IC or interstitial, and both of these are inaccessible compartments. This also explains why most of TKM studies do

not segregate EC into plasma and interstitial compartments. For experimental purposes, it is possible to measure intra-cellular concentration but the process is difficult to replicate in routine clinical settings. The additional benefit of multi-compartment model is that it can predict concentration changes in the inaccessible body compartments, which may be relevant to understanding side effects.

2.3.4 Regional Blood Flow Model

Earlier model representations consider the body as a series of compartments, and lacks sound physiological basis, e.g. administration of D_2O or T_2O bolus to the blood stream requires more than an hour to equilibrate in blood compartment [47]. This phenomenon cannot be explained by the two-pool representation of physiology. The delayed equilibration is explained by heterogeneous distribution of blood to the tissues. As shown in Figure 2.5, very small organs like kidneys, heart, brain etc. receive a major portion of blood flow. Based on this premise, the regional blood flow (RBF) model assumes that removal of toxins is flow limited rather than the diffusion limited. Small-sized organs like kidneys, heart, brain, and lungs in the body receives larger fraction of cardiac output (CO), while the large-sized organs receive only a small fraction of total CO. The former category of organs is designated as high flow region (HFR), while the latter as low flow region (LFR). The HFR constitutes only 20% of fluid volume, but receives almost 85% of total CO. On the other hand, LFR comprises 80% of fluid volume but receives only 15% of CO. This heterogeneous distribution of CO results in high clearance of HFR, and less or delayed clearance of LFR. This model representation was first proposed by Schneditz *et al*. [48].

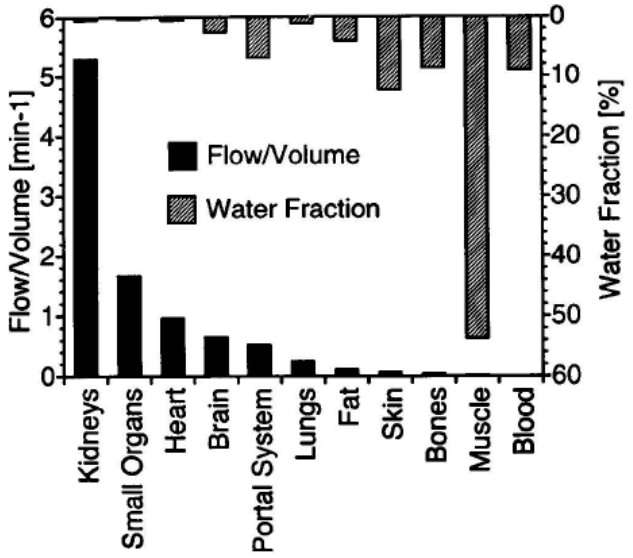

Figure 2.5: Blood flow/tissue water volume and water content of different organs under baseline condition [48]

At the start of dialysis, toxins are equilibrated thorough out the body, i.e. toxin concentration is the same; hence, the LFR contains significantly more amounts of toxins than HFR, owing to the larger fluid volume of the former. Owing to heterogeneous distribution of CO, HFR is thoroughly cleared, and LFR is insufficiently cleared of toxins. After dialysis, the toxin starts equilibrating between regions, and thus explains the post-dialytic rebound. Such conceptualization lays the foundation for RBF representation of physiology. Unlike the two-compartment model where compartments are arranged in series, the RBF representation is referred as parallel flow model [49, 50]. The RBF representation of physiology is presented in Figure 2.6. The RBF model equations are illustrated below.

$$k_{\mathrm{H}} + k_{\mathrm{L}} = 1 \tag{2.9}$$

$$\frac{\mathrm{d}(VC)_{\mathrm{HFR}}}{\mathrm{dt}} = Q_{\mathrm{H}}(C_{\mathrm{art}} - C_{\mathrm{H}}) - C_{\mathrm{art}}K_{\mathrm{r}} - k_{\mathrm{H}}Q_{\mathrm{uf}}C_{\mathrm{H}} + G_{\mathrm{HFR}} \tag{2.10}$$

$$\frac{\mathrm{d}(VC)_{\mathrm{LFR}}}{\mathrm{dt}} = Q_{\mathrm{L}}(C_{\mathrm{art}} - C_{\mathrm{L}}) - C_{\mathrm{art}}K_{\mathrm{r}} - k_{\mathrm{L}}Q_{\mathrm{uf}}C_{\mathrm{L}} + G_{\mathrm{LFR}} \tag{2.11}$$

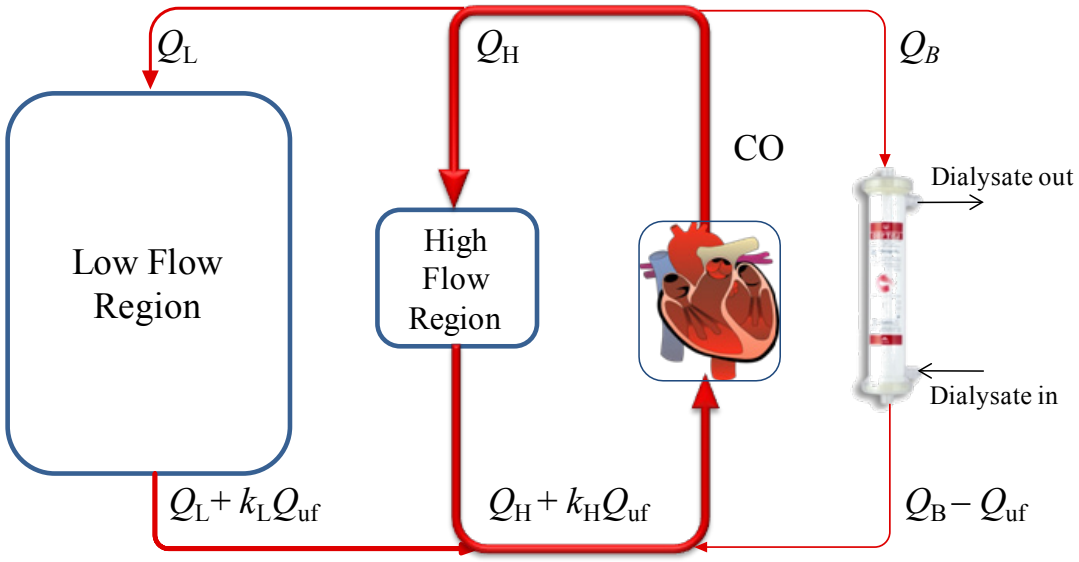

Figure 2.6: Regional blood flow representation of physiology. The flow line thickness is approximately proportional to the amount of cardiac output received. Q_H and Q_L represent the amount of blood flow received by HFR and LFR, respectively; Q_B is the blood flow to dialyzer; Q_{uf} is ultrafiltration rate; CO is cardiac output; k_H and k_L are fluid fraction of HFR and LFR, respectively.

Though this model is physiologically superior to the preceding two-pool model, it could not explain the kinetics of other smaller sized uremic toxins such as creatinine. This means that there is a need for further modification of RBF model – Chapter 3 will consider this problem in detail. Schneditz *et al*. [51] divided each region of RBF model into two-pool model, thus diffusion as well as flow was accounted in the new model, and the model was named as diffusion-adjusted RBF model. This model is complex due to the more number of unknown model parameters. This issue will also receive attention in Chapter 3.

2.4 Kinetics of other toxins

Urea based dialysis adequacy is the established marker of dialysis prescription. Insufficient removal of urea has been found to relate with morbidity and mortality [52]. However, it has been reported in the literature that increasing the dialysis dose defined by $K_D t / V_{urea}$ did not improve patient survival [53]. Even, restricting urea removal by

adding urea in dialysate did not cause clinically significant complication [26]. Numerous studies pointed out that urea removal does not extrapolate to other middle-sized uremic toxins. Moreover, other small-sized uremic toxins behave differently than urea. Hence, researchers started focusing on toxins other than urea, with the postulate that urea kinetics is not representative for kinetics of most other uremic toxins. Kinetic study of other uremic toxins can provide better understanding on evolution of pathophyiologcally important solutes. Some of the toxin kinetics studies are briefly discussed below.

2.4.1 Phosphate Kinetics

ESRD patients are often overloaded with phosphate, a condition known as hyperphosphatemia, which results in secondary hyperparathyroidism and ultimately to osteodystrophy. An easy maneuver for low serum phosphate is to control phosphate via dietary intake, but this may lead to protein-calorie malnutrition. Serum phosphate levels decline significantly during dialysis, but post-dialytic rebound is also more pronounced. Sometimes, during dialysis itself, the phosphate level starts rising after a steep decline. This complicates the phosphate kinetics, and early phosphate kinetics model could not explain such behavior [54, 55]. The best model to-date explaining the phosphate kinetics was proposed by Spalding *et al*. [56]. Their model comprises four pools of phosphate; two of them are conventional EC and IC (Figure 2.7). In addition, it was hypothesized that dialysis patients are likely to have pathologic stores of phosphate in bones, from where phosphate can potentially efflux. This was designated as the third pool, comprising phosphate not yet incorporated into the bone matrix. When phosphate concentrations are critically low, the fourth pool of phosphate inside IC can activate. This fourth pool containing glycophosphates in the IC could be involved in a short-term regulatory response mechanism [56].

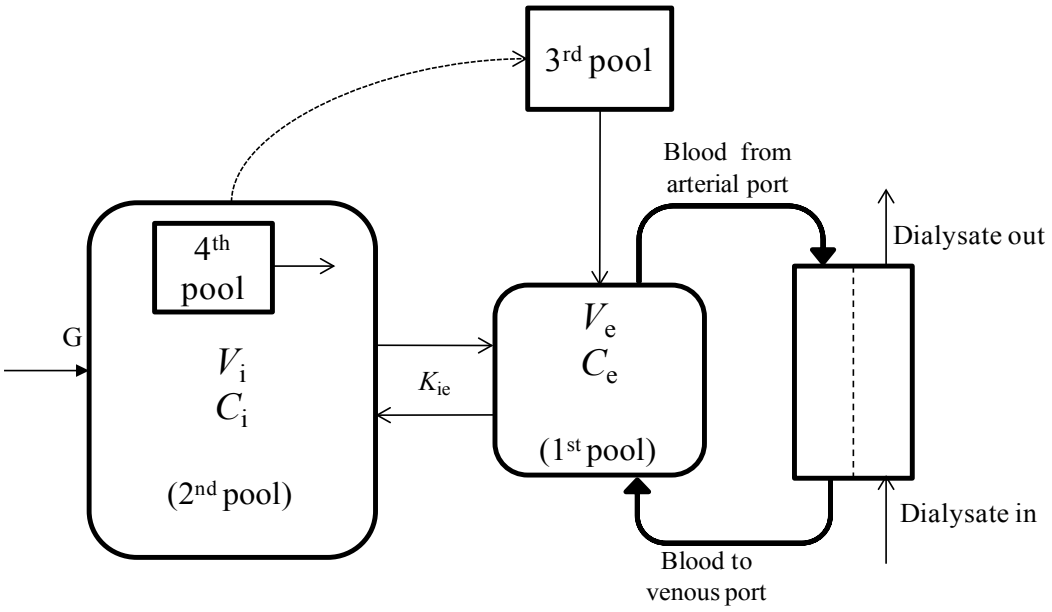

Figure 2.7: Phosphate kinetics model comprising four pools [56].

Phosphate removal by dialysis is abysmally low due to its complex kinetic behavior. Clinically, phosphate removal is often achieved by non-dialytic means such as phosphate binders, which binds with intestinal phosphate and prevents its intestinal absorption [57]. Patients are advised to take phosphate binders just before the meal. These binders are generally calcium, aluminum, or lanthanum based salts. They bind with phosphate present in ingested food and prevent its absorption into blood stream.

2.4.2 Sodium Kinetics and Profiling

Sodium is an important electrolyte which is responsible for homeostatic balance. The ideal sodium concentration in the serum is 140 mEq/L, a condition known as normonatremia. However, dialysis patients are often overloaded with sodium (hypernatremia). Excess sodium cascades on to increased thirst, fluid overload, hypertension, and cardiovascular mortality or deterioration of residual kidney function. Although sodium is the main constituent in EC, clinicians have referred it as a toxin due to its pathophysiological contribution [58, 59]. Sodium levels in dialysis patients can reach well above 140 mEq/L, and its removal is achieved by using the conventional

dialysate composition of 138 mEq/L. Slight decrease in serum sodium concentration below normonatremia can lead to condition known as hyponatremia, which immediately manifests in the form of cramps, giddiness, or similar intra-dialytic symptom, commonly known as intra-dialytic hypotensive (IDH) episodes. Incidence of IDH is observed in 30-35% of dialysis sessions, and is suggested to play a major role in cardiovascular mortality [60].

Increasing the sodium concentration in dialysate will result in less sodium removal and thus prevents the incidence of IDH. The downside of increased dialysate sodium is that it will result in increased thirst and eventually hypertension. Clinicians have thus investigated the ramping of dialysate sodium. In ramping, clinicians start with high sodium concentration and decrease it in piecewise constant steps or linearly until the end of dialysis session. Ramping of dialysate sodium is commonly known as sodium profiling; however, such intervention did not result in improved patient outcomes [61]. In such a scenario, controlling dialysate sodium via feedback mechanism is an obvious scheme [62]. This will require continuous measurement of serum sodium concentration, so that controller can take corrective actions to keep sodium within desirable limits. However, continuous measurement of sodium is very difficult and so secondary inference using a mathematical model is required, which is commonly referred as soft-sensing in chemical engineering. Early developments in sodium kinetics were proposed by Coli and Ursino *et al*. [62, 63], who also proposed model-based sodium profiling. The model-based profiling simulation also results in improved dialysate sodium control and suggests that first the dialysate sodium should be increased and then ramped down to certain level, such that the plasma sodium concentration does not reach to a point where it may culminate in hypotensive episode. An example of sodium profiling is shown in Figure 2.8 (results reproduced from Coli *et al*. [62]).

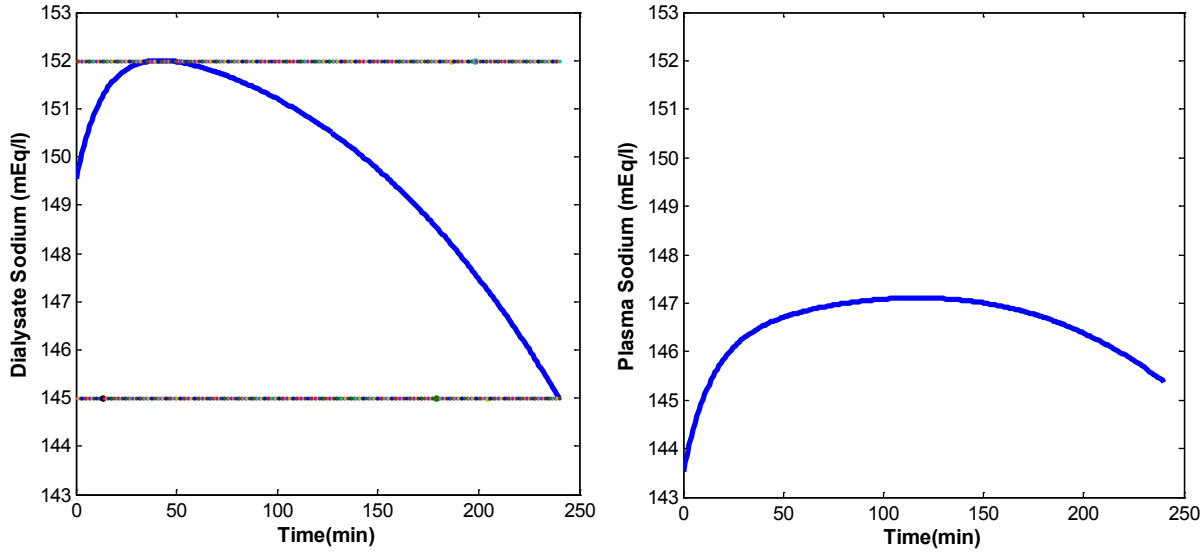

Figure 2.8: Dialysate sodium profile to control the serum sodium concentration

The concept of sodium profiling seems to stabilize the model patient, but in routine clinical settings sodium profiling could not result in better outcomes [64]. The prescribed dialysate sodium profile (Figure 2.8) will stabilize the patient but at the same time it does not remove sufficient sodium and results in high post-dialysis serum sodium concentration. In other words, dialysate sodium is a good maneuver for stabilizing the patient in the short-term, but at the cost of poor patient outcomes in the long-term. Until sodium profiling is realized in routine clinical settings, the best strategy to control the serum sodium is to restrict its intake [59].

2.4.3 Kinetics of Guanidino Compounds

Guanidino compounds (GCs) are large group of solutes resulting from protein and amino acid metabolism. Unlike urea, GCs can interfere with neuronal, cardiovascular, and blood cells functions, and are commonly referred to as neurotoxins [65]. In non-dialyzed subjects, the concentration of GCs was found to be very high when compared to controls, and correlated with morbidities [66]. The kinetics of GCs was first explored by Eloot *et al*. In their study, they employed two-pool model structure and considered 6 small and

water soluble GCs, namely, creatinine, guanidinosuccinic acid, guanidine, methylguanidine, guanidinoacetic acid, and creatine [67]. It was noted that though GCs are present in small concentration, their total distribution volume can be much higher than that of urea. The total distribution volume for creatinine (54 L), guanidinosuccinic acid (30.6 L), guanidine (89.7 L), methylguanidine (102.6 L) , guanidinoacetic acid (123.8 L), and creatine (98 L), was significantly higher the distribution volume for urea (42.7 L), except for guanidinosuccinic acid. Only mean values of 7 recruited patients are presented [67]. Note that the estimates of toxin distribution volume are higher than the body weight itself, which is infeasible. The authors suggested that larger the toxin distribution, the longer it will take to clear the toxin, as more body fluid needs to be processed. The conclusion is that urea kinetics is not representative of other small-sized uremic toxins, thus $K_D t / V_{urea}$ based dialysis adequacy should be abolished [68].

All these researches corroborate the idea that urea is not the best marker toxin and concept of adequacy must be revised. After decades of practice, the adequate dialysis concept has not improved mortality and morbidity. Some researchers have even suggested the introduction of $K_D t / V_{urea}$ concept as an unfortunate one [59, 69]. In summary, attention should be shifted from urea, as it cannot be a suitable representative of other uremic toxins, and a better marker is definitely required. Recently, middle molecules have been discussed extensively. Particularly, β_2-microglobulin (β_2M) has been considered as a marker of middle molecules [68]. Its pre-dialysis concentration has been found to correlate with mortality [38, 70]. After urea, β_2M is the most studied toxins. Numerous kinetic studies have been published to explain its kinetics [71-74]. In this thesis, β_2M is considered as a marker of toxin milieu and its kinetics is studied. Further details will be presented in Chapter 3.

2.5 Summary

More than 115 uremic toxins have been identified and supposedly more new toxins will be identified in the future. Dialysis, being a non-selective method (dependent on membrane pore size) of toxin removal, needs a marker whose removal can correlate with the removal of other uremic toxins. Urea is an established choice of marker and is the basis of current dialysis prescription. Urea based dialysis adequacy, emerged from kinetic studies of urea was an important step for standardizing the dialysis therapy. The kinetic studies are generally referred as toxin kinetic modeling (TKM), and a number of TKMs were reviewed in this chapter. TKM explained an important phenomenon known as rebound, which controls the net efficacy of dialysis. The advantage of these models is that predictions beyond the range of examined parameters are more robust, as they are based on fundamental physical principles (conservation of mass) [69]. TKM also assists in better understanding of physiology, based on which it is suggested that toxin transfer to dialysate is restricted both by physiological resistance as well as resistance in artificial kidney i.e. dialyzer.

3. Diffusion-adjusted Regional Blood Flow Model for β_2-Microglobulin[§]

"*All models are wrong, but some are useful.*"

- *George E. P. Box*

In the previous chapter, the importance of TKM paradigm in HD literature was discussed. The inadequacy of urea as marker toxin was elucidated. Hence, clinicians started focusing on uremic toxins other than urea. β_2-microglobulin (β_2M) is one such toxin which has received major attention from the nephrology community (Section 3.1). In this chapter, a comprehensive model for explaining β_2M kinetics is proposed (Section 3.2). The developed model comprises 7 unknown model parameters whose estimation is difficult from limited patient data. Hence, parameter reduction aspects using *a priori* identifiability analysis are discussed (Section 3.3). The model is calibrated using clinical data of 10 maintenance HD patients and parameter estimates are compared with those obtained for the existing two-pool model for β_2M (Section 3.4). The use of a mathematical model should not be limited to explaining the underlying phenomenon; rather it should also be employed to study interventions prior to their realization in clinical settings. In this direction, the calibrated model is employed to study the effect of exercise intervention during HD as exercise has been shown to improve the toxin removal. Based on the model simulations, a new hypothesis for explaining the exercise effect on physiology is presented (Section 3.5).

[§] The contents of this chapter have been published in: Vaibhav Maheshwari, Lakshminarayanan Samavedham, and Gade Pandu Rangaiah, A regional blood flow model for β_2-microglobulin kinetics and for simulating intra-dialytic exercise effect, *Annals of Biomedical Engineering*, 39:12, 2011

3.1 β_2-microglobulin and Kinetic Studies

β_2M is an undisputed marker of middle to large-sized uremic toxins [37, 68]. Higher pre-dialysis serum concentrations of β_2M have been associated with mortality and morbidity [38, 75]. β_2M is found on the surface of all nucleated cells. After being shed from cell surface, it is excreted by glomerular filtration. In subjects with renal insufficiency, it accumulates in the interstitium and plasma, and deposits as amyloid fibrils in osteoarticular structures [76, 77]. These deposits can lead to amyloidosis, carpal tunnel syndrome, or formation of bone cysts, which are causes of morbidity in long-term hemodialysis subjects [78]. Vanholder *et al.* have recommended that monitoring the serum level of β_2M alone might be sufficient for the evaluation of dialysis adequacy [68]. The kinetics of β_2M differs from that of small molecules (e.g., urea and creatinine) in that the former is distributed in extracellular (plasma + interstitium) compartment only [72], while the latter are distributed in both extracellular and intracellular compartments (Figure 3.1).

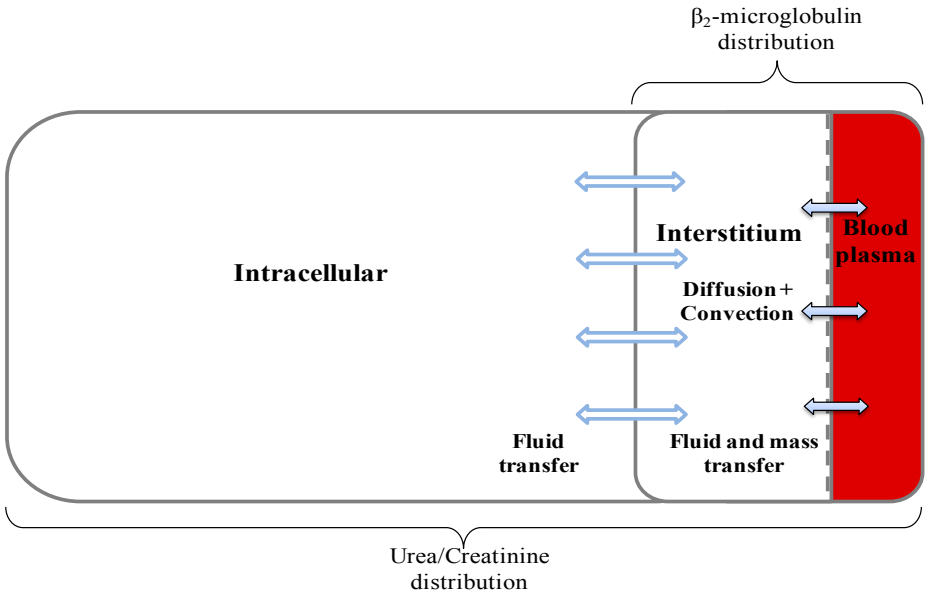

Figure 3.1: Compartmental representation of physiology. Toxins are distributed in intracellular (IC) and extracellular compartments (EC). Urea is distributed in both IC and EC, and β_2M is distributed in EC. The hollow arrows between IC and interstitium denote fluid movement, while solid arrows between interstitium and plasma represent the fluid as well as β_2M movement.

Though considerable interest has been shown for intra-dialytic removal of β_2M, urea is still considered to be the standard marker of dialysis adequacy in clinical practice. Incorporating β_2M in the prescription of adequate dialysis requires comprehensive mathematical models that can describe β_2M kinetics and motivate clinicians to accept its clinical use. Such models can also help in realizing the goal of optimal individualized treatment. So far, the two-pool model has been used to describe the kinetics of urea, creatinine [79], β_2M [73, 74, 80], guanidino compounds [29, 67], phosphate [80], and other toxins [81] in patients on renal replacement therapy. However, the practical application of the two-pool models has been limited, and primarily restricted to explain the effect of increased dialysis frequency or duration [80, 82, 83]. Alternatively, regional blood flow (RBF) model can also explain urea kinetics (Sub-section 2.3.4) [48]. It describes solute kinetics in terms of an unequal distribution of blood flow to different body organs, and appears to be better that the two-pool model. The reasons are that RBF model is closely related to physiology and explains certain aspects of kinetics which the two-pool model cannot, such as cardiopulmonary recirculation [84], and the effect of intra-dialytic exercise [85]. Recently, Schneditz *et al.* proposed a diffusion-adjusted RBF (DA-RBF) model structure [51], which encompasses the characteristics of both the two-pool and the simple RBF model, and brings it much closer to physiology.

Even after the improvements in the previous RBF model, the DA-RBF model has not been much valued by the research community. Probable reasons include the large number of parameters in the DA-RBF model [69, 86], which are difficult to estimate from limited patient data, and clinicians' reluctance to shift to a more complex model. Additionally, the DA-RBF model has not been validated using real-time clinical data for any toxin. Nevertheless, these reasons alone do not undermine the relevance of DA-RBF model in routine clinical setting. In the past, the DA-RBF model has been employed to simulate the

kinetics of small molecules like urea and creatinine only [51]. The applicability of DA-RBF model for larger molecules marker, such as β_2M, and its relevance for renal subjects, has yet to be evaluated.

3.2 Model Description

The original DA-RBF model was developed for urea which is distributed in both IC and EC [51]. To account for the distribution characteristics of β_2M, the existing DA-RBF model is modified in this study. Based on specific perfusion (ratio of blood flow rate to organ fluid volume), the body organs are divided into two major regions, namely, high flow region (HFR) and low flow region (LFR) (Figure 3.2). HFR comprises small organs like heart, brain, kidney, and liver with specific perfusion greater than 0.2 min^{-1}. They sum up to 20% of total body fluid volume, but are highly perfused and almost 85% of cardiac output goes to them. The remaining organs are part of LFR which mainly comprises the large body organs like skin, muscles, and bones. They sum up to 80% of total fluid volume and perfused by only 15% of total cardiac output [86, 87]. Heart pumps blood to various body organs; HFR and LFR plasma flows (Q_{hp} and Q_{lp}) move the toxin between plasma compartments and dialyzer. Both HFR and LFR behave as a two-compartmental structure where mass transfer between compartments is controlled by inter-compartmental mass transfer coefficient (K_{ip}). It can be observed that this model structure comprises 2 two-pool compartments in parallel, or it can be called as parallel-cum-series representation of physiology (Figure 3.2). In the following, all model equations are described.

Mass balance during dialysis

Toxin exchange between compartments depends on the concentration difference (diffusive flux), and fluid movement due to ultrafiltration (convective flux). Additionally,

constant toxin generation and constant non-renal clearance (K_{NR}) also contribute to toxin accumulation. For example, toxin accumulation in HFR plasma compartment depends on the following factors; (i) diffusive flux from interstitium to plasma, (ii) toxin transfer from interstitium to plasma with ultrafiltered fluid, (iii) toxin transfer from plasma to systemic circulation with ultrafiltered fluid, (iv) convective removal with systemic circulation, (v) non-renal clearance from plasma compartment, and (vi) constant toxin generation. Here systemic circulation refers to the distribution of cardiac output to various regions. All these factors appear in the same order in the right hand side of equation (3.1). Toxin balance equations for other compartments are written in the similar manner.

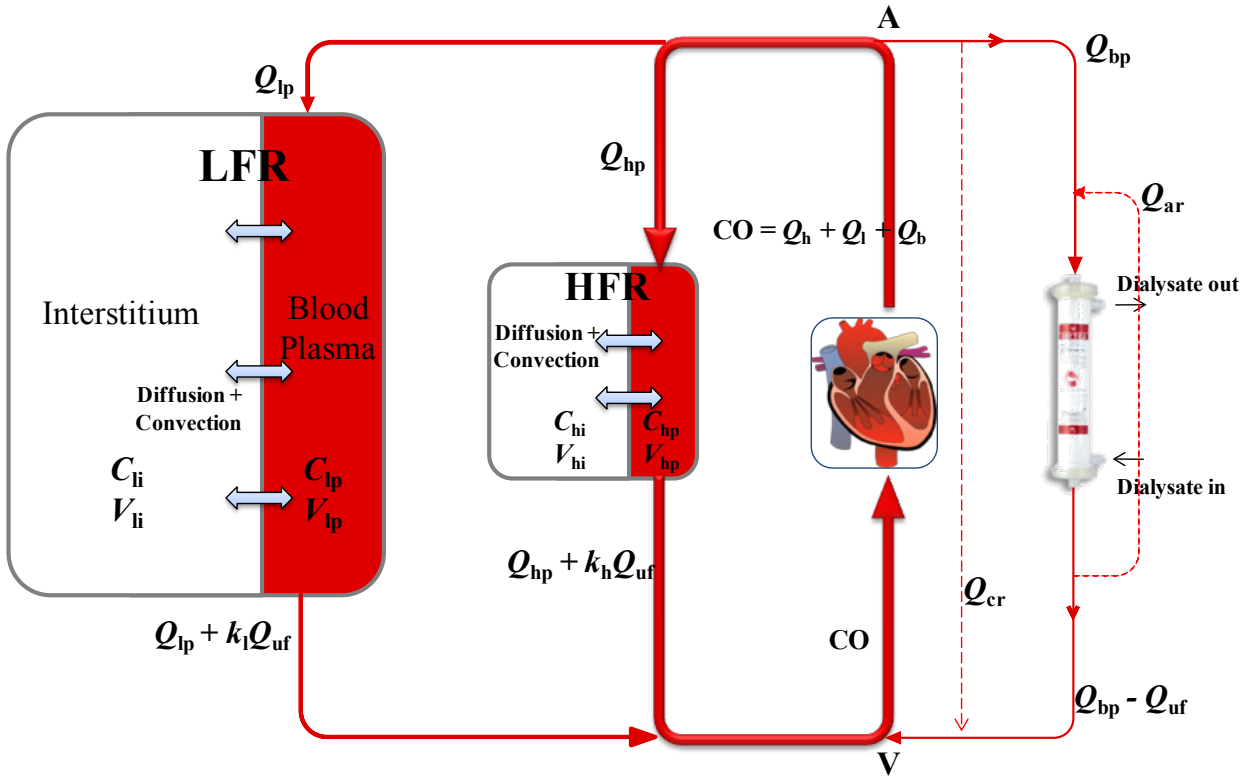

Figure 3.2: Diffusion-adjusted regional blood flow model (parallel-cum-series representation of physiology) for explaining β_2M kinetics. Toxin transfer is due to diffusion across capillary endothelium, and blood/plasma circulation causes convective transport. Q_h/Q_{hp}, Q_l/Q_{lp}, and Q_b/Q_{bp} are blood/plasma flows to HFR, LFR, and dialyzer, respectively. Q_{cr} and Q_{ar} are cardiopulmonary and access recirculation, respectively. Shaded compartments represent contact with blood (A – arterial node and V – venous node). Here, IC is not presented because β_2M distribution is restricted to EC alone.

HFR plasma mass balance:

$$\frac{\mathrm{d}(C_{\mathrm{hp}}V_{\mathrm{hp}})}{\mathrm{dt}} = k_{\mathrm{h}}K_{\mathrm{ip}}(C_{\mathrm{hi}} - C_{\mathrm{hp}}) + k_{\mathrm{h}}Q_{\mathrm{uf}}C_{\mathrm{hi}} - k_{\mathrm{h}}Q_{\mathrm{uf}}C_{\mathrm{hp}} + Q_{\mathrm{hp}}(C_{\mathrm{art}} - C_{\mathrm{hp}}) - k_{\mathrm{h}}K_{\mathrm{NR}}C_{\mathrm{hp}} + k_{\mathrm{h}}G_{\beta 2\mathrm{M}}f_{\mathrm{P}} \tag{3.1}$$

HFR interstitium mass balance:

$$\frac{\mathrm{d}(C_{\mathrm{hi}}V_{\mathrm{hi}})}{\mathrm{dt}} = -k_{\mathrm{h}}K_{\mathrm{ip}}(C_{\mathrm{hi}} - C_{\mathrm{hp}}) - k_{\mathrm{h}}Q_{\mathrm{uf}}C_{\mathrm{hi}} + k_{\mathrm{h}}G_{\beta 2\mathrm{M}}(1 - f_{\mathrm{P}}) \tag{3.2}$$

LFR plasma mass balance:

$$\frac{\mathrm{d}(C_{\mathrm{lp}}V_{\mathrm{lp}})}{\mathrm{dt}} = k_{\mathrm{l}}K_{\mathrm{ip}}(C_{\mathrm{li}} - C_{\mathrm{lp}}) + k_{\mathrm{l}}Q_{\mathrm{uf}}C_{\mathrm{li}} - k_{\mathrm{l}}Q_{\mathrm{uf}}C_{\mathrm{lp}} + Q_{\mathrm{hp}}(C_{\mathrm{art}} - C_{\mathrm{lp}}) - k_{\mathrm{l}}K_{\mathrm{NR}}C_{\mathrm{lp}} + k_{\mathrm{l}}G_{\beta 2\mathrm{M}}f_{\mathrm{P}} \tag{3.3}$$

LFR interstitium mass balance:

$$\frac{\mathrm{d}(C_{\mathrm{li}}V_{\mathrm{li}})}{\mathrm{dt}} = -k_{\mathrm{l}}K_{\mathrm{ip}}(C_{\mathrm{li}} - C_{\mathrm{lp}}) - k_{\mathrm{l}}Q_{\mathrm{uf}}C_{\mathrm{li}} + k_{\mathrm{l}}G_{\beta 2\mathrm{M}}(1 - f_{\mathrm{P}}) \tag{3.4}$$

Calculation of arterial toxin concentration (C_{art})

During dialysis, blood is taken from the arterial port (C_{art}) and rendered to dialyzer; after purification, it is infused back through the venous port. Blood sampling is limited to this arterial blood, which is not purely from HFR or LFR; therefore, an expression relating arterial concentration to HFR and LFR plasma concentration is needed. According to Figure 3.2, plasma mass balance across dialyzer (in lumen side) can be described by:

$$Q_{\mathrm{bp}}C_{\mathrm{art}} - (Q_{\mathrm{bp}} - Q_{\mathrm{uf}})C_{\mathrm{ven}} = \text{Amount transferred to dialysate} = K_{\mathrm{D}}C_{\mathrm{art}} \tag{3.5}$$

Fluid (blood/plasma) balance across arterial node ('A' in Figure 3.2):

$$\mathrm{CO} = Q_{\mathrm{h}} + Q_{\mathrm{l}} + Q_{\mathrm{b}} \tag{3.6}$$

$$(1 - \mathrm{HCT})\mathrm{CO} = Q_{\mathrm{hp}} + Q_{\mathrm{lp}} + Q_{\mathrm{bp}} \tag{3.7}$$

Plasma mass balance across venous node ('V' in Figure 3.2):

$$(1 - \mathrm{HCT})\mathrm{CO}.C_{\mathrm{art}} = (Q_{\mathrm{hp}} + k_{\mathrm{h}}Q_{\mathrm{uf}})C_{\mathrm{hp}} + (Q_{\mathrm{lp}} + k_{\mathrm{l}}Q_{\mathrm{uf}})C_{\mathrm{lp}} + (Q_{\mathrm{bp}} - Q_{\mathrm{uf}})C_{\mathrm{ven}} \tag{3.8}$$

Rearrangement of equation (3.8) using equations (3.5) and (3.7) gives:

$$C_{art} = \frac{(Q_{hp} + k_h Q_{uf})C_{hp} + (Q_{lp} + k_l Q_{uf})C_{lp}}{Q_{hp} + Q_{lp} + K_D} \tag{3.9}$$

Volume balance during dialysis

During dialysis fluid is removed from both IC and EC (interstitium + plasma). Fraction '*e'* of total ultrafiltered fluid comes from EC and rest from IC. The fluid removal from EC is further divided into two components, (i) removal from interstitial compartment and (ii) removal from plasma compartment, based on plasma volume fraction in EC (f_P). It is assumed that fluid removal from any compartment will be in proportion of that compartment fluid volume [73, 74].

HFR plasma volume depletion:

$$\frac{dV_{hp}}{dt} = -eQ_{uf}k_h f_P \tag{3.10}$$

HFR interstitial volume depletion:

$$\frac{dV_{hi}}{dt} = -eQ_{uf}k_h(1 - f_P) \tag{3.11}$$

LFR plasma volume depletion:

$$\frac{dV_{lp}}{dt} = -eQ_{uf}k_l f_P \tag{3.12}$$

LFR interstitial volume depletion:

$$\frac{dV_{li}}{dt} = -eQ_{uf}k_l(1 - f_P) \tag{3.13}$$

Summing up all the volume balance equations (equations 3.10 to 3.13) will give the total fluid removal from extracellular compartment.

Auxiliary equations

Sum of HFR and LFR volume fraction must be equal to 1. Therefore,

$$k_h + k_l = 1 \tag{3.14}$$

A part of cardiac output goes to dialyzer (Q_b), and rest goes in systemic circulation (Figure 3.2). In blood, β_2M is found in plasma only, so, only a portion of systemic circulation participates in mass transfer which is called as systemic plasma (Q_s).

$$Q_s = (1 - \mathrm{HCT})(\mathrm{CO} - Q_b) \tag{3.15}$$

This systemic plasma is sub-divided into two parts, one going to HFR and other to LFR, thus plasma flow fraction to HFR and LFR:

$$\begin{aligned} Q_{hp} &= f_h Q_s \\ Q_{lp} &= f_l Q_s \end{aligned} \tag{3.16}$$

Sum of blood flow fraction to HFR and LFR must be equal to 1. Therefore,

$$f_h + f_l = 1 \tag{3.17}$$

Model equations during inter-dialysis period

During inter-dialysis period, all the equations are modified by setting dialyzer clearance (K_D), ultrafiltration rate (Q_{uf}), and blood flow to dialyzer (Q_b) equal to zero. It is assumed that distribution of fluid intake will be in proportion to compartmental fluid volume, i.e. part of fluid intake, proportional to intracellular fluid volume will move to IC. Sample equation describing the HFR plasma compartment is shown below; toxin accumulation in HFR plasma compartment depends on (i) diffusive flux from interstitium to plasma, (ii) toxin transfer from plasma to systemic circulation, (iii) non-renal clearance from plasma compartment, (iv) constant toxin generation, and (v) convective flux from plasma to interstitium with fluid intake. Similar equations hold for mass and volume balances in other compartments as well.

HFR plasma mass balance:

$$\frac{\mathrm{d}(C_{hp}V_{hp})}{\mathrm{dt}} = k_h K_{ip}(C_{hi} - C_{hp}) + Q_{hp}(C_{art} - C_{hp}) - k_h K_{NR} C_{hp} + k_h G_{\beta 2M} f_P - k_h \alpha C_{hp} e(1 - f_P) \tag{3.18}$$

HFR plasma volume balance:

$$\frac{\mathrm{d}V_{\mathrm{hp}}}{\mathrm{dt}} = ek_{\mathrm{h}}f_{\mathrm{P}}\alpha \tag{3.19}$$

3.3 Model Parameter Reduction and Estimation

Patient data are obtained from a previously published study of 10 patients (8 men and 2 women) treated with post-dilution hemodiafiltration (HDF) [74]. Briefly, HDF is also an extracorporeal method of blood purification, and has shown its superiority over conventional HD in the removal of middle-sized uremic toxins. Further details of HDF, associated clinical outcomes, modes of operation are detailed in Chapter 4. The data used for parameter estimation was obtained under same treatment conditions for all recruited patients [74]. Blood and dialysate flow rates were kept constant at 280 mL min^{-1} and 500 mL min^{-1}, respectively. Treatment time was 240 min for all patients. Blood samples from arterial line were collected at the beginning of dialysis and subsequently at 60, 120, and 240 min during the session. Immediately after HDF, a sample was collected 20 sec later; subsequent samples were collected at 5, 10, 30, 60, 90, 120, and 240 min for capturing the post-dialysis rebound (Figure 3.3). Blood sample just before the next treatment session was also collected for each patient to calculate toxin generation rate ($G_{\beta 2M}$).

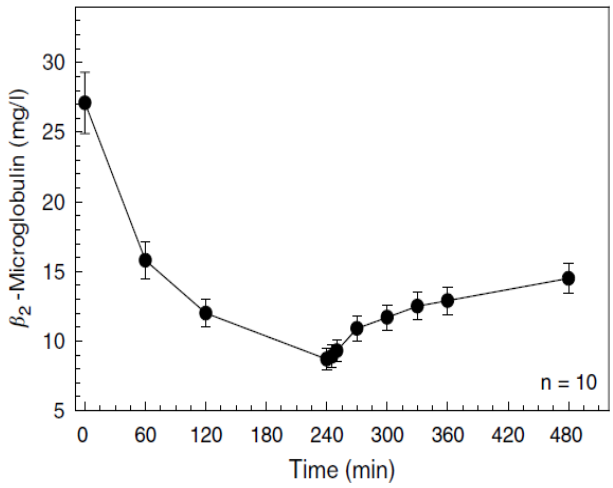

Figure 3.3: Plasma β_2M concentrations during 240 min dialysis treatment and for 4 hours following the treatment. Data is presented as mean± standard error of mean (s.e.m.) [74].

The developed model has 7 unknown parameters, namely, inter-compartmental clearance or inter-compartmental mass transfer coefficient (K_{ip}), toxin distribution volume (V_d), cardiac output (CO), HFR flow fraction (f_h), HFR volume fraction (k_h), EC volume fraction (e), and plasma volume fraction in EC (f_P). It is not possible to estimate all these parameters with precision from limited patient data, and one should replace weakly identifiable parameters with constants. To reduce the number of parameters, *a priori* identifiability analysis proposed by Yao *et al*. is employed [88]. It helps to determine the subset of potentially identifiable parameters, and is based on the calculation of parametric sensitivities (equation 3.20). Large sensitivity indicates the strong influence of that parameter on measured output state, and so the parameter can be better estimated from available data.

$$\left.\frac{\partial C_{art}}{\partial t}\right|_{\substack{p_j=\text{cons}\\ j\neq i}} ; p_i = K_{ip}, V_d, \text{CO}, f_h, k_h, e, f_P \tag{3.20}$$

Scaled sensitivities are calculated at each sample time to form the scaled sensitivity matrix, which is evaluated for initial parameter estimates [88].

$$Z = \begin{bmatrix} \left(\frac{K_{ip}}{C_{art}|_{t=0}}\right)\left.\frac{\partial C_{art}}{\partial K_{ip}}\right|_{t=0} & \left(\frac{V_d}{C_{art}|_{t=0}}\right)\left.\frac{\partial C_{art}}{\partial V_d}\right|_{t=0} & \cdots & \left(\frac{f_P}{C_{art}|_{t=0}}\right)\left.\frac{\partial C_{art}}{\partial (f_P)}\right|_{t=0} \\ \left(\frac{K_{ip}}{C_{art}|_{t=60}}\right)\left.\frac{\partial C_{art}}{\partial K_{ip}}\right|_{t=60} & \left(\frac{V_d}{C_{art}|_{t=60}}\right)\left.\frac{\partial C_{art}}{\partial V_d}\right|_{t=60} & \cdots & \left(\frac{f_P}{C_{art}|_{t=60}}\right)\left.\frac{\partial C_{art}}{\partial (f_P)}\right|_{t=60} \\ \vdots & \vdots & \cdots & \vdots \\ \left(\frac{K_{ip}}{C_{art}|_{t=480}}\right)\left.\frac{\partial C_{art}}{\partial K_{ip}}\right|_{t=480} & \left(\frac{V_d}{C_{art}|_{t=480}}\right)\left.\frac{\partial C_{art}}{\partial V_d}\right|_{t=480} & \cdots & \left(\frac{f_P}{C_{art}|_{t=480}}\right)\left.\frac{\partial C_{art}}{\partial (f_P)}\right|_{t=480} \end{bmatrix} \tag{3.21}$$

Absolute sum of elements in all columns of matrix Z provides the basis to identify the significant parameters. Larger column sum suggests that corresponding sensitivities are large i.e. change in state (C_{art}) with respect to change in the parameter is significant. After

selecting the most significant parameter, scaled sensitivity matrix is deflated (i.e., removing inter-dependence among parametric sensitivities to evaluate the "net influence" of each parameter) using the column corresponding to the largest sum, and second important parameter is then obtained. This process is iterative and continued till all the parameters are ranked according to their column sum. The involved steps are outlined below.

1. Calculate the absolute column sum (corresponding to each parameter) of matrix *Z*.
2. Select the first important parameter corresponding to largest column sum, and mark the corresponding column as X_{L} ($L = 1$ for first iteration).
3. Calculate Z_{L}, the prediction of full sensitivity matrix, *Z*, using the X_{L}: $Z_{\mathrm{L}} = X_{\mathrm{L}}(X_{\mathrm{L}}^{\mathrm{T}} X_{\mathrm{L}})^{-1} X_{\mathrm{L}}^{\mathrm{T}} Z$
4. Calculate the deflated matrix/residual matrix: $R_{\mathrm{L}} = Z - Z_{\mathrm{L}}$
5. Calculate the column sum and select the second most important parameter corresponding to highest column sum.
6. Augment the X_{L} by including new column. Repeat the procedure until all the parameters are ranked in the decreasing order of their column sum.

The procedure can be understood by the following illustration, where following initial guesses are selected for individual patient. The initial guesses are close approximation of physiology. The initial guess for each parameter is stored in a parameter vector θ_0.

$$\theta_0 = [K_{\mathrm{ip}}, V_{\mathrm{d}}, \mathrm{CO}, f_{\mathrm{h}}, k_{\mathrm{h}}, e, f_{\mathrm{P}}] = [100,\ 14,\ 6,\ 0.85,\ 0.2,\ 0.4,\ 0.25]$$

Using the Patient 1 data, the following estimates are obtained.

$$\theta_{\mathrm{e}} = [78,\ 17.62,\ 9.9,\ 0.74,\ 0.73,\ 0.4,\ 0.32]$$

Obtained estimates are used to calculate the scaled sensitivity matrix (Z) (equation 3.21), and following the above mentioned steps, all parameters are ranked. The column sums (CS) of all parameters and their % contribution ($CS_{\%}$) are:

$$\mathrm{CS} = \begin{bmatrix} K_{\mathrm{ip}} & 0.45 \\ V_{\mathrm{d}} & 5.30 \\ \mathrm{CO} & 0.0008 \\ f_{\mathrm{h}} & 0.0001 \\ k_{\mathrm{h}} & 0.001 \\ e & 0.005 \\ f_{\mathrm{P}} & 1.33 \end{bmatrix} \Rightarrow \mathrm{CS\%} = \begin{bmatrix} K_{\mathrm{ip}} & 6.38 \\ V_{\mathrm{d}} & 74.8 \\ \mathrm{CO} & 0.02 \\ f_{\mathrm{h}} & 0.0 \\ k_{\mathrm{h}} & 0.01 \\ e & 0.07 \\ f_{\mathrm{P}} & 18.8 \end{bmatrix}$$

It is evident that cumulative contribution of parameters V_{d}, f_{P}, and K_{ip} is ~99.9%, and thus selected as the important parameters. In other words, the effect of change in CO, f_{h}, e, and k_{h} on arterial blood plasma concentration (C_{art}) is very small in comparison to the effect of change in V_{d}, f_{P}, and K_{ip}. The remaining four parameters (CO, f_{h}, e, and k_{h}) are replaced by constants. The constants for model parameters and other physiological constants are presented in Table 3.1. Same parameter sub-set results are obtained for other patients too.

Note that the previous two-pool β_2M kinetic studies have assumed the removal of accumulated fluid from EC alone [73, 74], which is infeasible, as fluid removal from blood compartment will induce the fluid movement from interstitial compartment and then from IC. To make it realistic, the two-pool model assumption pertaining to fluid removal is modified, and is discussed in the following. The net fluid removal is considered from both EC and IC. Further, it is assumed that fluid removal from any compartment will be in proportion of that compartmental fluid volume [89]. Hence, fluid removal from EC will be in proportion of volume fraction of EC (e), which is later assumed to be a constant based on *a priori* identifiability analysis. It is assumed that about 33% of fluid is removed from EC and the remaining 67% comes from IC [89-91].

Considering this information, EC volume fraction (e) is replaced by factor of 1/3 in the equations for rate of volume depletion (Table 3.1).

Table 3.1: Constant model parameters for all patients

Symbol	Description	Value	Reference
HCT	Hematocrit	0.35	[74]
k_h	Volume fraction of high flow region	0.2	[92]
CO	Cardiac output (L min^{-1})	5.8	[84, 93]
e	Extracellular fluid fraction	1/3	[89]
f_h	Blood flow fraction to high flow region	0.85	[84, 92]
K_{NR}	Non-renal clearance (mL min^{-1})	3	[74]

After replacing the four insensitive parameters by suitable constant values, the three important parameters are re-estimated. The estimated post-dialysis toxin distribution volume (V_d) is 14.22±0.75 L (equivalent to 20.3±1.3% of end-dialysis body weight), plasma fraction in EC (f_P) is 0.39±0.03, and inter-compartmental mass transfer coefficient (K_{ip}) is 44±4.1 mL min^{-1}. Estimated values of model parameters for each patient are listed in Table 3.2. For comparison, parameter estimates from two-compartment model approach are also presented [74]. Obtained estimates of V_d are larger than those obtained from the two-pool model (10.2±0.6 L). Also, the obtained estimates for f_P are larger than f_P of 0.25 in normal subjects. Toxin generation rate is 0.131±0.007 mg min^{-1}, which is calculated using estimated V_d and toxin concentration measured at the beginning of next dialysis session. Note that results are presented as mean ± s.e.m. (standard error of mean).

Table 3.2: Estimated model parameters for β_2-microglobulin kinetics

Patient No.	Diffusion adjusted regional blood flow model				Two-compartment model (Ward *et al.* [74])		
	Inter-compartmental clearance, K_{ip} (mL min^{-1})	Toxin distribution volume, V_d (L)	Plasma Fraction in extracellular compartment, f_P	Generation Rate, $G_{\beta 2M}$ (mg min^{-1})	Inter-compartmental clearance, K_{ip} (mL min^{-1})	Toxin distribution volume, V_d (L)	Generation Rate, $G_{\beta 2M}$ (mg min^{-1})
1	43	18.47	0.41	0.134	100	13.27	0.131
2	46	10.51	0.43	0.121	86	7.52	0.131
3	51	14.28	0.27	0.125	63	8.10	0.144
4	48	15.03	0.38	0.091	75	12.31	0.091
5	39	15.21	0.27	0.136	53	8.57	0.140
6	28	16.26	0.33	0.128	57	9.25	0.125
7	54	14.39	0.46	0.122	108	11.99	0.131
8	24	10.84	0.54	0.155	102	9.91	0.165
9	40	13.10	0.39	0.171	74	9.31	0.182
10	70	14.12	0.42	0.126	107	11.37	0.115
Mean ± s.e.m.	44 ± 4.1	14.22 ± 0.75	0.39 ± 0.03	0.131 ± 0.007	82.5 ± 6.7	10.2 ± 0.6	0.136 ± 0.008

The reduced DA-RBF model adopts similar assumptions as in the two-pool study [74]. In the absence of any literature evidence, membrane sieving coefficient is considered as one, inferred from the study by Harper *et al*., where they revealed *in vivo* that uremia enhances the membrane permeability [94]. However, as dialysis progresses, uremia decreases; hence, membrane permeability and K_{ip} should continuously decrease. Nevertheless, the sieving coefficient and K_{ip} are considered as constant, which is the assumption in all previously developed kinetic models for urea, creatinine, and β_2M. This may not be valid in reality. Experimental studies are required to find out how the sieving coefficient and K_{ip} changes with the decrease in uremia. Secondly, even though the DA-RBF model can account for access recirculation (Q_{ar}), it is neglected in the current study due to the absence of relevant individual patient data, and to make a valid comparison between the outputs of the developed model and that of the existing two-pool model [94]. Q_{ar} dilute the inlet blood to dialyzer and reduce the toxin concentration. As a result of this reduced concentration, toxin removal or access clearance reduces, or post-dialysis toxin concentration increases. The effect of Q_{ar} is not limited to β_2M alone, rather affects all toxins equally, and leads to reduction in the measure of dialysis adequacy $K_D t / V_{urea}$. As dialyzer clearance (K_D) and time of dialysis (t) are independent of recirculation, only increase in distribution volume (V_d) can explain the decreased adequacy index. Hence, inclusion of Q_{ar} will result in larger estimates of toxin distribution volume [92, 95].

3.4 Interpretation of Parameter Estimates

The toxin distribution volume for β_2M obtained from fitting the model to experimental data (14.22±0.75 L or 20.3±1.3% of end-dialysis body weight) is greater than that estimated by anthropometric formulae given by Watson *et al*. [96], (12.62±0.57 L or 17.6±0.4% of end dialysis body weight). The difference could be because anthropometric formulae were derived for normal subjects, and not for renal patients, who always have

excess fluid. On the other hand, significant difference is observed between the results obtained here and from the two-pool study for V_d (10.2±0.6 L) [74]. This can be attributed to the improved physiological representation in the form of DA-RBF model, and the assumption that about 33% of ultrafiltered volume comes from EC and rest comes from IC. In clinical scenario, one can validate one of the two models by measuring the toxin concentration in blood serum, and comparing it with that obtained by both the models. The correct (validated) model can be used to decide the dialysis dose. The parameter estimate for plasma fraction in EC is 0.39±0.03, which is greater than plasma fraction found in normal subjects. It can be understood that this excess fluid contributes to blood volume; the obtained parameter estimates also explain the reason for most renal patients being hypertensive. Distinctively, f_P for Patient 8 (0.54) is much higher than rest of the patients, probably because there is no fluid removal for this patient during dialysis (pre- and post-dialysis weight are same).

Toxin generation is assumed to be in both interstitium and plasma compartments, and it is calculated after estimating toxin distribution volume. Toxin concentration at t = 480 min (with t = 0 min denoting start of dialysis) and pre-dialysis toxin concentration measured before next dialysis session are used for this purpose (assuming constant toxin generation rate). The calculated generation rate (0.131±0.007 mg min^{-1}) is similar to the results obtained for the same patient group using the two-pool study (0.136±0.008 mg min^{-1}) [74], and in other hemodialysis subjects using the two-pool modeling approach (0.132±0.006 mg min^{-1}) [71]. Estimated inter-compartmental clearance (K_{ip}) between interstitium and plasma compartment is 44±4.1 mL min^{-1}, which is much smaller than reported value of 82±7 mL min^{-1} in the two-compartment study [74]. In this study, measured dialyzer clearance (K_D) of β_2M is 73±2 mL min^{-1}. Despite this high K_D, mass transfer is limited by smaller K_{ip}, which is evident from the obtained parameter estimates

for individual patient, i.e. toxin removal is primarily controlled by membrane resistance. The smaller value of K_{ip} than K_D explains, why convection based dialysis (hemodiafiltration) does not result in significantly improved toxin removal, and is limited to toxin removal from blood compartment only [74]. This also implies that physiological resistance confer the major resistance for toxin removal [74].

Measured toxin concentrations and model fit are shown in Figure 3.4, while toxin concentration in each compartment is illustrated in Figure 3.5 (for Patients 1 and 10). There is consistent difference between concentrations of C_{hp} and C_{lp} from the onset of dialysis, as the unequal distribution of cardiac output creates a concentration difference between HFR and LFR. Nevertheless, one can observe that HFR and LFR plasma concentration equilibrate immediately after dialysis due to systemic circulation (Figure 3.5). This explains the cause of sharp rebound after dialysis. One can also observe that major contribution to rebound is concentration difference between interstitium and plasma compartment. In summary, the developed model gives better insight into toxin distribution in various compartments. It can be employed for precise estimation of toxin distribution volume i.e. extracellular fluid volume, which is one of the greatest challenges to practicing nephrologists [97]. This may further help in accurate dialysis dose prediction for hemodialysis subjects based on modified dialysis adequacy index considering β_2M ($K_Dt/V_{\beta 2M}$) as a global marker of toxin milieu.

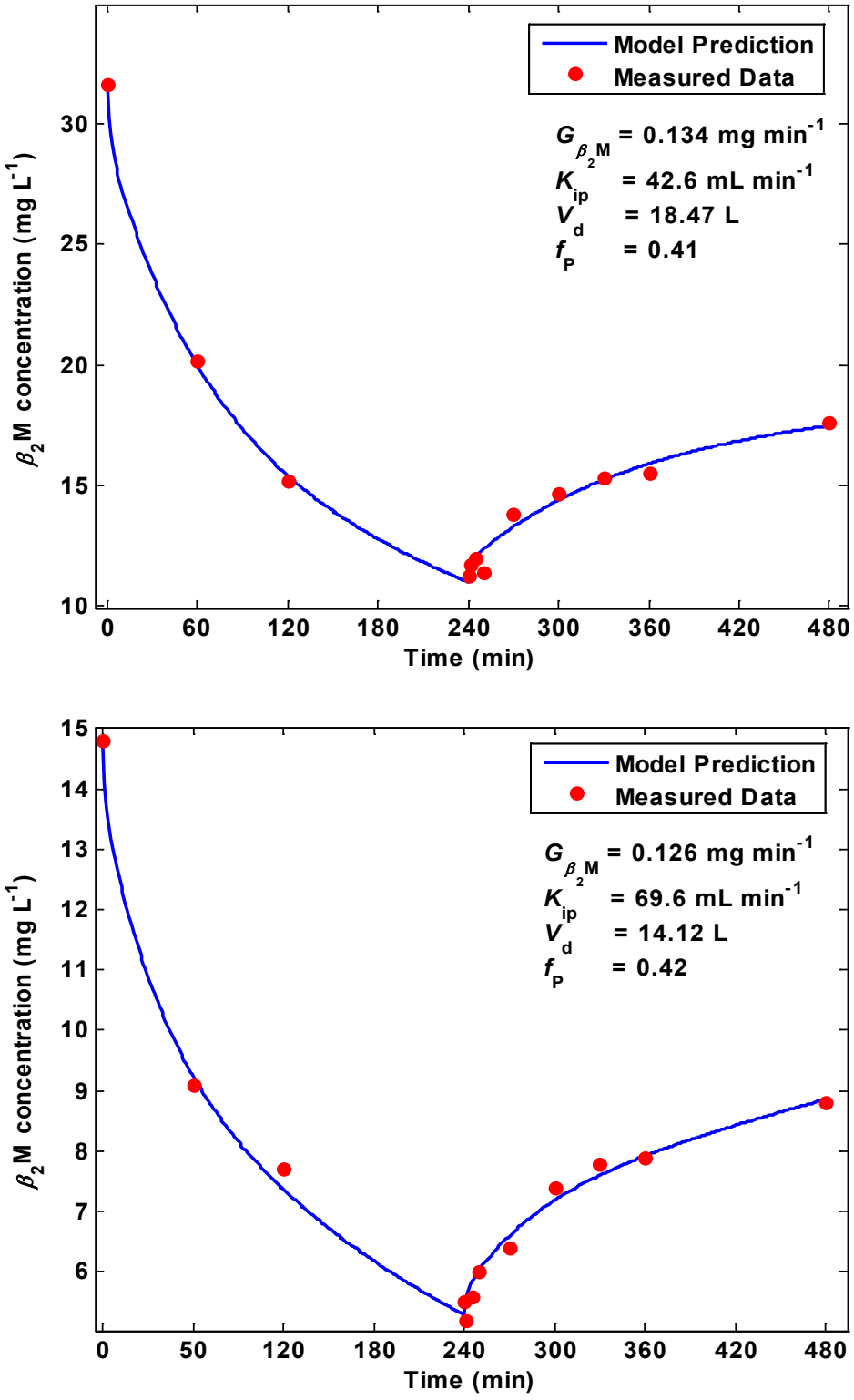

Figure 3.4: Arterial plasma concentration profile (model fit) and measured concentration of β_2-microglobulin for Patient 1 (top) and Patient 10 (bottom)

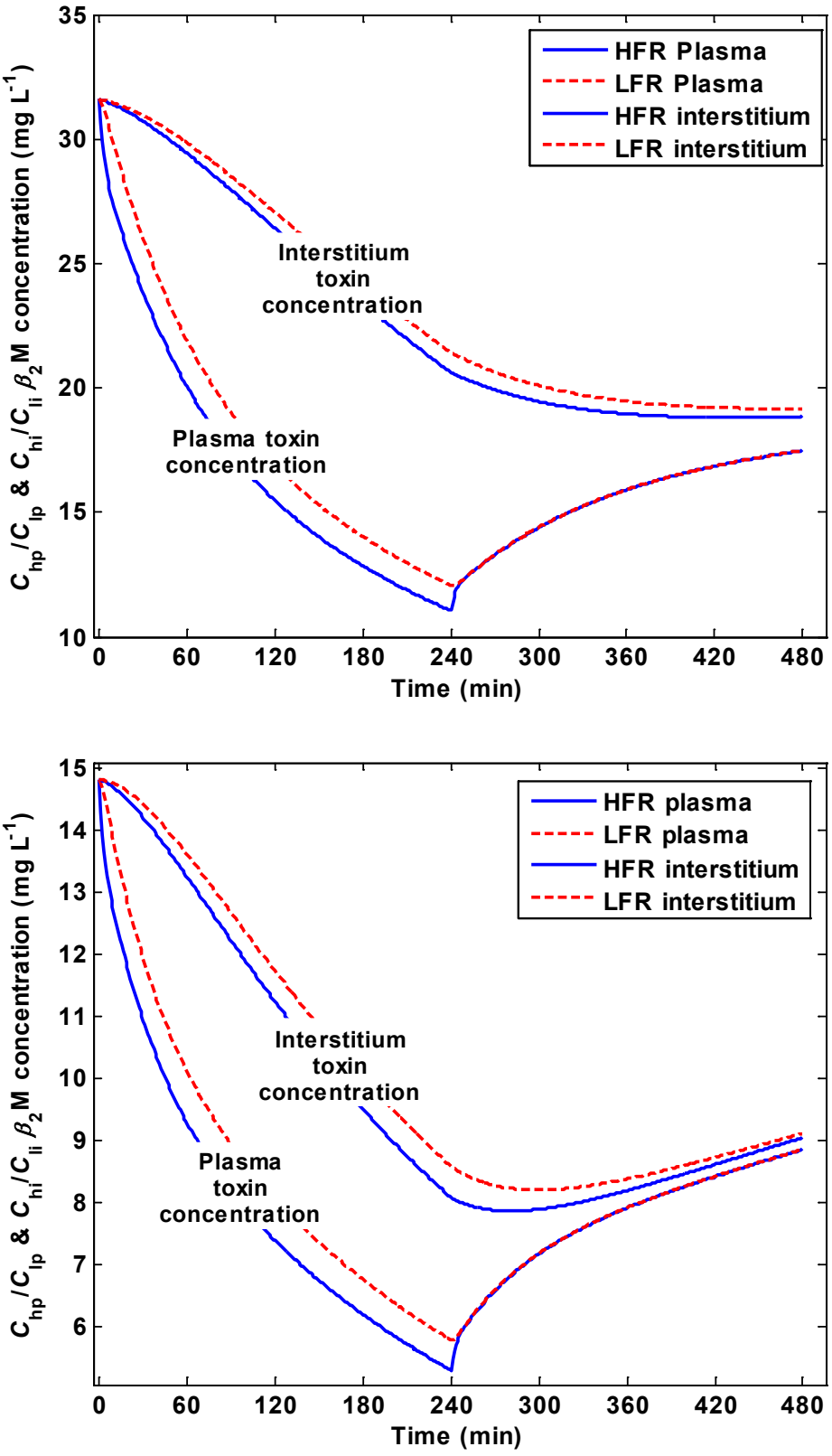

Figure 3.5: β_2-microglobulin concentration profile in different body compartments for Patient 1 (top) and Patient 10 (bottom).

3.5 Model Applications

It is evident that DA-RBF model results in better parameter estimates for HD patients which explain the physiology of HD patients. Nevertheless, developing a good model is the first step to understand a system, and model is not restricted to predict the underlying behavior only. Hence, the developed model is employed to estimate the removed toxin mass and also study the effect of exercise on toxin removal.

3.5.1 Estimation of Removed Toxin Mass

The DA-RBF model is employed to estimate the removed toxin mass during HDF. This calculation can be performed using initial (at t = 0 min) and final toxin concentration after dialysis (at t = 240 min) and obtained estimates of toxin distribution volume,

$$MR = M_0 - M_{240} = C_0 V_0 - C_{240} V_{240} \tag{3.22}$$

However, above formulation will overestimate the removed toxin mass due to post-dialysis rebound. Thus, adjusting for post-dialysis rebound will result in,

$$MR = M_0 - M_{480} = C_0 V_0 - C_{480} V_{480} \tag{3.23}$$

where C_0, C_{240}, and C_{480}, represent pre-dialysis toxin concentration (at t = 0), concentration at the end of dialysis (at t = 240 min), and concentration after 240 min of dialysis (at 480th min from the beginning of dialysis), respectively. The estimates of removed toxin mass using the developed model are 196.31±19.7 mg, which are higher than 141.45±14.17 mg, obtained by the existing two pool model (Table 3.3). The larger estimates of removed toxin mass from DA-RBF model can be explained by the bigger estimates of V_d when comapred with that obtained in the two-pool model. This simple approach can be used to validate the superiority of one toxin kinetic model over another.

Table 3.3: Estimates of removed toxin mass (mean±s.e.m.)

Patient No.	Mass removed, mg (estimated by the DA-RBF model)	Mass removed, mg (estimated by the Two-pool model [74])
1	268.63	208.42
2	218.76	160.39
3	190.19	112.99
4	110.67	88.91
5	189.69	115.47
6	268.22	158.17
7	241.70	199.41
8	144.77	121.64
9	236.25	171.38
10	94.26	77.69
Mean ± s.e.m.	196.31±19.7	141.45±14.17

3.5.2 Simulating Effect of Exercise

Exercise during dialysis (intra-dialytic exercise) has shown to improve the toxin removal [98, 99]. Smye *et al*. first employed the simple RBF model and demonstrated via simulations that increase in cardiac output or increased perfusion of the skeletal muscles results in reduced post-dialysis rebound [85]. It has been suggested in the past that, as a result of intra-dialytic exercise, a large fraction of increased CO reaches the LFR, where major portion of toxin is present in comparison to HFR [84]. This increased perfusion of LFR results in higher toxin removal through convection, and thus reduced post-dialysis rebound. To observe the same, the effect of increased CO (6 L min^{-1} in normal condition to 12 L min^{-1} during exercise [85]) on arterial plasma concentration is studied for all 10 patients. Exercise is given to *in silico* patients at t = 150 min, and sustained till the end of session (t = 240 min). Quantitatively, the 100% increase of CO results in only ~1% decrease in post-dialysis toxin concentration at t = 480 min. Similar results are observed

for rest of the patients too (Table 3.4). Figure 3.6 illustrates the effect of 100% increase in cardiac output due to intra-dialytic exercise. However, exercise has shown to decrease the post-dialytic toxin rebound much more than 1 %; e.g. in the study of Kong *et al*., the creatinine rebound decreased 4% [100]. Similar results were obtained for phosphate removal, where weekly phosphate removal increased in exercises intervention [99]. Though there is no clinical trial studying the effect of intra-dialytic exercise on any of middle-sized uremic toxin removal, it can be assumed that exercise will result in similar quantum of decrease in % rebound. This leads to the question – how does intra-dialytic exercise lead to reduced rebound when the effect of increased cardiac output is not significant?

To explain the phenomenon, it is hypothesized that intra-dialytic exercise increases both CO and K_{ip}. It is known that exercise to lower extremity causes increased blood flow to LFR. The increased flow is hypothesized to dilate capillaries/membranes so that the excess blood flow can be accommodated [98]; this will increase the membrane surface area. Additionally, dilation will lead to larger membrane pore size. These two reasons, namely, increased surface area of capillaries and increased membrane pore size will increase the membrane permeability i.e. increase in inter-compartmental mass transfer clearance (K_{ip}), and hence more toxin transfer to blood compartment. This transferred toxin will be swept away by increased blood flow.

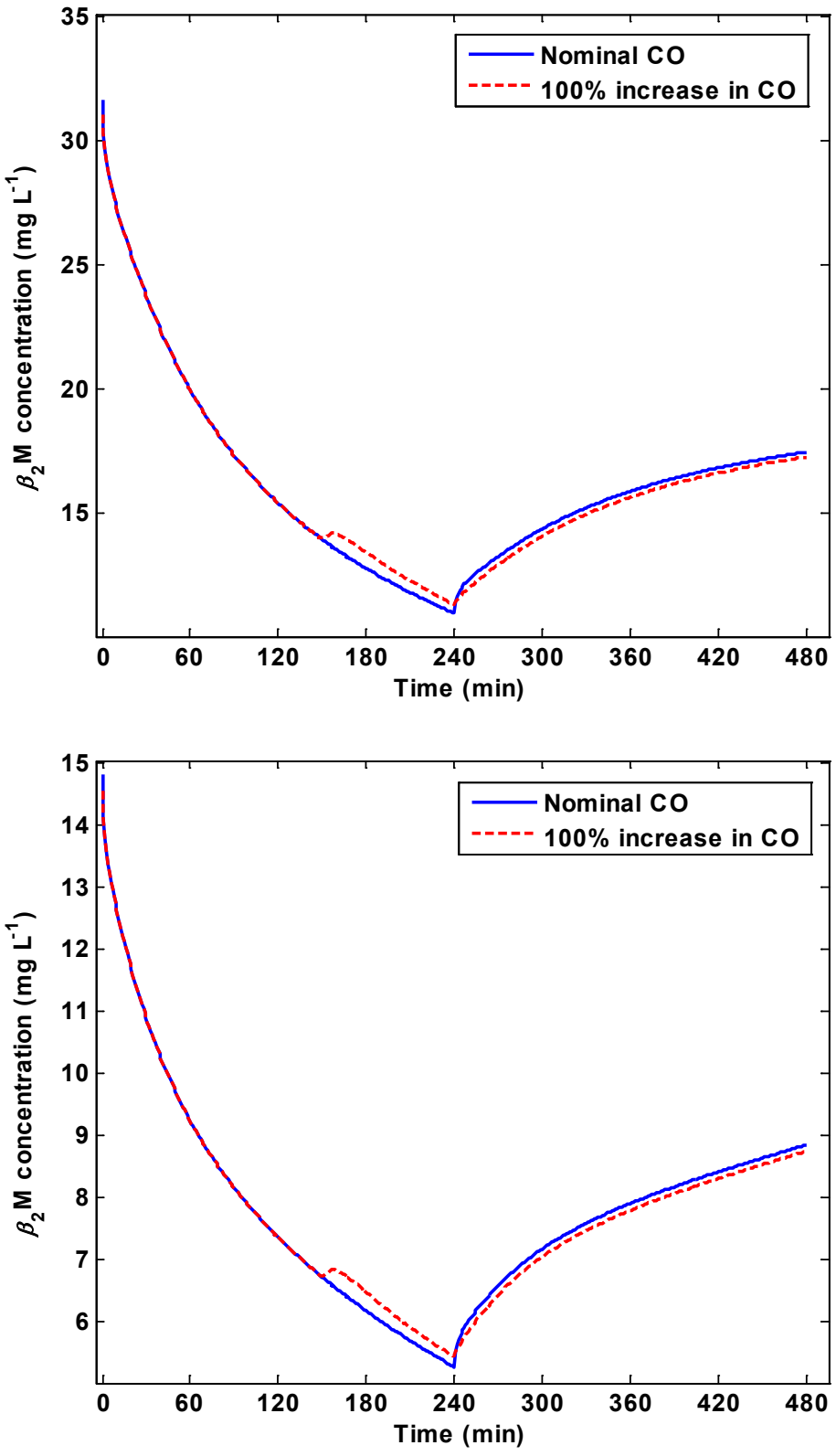

Figure 3.6: Simulation of effect of intra-dialytic exercise for Patient 1 (top) and Patient 10 (bottom) – Decrease in post-dialysis rebound due to 100% increase in cardiac output.

To compare their individual effect on toxin removal, increase in both factors is studied independently. (i) The model is simulated for CO = 6 L min^{-1} (without exercise) and CO = 12 L min^{-1} (with intra-dialytic exercise) keeping K_{ip} constant. To simulate the toxin kinetics during exercise, the HFR blood flow remained same as in no exercise condition [85], thus rest of the increased cardiac output will perfuse LFR. (ii) To observe the effect of increase in K_{ip}, a hypothetical increase of 15% is studied (keeping cardiac output constant at 6 L min^{-1}). In all the cases, the post-dialysis rebound is calculated using the following equation [72].

$$\%Rebound = \frac{C_{480} - C_{240}}{C_0 - C_{240}} \times 100 \tag{3.24}$$

Difference in percentage rebound is calculated for CO = 6 and 12 L min^{-1}; similar calculations are performed between nominal K_{ip} and 15% increased K_{ip}. Table 3.4 comprises the quantitative results corresponding to both scenarios. It is observed that 15% increase in K_{ip} can result in similar decrease as obtained with 100% increase in CO. Hence, it can be concluded that intra-dialytic exercise not only increases the CO but also increases the K_{ip}. To substantiate this hypothesis, further clinical studies need to be carried out so as to segregate the effect of CO and K_{ip} on arterial toxin plasma concentration, and formulating a relationship between the effect of exercise and toxin removal. Such clinical studies can also help in quantifying the effect of exercise on inter-compartmental clearance.

Table 3.4: Simulating effect of intra-dialytic exercise – Decrease in rebound % (a) for 100% increase in cardiac output (CO) and (b) for 15% increase in inter-compartmental mass transfer coefficient (K_{ip})

Patient No.	Effect of increase in CO, keeping K_{ip} constant			Effect of increase in K_{ip}, keeping CO constant		
	Rebound % during normal dialysis (CO = 6 L min^{-1})	Rebound % with intra-dialytic exercise (CO = 12 L min^{-1})	Decrease in Rebound % due to exercise	Rebound % during normal dialysis (K_{ip} = nominal)	Rebound % with intra-dialytic exercise (K_{ip} = 1.15 × nominal)	Decrease in Rebound % due to exercise
1	31.37	30.07	1.30	31.76	31.00	0.75
2	23.38	22.64	0.74	24.71	23.92	0.80
3	32.91	32.06	0.85	34.95	33.60	1.35
4	37.18	36.49	0.69	37.75	36.59	1.17
5	39.21	38.78	0.43	40.48	39.31	1.17
6	33.57	32.90	0.68	35.35	34.57	0.78
7	25.63	24.25	1.38	25.31	24.30	1.01
8	33.95	33.31	0.64	33.73	32.91	0.82
9	33.38	32.70	0.68	34.13	33.17	0.97
10	37.45	36.25	1.21	37.20	36.20	1.00

3.6 Summary

A comprehensive model (diffusion-adjusted regional blood flow model) describing the removal kinetics of middle-sized marker toxin, β_2-microglobulin, has been presented. Based on *a priori* identifiability analysis, the number of estimable parameters is reduced from seven to three. The estimates for toxin distribution volume (V_d) are greater than those obtained with two-compartment models, which can be justified by the fact that patients on maintenance hemodialysis are fluid overloaded. Estimates of plasma fraction in extracellular compartment (f_P) suggest that more of this excess fluid stores in plasma compartment, which explains the reason for renal patients being hypertensive. In summary, the reduced parameter DA-RBF model results in improved understanding of β_2-microglobulin kinetics. The developed model results in higher estimate of removed toxin mass than that obtained by the two-pool model. This information can be used to validate the existing models and select the one that is the best representative of physiology. To demonstrate the clinical application of the developed model, the effect of intra-dialytic exercise is examined. Based on the simulation results, it is suggested that increase in cardiac output alone cannot explain the decrease in rebound, and it is hypothesized that stating that intra-dialytic exercise not only increases the cardiac output but also increases the inter-compartmental mass transfer coefficient (K_{ip}). When combined together, both these manifests as lower post-dialysis rebound i.e. increased toxin removal. Further clinical studies are required to study the effect of exercise on toxin removal and to quantify the associated physiological changes. After confirming the intra-dialytic exercise effect in prospective clinical trials, the developed model can be utilized for systematic introduction of intra-dialytic exercise and synergizing its effect with dialysis to obtain improved patient outcomes.

4. Clinical Study to Compare Toxin Removal in Hemodialysis, Hemodiafiltration, and Hemodialysis with Exercise[§]

"The strongest arguments prove nothing so long as the conclusions are not verified by experience. Experimental science is the queen of sciences and the goal of all speculation."

- Roger Bacon

The previous chapter described a comprehensive model for β_2-microglobulin kinetics. Employing the developed model, the effect of exercise during dialysis was studied. To explain the existing clinical evidence pertaining to enhanced toxin removal by exercise, it is hypothesized that intra-dialytic exercise not only increases the perfusion of remote body compartments, but also decreases the inter-compartmental resistance. To advance further, clinical studies are required to test the proposed hypotheses. In this direction, a pilot clinical research to investigate the effect of exercise during dialysis on toxin removal is designed. The primary focus of this clinical research is to investigate the physiological changes associated with intra-dialytic exercise.

As discussed in sub-section 1.3.2, hemodiafiltration (HDF) has also shown to improve the toxin removal; hence, it is also studied for comparison purpose. The HDF details and associated literature evidence are presented in Section 4.1. In Section 4.2, clinical evidences for exercise and involved hypotheses are presented. The clinical trial design aspects are presented in Section 4.3. Information on study patients and dialysis

[§] A portion of this chapter has been published in: Vaibhav Maheshwari, Lakshminarayanan Samavedham, Gade Pandu Rangaiah, Yijun Loy, Lieng Hsi Ling, Sunil Sethi and Titus Lau Wai Leong. Comparison of toxin removal outcomes in online hemodiafiltration and intra-dialytic exercise in high-flux hemodialysis: A prospective randomized open-label clinical study protocol; *BMC Nephrology*, 13: 156, 2012

prescription are provided in Section 4.4. The results and discussion are presented in Sections 4.5 and 4.6, respectively.

4.1 Hemodiafiltration

According to single-pool assumption, the toxin removal is primarily hindered by dialyzer membrane pore size. Hence, an easy maneuver for increasing the toxin removal is to increase the membrane pore size. Two randomized clinical trials, Hemodialysis study and Membrane Permeability Outcome study have shown the superiority of large pore size membrane (high flux dialyzers) over small pore size membrane (low flux dialyzers) in decreasing the mortality and morbidity [101, 102]. Nevertheless, the removal of middle-sized toxins is poor with high-flux membranes, and CHD patients are often overloaded with middle-sized uremic toxins. The reason is that toxin removal in CHD is primarily controlled by diffusion. Since diffusion is inversely proportional to molecular weight or size [103], removal of middle-sized toxins is relatively smaller than that of small-sized toxins. Also, membrane pore size cannot be increased beyond certain limits because it may translate in loss of important constituents of blood such as glucose, proteins, etc.

HDF augments the toxin removal by convection, which mobilizes the toxins and thus enhances their removal. Understanding the toxin removal in dialyzer can clearly elucidate the role of diffusion and convection in toxin removal. In TKM, the dialyzer performance is quantified by dialyzer clearance (K_D), which determines the removal rate. Following Figure 4.1, the K_D can be calculated as [46],

$$K_D C_{Bi} = Q_{Bi} C_{Bi} - Q_{Bo} C_{Bo} \tag{4.1}$$

where Q_{Bi} and Q_{Bo} denote blood flow at the inlet and outlet of dialyzer (mL/min), C_{Bi} and C_{Bo} are corresponding concentrations of uremic toxin.

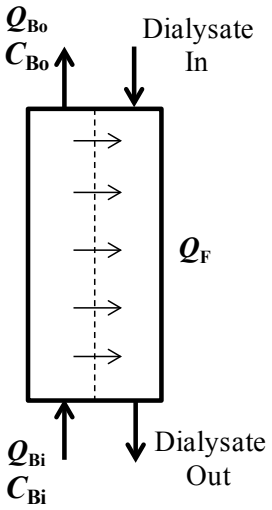

Figure 4.1: Blood and dialysate flow along dialyzer length. Horizontal arrows represent transfer of accumulated toxins and excess fluid from blood to dialysate stream

Along the dialyzer length, fluid is removed at a certain rate. If the rate of fluid removal is Q_F, then

$$Q_{Bo} = Q_{Bi} - Q_F \tag{4.2}$$

Replacing Q_{Bi} simply by Q_B, equation 4.1 simplifies to a general formula for dialyzer clearance,

$$\begin{aligned} K_D &= Q_B \frac{C_{Bi} - C_{Bo}}{C_{Bi}} + Q_F \frac{C_{Bo}}{C_{Bi}} \\ \Rightarrow K_D &= (Q_B - Q_F) \frac{C_{Bi} - C_{Bo}}{C_{Bi}} + Q_F \end{aligned} \tag{4.3}$$

Hence, to calculate K_D, blood samples at the inlet and outlet of dialyzer should be collected. During dialysis, the membrane permeability would decrease thus K_D will also decrease; however, clinical studies found that K_D remains almost constant during 4 hour dialysis [46, 74]. The first term in equation 4.3 describes the effect of diffusion on toxin removal and the second that of convection. In CHD, the fluid removal rate is 10-15 mL/min, which is decided based on the amount of weight gain during inter-dialysis period. This is very small when compared with the diffusive component. In HDF, the Q_F contribution is increased by removing excess fluid along dialyzer length, which is

compensated by addition of sterile fluid before blood goes back to the patient. Typical replacement fluid volume during 4 hour HDF process is ~20 L, which corresponds to Q_F = 80 mL/min. The HDF can be performed in pre-dilution and post-dilution mode, depending on the point of fluid infusion. Figure 4.2 schematically presents both modes of HDF.

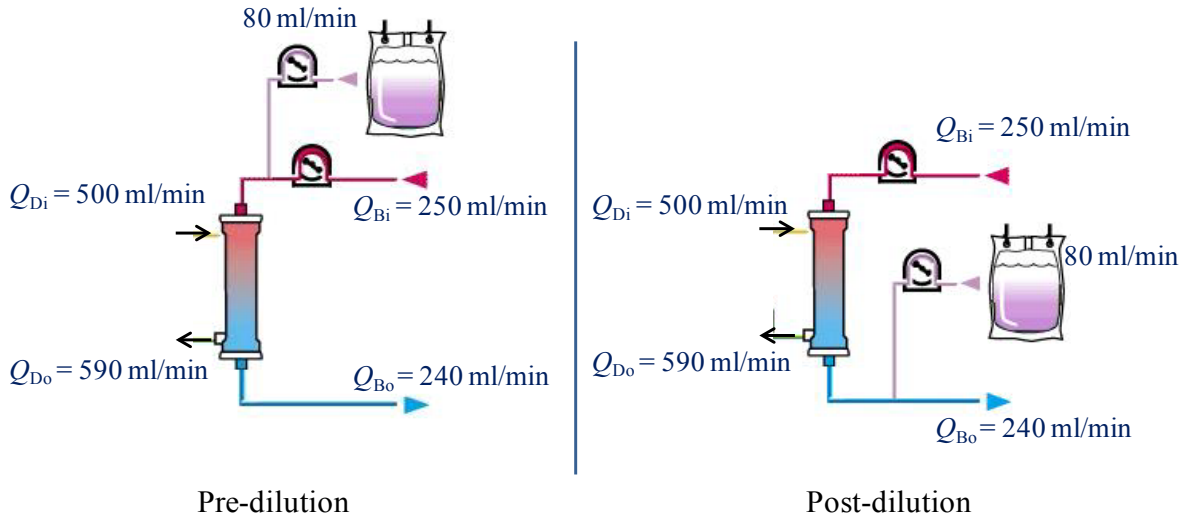

Figure 4.2: Pre- and post-dilution modes of hemodiafiltration. The given blood and dialysate flow rate are usual numbers practiced in routine dialysis settings. The replacement fluid rate is assumed to be 80 mL/min.

The utmost requirement of HDF is the availability of non-pyrogenic sterile replacement fluid, which can be added to the blood stream. In the past, the replacement fluid was provided in sterile bags, but the extremely high cost prohibited this practice. On-line regeneration of replacement fluid has decreased this cost [104, 105], and resulted in increased acceptability of HDF. This mode of HDF is known as online-HDF.

4.1.1 Clinical Evidences for HDF

HDF is increasingly being considered as superior to CHD, and is a subject of major research [19, 106]. Numerous randomized controlled trials have studied its efficacy for toxin removal and clinical outcomes [20, 107-111]. As discussed earlier, the basic premise for encouraging HDF is the forced ultrafiltration rate that results in increased

removal of middle and large-sized toxins via convection [112, 113]. Despite numerous documented benefits of HDF, there is lack of evidence from various clinical trials that HDF can improve the toxin removal. This points to a need of properly designed randomized controlled clinical trials [19, 114].

Among clinical trials studying HDF, a prospective clinical study comparing online-HDF and high flux HD has shown that both small (urea and creatinine) and large (β_2M and complement factor D) sized toxin removal were greater for HDF when compared to high-flux HD. However, this increased removal of urea and creatinine did not result in lower pre-treatment serum concentration in both groups. In the context of large-sized molecules, it was found that, after one year, pre-treatment serum β_2M levels were similar in both regimens, but significant decrease was observed for complement factor D [20]. Complement factor D is one of the toxins distributed in blood plasma. Based on these evidences, it was concluded that efficacy of HDF is largely limited to blood compartment only and is restricted by inter-compartmental resistance [74]. Toxins, which are distributed in intracellular and/or interstitial compartments, in addition to blood plasma compartment, are severely restricted by cellular membrane or capillary endothelium. This also explained the significant removal of complement factor D, for its distribution is limited to blood compartment only. Since majority of uremic toxins are distributed in both IC and EC, HDF and high-flux HD seem to detoxify the blood compartment primarily. These arguments also led to conclude that, after a certain volume of replacement fluid in HDF, there will not be significant benefit for toxin removal, as blood plasma compartment will almost be devoid of toxins and inflow of toxins from remote compartments is restricted by inter-compartmental resistance. This explains why even with very high volume of replacement fluid (60 L), there was no significant improvement in toxin removal [115]. The only plausible way to overcome this resistance is to opt for

intensive dialysis, i.e. prescribe long nocturnal dialysis or increased frequency of dialysis, which have been found to be more efficacious than the high flux HD [57, 116].

In another clinical study performed on 20 subjects, removal outcomes of HDF and low flux HD were compared for asymmetric dimethylarginine (ADMA), which is one of the guanidino compounds. There was no benefit from HDF over HD in lowering the ADMA concentration; rather, authors found that low-flux HD was superior in increasing the L-arginine/ADMA ratio [117]. The reason for insignificant ADMA removal was associated with protein binding of ADMA. However, it is noted that ADMA is a metabolic by-product of protein modification process in human cells, thus it may also be chiefly intra-cellular, and so HDF will be inefficient for its removal. This further strengthens the conclusion of Ward *et al*. that inter-compartmental resistance is the major barrier for toxin removal [74].

Recent Turkish online-HDF study [110] comparing high-flux HD and HDF observed decreased incidence of cardiovascular mortality in patients with high amount of replacement fluid. Nevertheless, the positive outcomes cannot be associated with increased toxin removal in HDF because authors could not find statistically significant difference in pre-dialysis serum concentration of urea, creatinine, phosphate, and β_2M after two years [110]. The superiority of HDF over conventional high-flux HD in long term clinical trials is still debated [114], and this thesis does not intend to delve on this debate. Rather, the intention here is to see – how we can further improve the toxin removal performance of CHD or HDF by overcoming the physiological barrier. Exercise during dialysis has been found to improve the toxin removal, although acceptance of exercise intervention in clinical setting is poor.

4.2 Exercise during Dialysis

Intra-dialytic exercise was first studied by Painter *et al*. in prospective clinical trials for routine outpatient HD patients [118]. Since then, exercise has been proposed as adjunctive intervention for maintenance HD patients. It is known that exercise increases the cardiac output (CO). The major portion of this increased CO is rendered to LFR, where majority of toxins reside. Based on the model simulations (presented in Chapter 3), it is hypothesized that exercise decreases the inter-compartmental resistance, which is often termed as major resistance for toxin removal [74]. The decrease in inter-compartmental resistance is anticipated due to increased capillary surface area and increased membrane pore size. Hence, both increased CO and decreased inter-compartmental resistance supposedly lead to enhanced toxin removal. This is evident from a number of clinical trials where intra-dialytic exercise has shown its potential for removal of uremic toxins. In the study of Parson *et al*., a consistent decrease in pre-dialysis serum creatinine concentration was observed; this is equivalent to increased creatinine removal [98]. In the study of Kong *et al*., both urea and creatinine % rebound (equation 3.24) decreased by statistically significant amounts [100]. Vaithilingam *et al*. oberserved increased phosphate removal due to intra-dialytic exercise [99]. Few other studies have also discussed the benefits of exercise for toxin removal [119, 120]. Exercise not only improves toxin removal but also provides numerous other benefits such as improved physical functioning [98, 121], decreased heart disease risk factors [122], decreased use of antihypertensive medicines [123], and most importantly, improved quality of life such as improved cognitive function, decreased stress levels, etc. [121].

Despite the documented benefits, nephrologists as well as patients are not enthusiastic to accommodate exercise in routine dialysis care, and exercise is still considered as intervention rather than as part of routine care. Intra-dialytic exercise sustainability in

routine HD setting is poor [124]. It will not be a mistake to say that exercise is one of the most underrated clinical interventions in HD care. One reason behind this could be the requirement of individualized prescription for intra-dialytic exercise [124]. Before we aim for individualized prescription, it is important to understand what physiological changes are responsible for enhanced toxin removal. In addition to increased CO and decreased peripheral vascular resistance, exercise induced physiological changes may also occur due to increased body core temperature. This is discussed in the following section.

4.2.1 Exercise and Temperature

It is hypothesized that exercise will increase the body core temperature which will further dilate the blood vessels or vasculature, i.e. decrease the inter-compartmental resistance. This hypothesis is based on results from another clinical research which studied the effect of dialysate temperature on urea removal and patient hemodynamic stability [125]. Dialysate temperature plays an important role in patient hemodynamic stability and conventional dialysate temperature is set at 36°C or 36.5°C, while body core temperature is presumably 37°C. In the study of Kaufmann *et al*. comprising 15 HD subjects, effect of cool dialysate (35.5°C) and thermo-neutral dialysate (37°C) was studied. It was noted that cooled dialysate decreased the body core temperature by 0.22 ± 0.04 °C, while thermo-neutral dialysate increased it by 0.31 ± 0.05 °C. The increase in body core temperature in thermo-neutral dialysate was associated with inflammatory response. The cool dialysate provided better hemodynamic stability. Nevertheless, cooling also resulted in ~400% increase in peripheral vascular resistance index, when compared with thermo-neutral dialysate. Interestingly, increased peripheral vascular resistance index did not affect the urea removal and % rebound was similar in both cool and thermo-neutral dialysate [125].

Peripheral vascular resistance index, also known as systemic vascular resistance index, can be considered as surrogate of inter-compartmental resistance. Increased peripheral vascular resistance index could not affect the urea removal, because urea is small in size and its kinetics is primarily flow controlled (Sub-section 2.3.4) [84]. Also, rapid equilibration of urea across the cell membrane is essentially due to facilitated transport by selective urea transporters [126]. This suggests that, even with vasoconstriction, urea can easily pass through the cellular membrane and its removal is not affected. However, the conclusion should not be extrapolated to other uremic toxins, and their removal may be compromised in cool dialysate.

It is known that exercise increases the body core temperature due to increased oxygen uptake and increased metabolism in cells [127]. To decrease the body core temperature or to remove the accumulated heat, the blood flow to skin increases, and the person sweats. In the context of HD subjects under intra-dialytic exercise, this increased blood flow will mobilize toxins from remote compartments. However, there is no clinical study to investigate the effect of intra-dialytic exercise on body core temperature. It is hypothesized that exercise will increase the body core temperature, which will decrease the inter-compartmental resistance and result in increased toxin removal. To study change in peripheral vascular resistance index, patients were subjected to echocardiogram during the exercise session.

4.3 Clinical Trial Design

Following the preceding discussion, the proposed clinical trial was aimed to investigate the exercise induced physiological changes. The inter-compartmental resistance cannot be measured, and so change in peripheral resistance index is used as surrogate. The resistance index is measured via echocardiogram, also referred as Doppler ultrasound,

which is a non-invasive way to quantify the physiological changes (see Sub-section 4.3.4). The specific aims of study are:

1. Investigate the effect of intra-dialytic exercise on physiological changes, namely, decrease in inter-compartmental resistance, increase in CO, and increase in body core temperature due to exercise. The decrease in inter-compartmental clearance will be assessed by decrease in peripheral vascular resistance index.
2. Investigate the effect of intra-dialytic exercise on removal of middle molecule marker toxin, β_2-micorglobulin and compare the same with CHD and HDF. This is the first study to investigate the effect of exercise on β_2-micorglobulin removal. The toxin removal outcome will be assessed by 2 hour post-dialysis % rebound. The rebound % will also be compared for conventional toxins: urea, creatinine, and phosphate.

4.3.1 Study Design and Ethics Approval

This study was single center, open label, self-controlled (within subject design), randomized prospective, efficacy study involving patients undergoing conventional high-flux HD. Blinding is an important aspect for randomized study; this helps in preventing the investigator and subject bias. However, blinding was not feasible because the changes in conventional HD are immediately visible to both study subjects and investigators.

The domain specific review board affiliated with the National Healthcare Group (NHG), Singapore has approved the trial. The study has undergone routine quality assurance review conducted by the ethics board. The ethics board also received timely progress status report and promptly informed of any adverse events owing to the intervention during the course of the study. The study was conducted at outpatient dialysis center of

the National University Hospital (NUH), Singapore. The study is registered in ClinicalTrials.gov with trial registration NCT01674153.

4.3.2 Patient Recruitment and Inclusion-Exclusion Criteria

Patient safety is the uppermost in any clinical research. The inclusion-exclusion criteria ensure the uniformity of recruited subjects and minimize the occurrence of any adverse event during the conduct of clinical research. Before contacting the patients, existing patients' database was reviewed for a number of conditions such as hemoglobin level and ejection fraction on prior test results, existing chronic obstructive pulmonary disease (COPD), angina, and history of heart-attack. All the study subjects have negligible residual renal function (defined by urine output < 200 mL/day). Potential subjects satisfying the above mentioned criteria were identified and subsequently contacted for preliminary tests where patients were explained about the study protocol, effectiveness of HDF, and intra-dialytic exercise. Agreed patients satisfying the inclusion-exclusion criteria signed the patient information sheet and consent form. A copy of signed form was given to the patients. Total of 15 subjects consented for the study. All study procedures followed the declaration of Helsinki and adhered to Good Clinical Practices (GCP) guidelines. Below is the list of all inclusion-exclusion criteria pre-defined in the research.

Inclusion Criteria:

1. Adult patients male or female (Age > 21 years)
2. Minimum dialysis vintage of 2 months
3. Stable on hemodialysis
4. Minimum Hemoglobin level of 10 g/dL
5. Blood access capable of delivering the blood flow rate greater than 250 mL/min
6. Preserved left ventricular ejection fraction (> 50%) on prior imaging study

7. Desirable performance in 6-min walk test (6 MWT)

Exclusion Criteria:

1. History of recurring or persistent hypotension in the past 2 months
2. Pregnant woman
3. Severely Hypertensive patients (systolic blood pressure > 180 mmHg and/or diastolic blood pressure > 115 mmHg)
4. History of recent myocardial infarction or unstable angina (within the past 6 months)
5. Significant valvular disease, i.e. severe aortic stenosis and moderate-severe mitral regurgitation.
6. Patients with end stage organ disease e.g. COPD, recent or debilitating cerebrovascular accident (CVA)
7. Patient with recent stroke (within the past 6 months)
8. Anemic patients
9. History of known arrhythmia
10. Participation in another clinical intervention trial
11. Moderate to severe osteoarthritis of knee(s)
12. Unable to consent

The consented subjects were called for 6 MWT, which was performed according to the standard guidelines prescribed by American Thoracic Society [128]. This test has been considered as appropriate sub-maximum test to assess patient's functional and physiological response, cardiovascular fitness, and suitability for intra-dialytic exercise in ESRD population [129]. Patients walked along a measured circuit (30 m), instructed to cover as much distance as they can within 6 min. Patients were not allowed to run. Blood

pressure (BP), heart rate (HR) and rate of perceived exertion (RPE) were assessed at pre- and post- 6 MWT. HR and RPE were measured at every minute of the test, as well as at 8 and 10 min to assess heart rate recovery (HRR) and blood pressure. Patients who ambulated less than 300 m over 6 min were excluded from the test due to the likelihood that they may not tolerate the exercise protocol (described in Sub-section 4.3.4). Patients were also supposed to demonstrate acceptable physiological response during the test, e.g. HRR, hemodynamic parameters within safe guidelines for exercise. The 6 MWT was conducted by a trained physiotherapist.

4.3.3 Study Interventions

All recruited study subjects underwent three different study dialysis sessions, namely, HD, HDF, and HD with intra-dialytic exercise (HD-Ex) within a maximum time interval of 6 months between the first and last study session. Minimum one week gap was maintained between study sessions for each individual patient. The one-week gap should remove any carry-over effect of previous study session and bring the patients to their nominal toxin concentration level. High-flux HD was conducted as per the patient routine dialysis session; HDF was conducted with 18 L of target replacement fluid. Patients' medications such as phosphate binder, medication for hypertension, erythropoietin dose, etc. were not changed during the study period. Patients were also advised to keep their diet fairly constant during the study period. The study sessions were conducted in mid-week or end-week setting; however, study sessions for an individual subject were on the same day of the week. To avoid the effect of confounding factors, same dialysis conditions were used in all study dialysis sessions.

The intra-dialytic exercise was conducted in conventional high-flux HD setting with exercise prescription in three bouts. The first exercise bout started from 40–60 min,

second from 80–100 min, and third from 120–140 min. If patients were unable to adhere to the prescribed exercise intervention, then they were advised to perform a total of 60 min exercise during the dialysis. The exercise was sustained till the achievement of 70% of maximum heart rate, and given via active cycling movement (ACM) using calibrated Monark 881E cycle ergometer (Monark, Sweden). The maximum heart rate is calculated by subtracting patient age from 220. Various hemodynamic responses, namely, heart rate, blood pressure, arterial and venous blood temperature were measured during all study sessions. Additional hemodynamic responses, namely, CO and peripheral vascular resistance index, were also assessed by measuring left ventricular stroke volume using Doppler echocardiography. The echocardiogram images were taken just before starting of HD-Ex session, before starting first bout of exercise, at 5-minute intervals during exercise, and after termination of first exercise bout. But they were not taken during the second and third bouts of exercise because similar cardiac responses were anticipated. Systemic vascular resistance and parameters of ventricular-arterial coupling were derived to determine the stroke volume response to exercise. The echocardiography was also used to assess cardiac structure and function before and during exercise – any new or unexpected abnormality, e.g. regional dysfunction. Any abnormality was recorded and best possible clinical judgment was taken to ensure patient safety. If during exercise, patient's systolic blood pressure exceeds beyond 180 mm Hg, the patient was asked to stop exercise till the pressure attains the safe level of below 180 mm Hg.

4.3.4 Data collection

Blood sampling:

Three arterial blood samples, namely, pre-dialysis (t = 0 min), end-dialysis (t = 240 min), and post-rebound (t = 360 min) were collected in each study session. Each blood sample

was analyzed for uremic toxins, namely, urea, creatinine, phosphate, and β_2M. The volume of each collected blood sample was ~4 mL. All the blood samples were sent to NUH clinical laboratory immediately after collection. These toxins/solutes concentrations were used for calculating the post-dialytic % rebound for each toxin. Conventionally, the blood samples are collected in tubes containing EDTA, which is a strong anticoagulant [74]. The anticoagulant prevents the blood clotting. This practice can plausibly equilibrate the toxin concentration between blood cells and plasma. However, as discussed earlier (Figure 3.5), dialysis process results in the concentration gradient between inaccessible cellular/interstitial compartments and accessible blood compartment. To prevent the concentration equilibration, all blood samples were collected in serum separator tubes (SST II), also referred as gold cap tubes. These tubes are coated with clot activator which expedites the blood clotting. The faster blood clotting prevents the equilibration of toxin among blood plasma and blood cells. The gel inside SST II tubes separates the blood plasma and blood cells, so that plasma extraction after centrifugation becomes relatively easier.

Blood temperature monitoring:

Arterial and venous blood temperature was continuously monitored using blood temperature monitor, abbreviated as BTM (Fresenius, Bad Homburg, Germany). As discussed earlier, intra-dialytic exercise will increase the body core temperature (Sub-section 4.2.1). The dialysate temperature directly affects the blood temperature; hence, it was kept same for all three study sessions for each individual patient. The dialysate temperature was measured during HD-Ex session alone. During standard HD or HDF, the blood temperature change is insignificant (Figure 4.3); hence, during these sessions, blood temperature was not measured. The schematic flow chart of clinical trials is

presented in Figure 4.4. To maintain patient confidentiality, all the collected samples and data were assigned a unique study number.

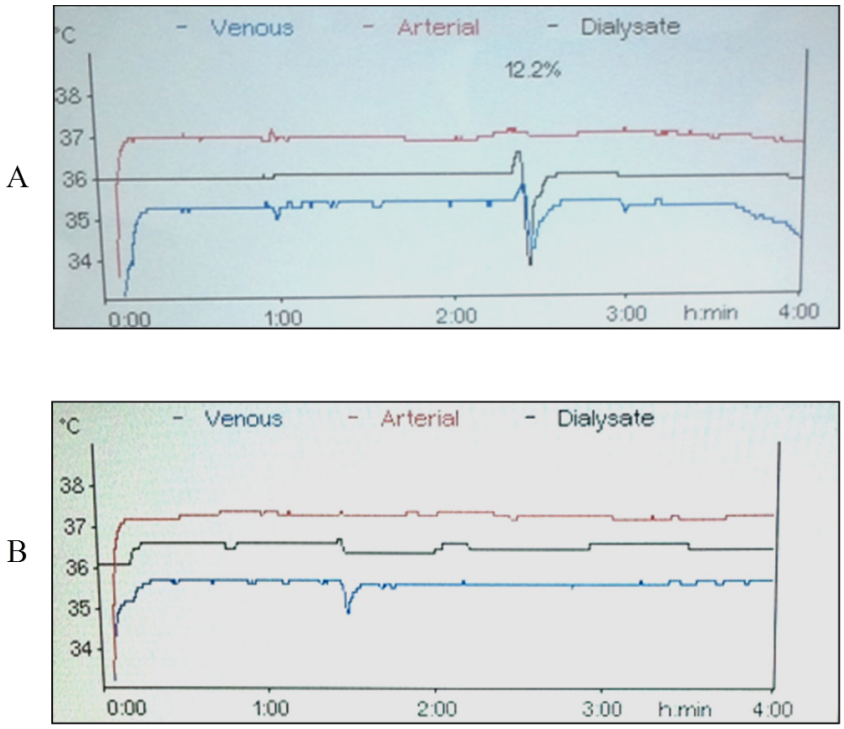

Figure 4.3 Blood temperature snapshot during HD session for two sample patients. In panel A, the kink in dialysate and venous temperatures is due to the measurement of access recirculation.

4.4 Patient and Dialysis Information

A total of 15 patients consented to participate in the study. Two patients could not fulfill the inclusion-exclusion criteria. Information pertaining to individual subjects who underwent the study intervention is provided in Table 4.1. Among 13 patients, one patient was prohibited to continue on HD-Ex session owing to poor baseline ejection fraction (25%); according to the inclusion-exclusion criteria, the baseline ejection fraction should be at least 50%. To prevent any adverse event, this particular patient was not allowed to undergo HD-Ex session. Hence, a total 38 study sessions were performed. Among the 12 patients who completed all 3 study sessions, echocardiogram could not be performed for one subject. Nevertheless, exercise intervention was followed as per the protocol

discussed in Sub-section 4.3.3 and blood samples were collected as per the protocol discussed in Sub-section 4.3.4.

Table 4.1: Patient demographics at the time of consent

Patient ID	Gender	Age	Hemoglobin (mg/dL)	Ejection fraction (on prior imaging)	Distance covered in 6 MWT (m)
P1	M	51	11.6	74	470
P2	M	66.5	13.9	75	460
P3	F	42	10.1	67	360
P4	M	55	12.7	56	423
P5	M	56	12.7	61	510
P6	F	63	12.6	72	368
P7	M	52	12	56	405
P8	F	40.5	11.6	58	425
P9	F	42	12.7	54	375
P10	F	55	11.5	55	397
P11	M	56	11.2	61	430
P12	F	54	11.4	55	570
P13	M	23	11.6	72	576
Mean ± std		**50.5 ± 11.3**	**12 ± 0.95**	**63 ± 8 %**	**444 ± 71**

All HD and HD-Ex sessions were conducted on Fresenius 4008S, and HDF sessions were performed on Gambro AK200. The dialyzer was same in all study sessions for an individual patient. All dialysis related parameters such as dialysate temperature, dialysate composition, were kept same in the study sessions of an individual patient to minimize the confounding factors. However, the ultrafiltration or fluid removal rate during each study session was calculated based on inter-dialytic weight gain, and was different for different sessions. It is assumed that excess fluid removal via ultrafiltration will insignificantly contribute towards toxin removal. The mean convective fluid volume in HDF was 21.2 ± 3.7 L, with minimum and maximum at 15.8 and 29.1 L, respectively.

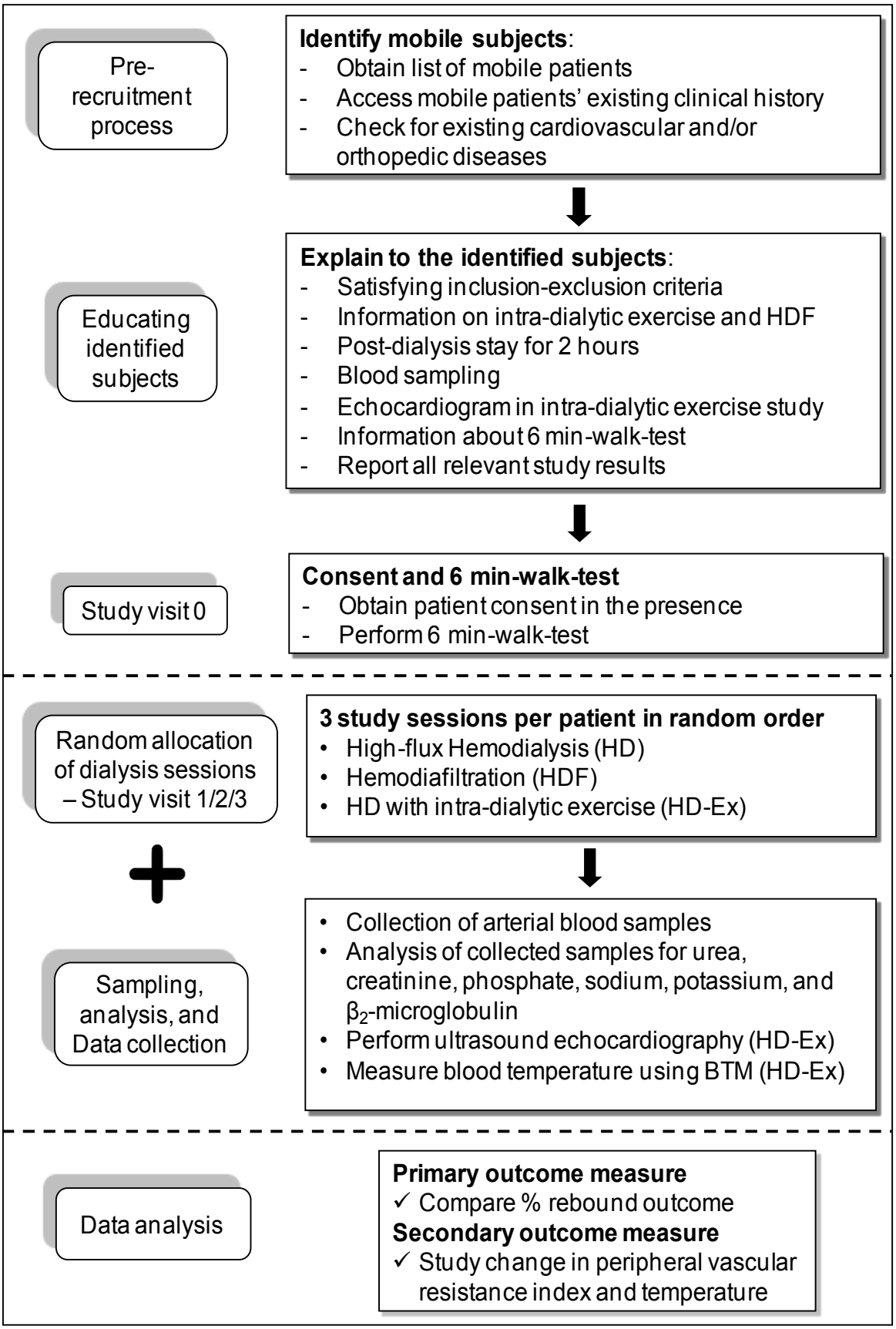

Figure 4.4: Schematic flow-chart of clinical trial

4.5 Results from the Clinical Study

The toxin removal is adjudged by % rebound calculation. The mean % rebound in HD, HDF, and HD-Ex for uremic toxins: urea, creatinine, phosphate, and β_2M are presented in Table 4.2. The rebound was calculated using pre-dialysis (t = 0 min), end-dialysis (t = 240 min), and post-rebound (t = 360 min) plasma toxin concentration (equation 3.24).

Table 4.2: Percentage rebound for each uremic toxin in different dialysis protocols

Dialysis Protocol	Urea	Creatinine	Phosphate	β_2-microglobulin
HD	13.4 ± 3.3	22.7 ± 4.2	37 ± 8.1	29.1 ± 14.5
HDF	14.4 ± 5.4	22.8 ± 4.5	23.5 ± 16.5	24.5 ± 3.0
HD-Ex	13.5 ± 4.0	22.0 ± 3.6	52.1 ± 21.6	27.4 ± 5.9

In Table 4.2, the mean % rebound results for HD corresponds to 12 patients. For one patient, the post-rebound sample was corrupted due to dilution while sampling blood. For HDF, phosphate rebound for one patient was negative because the post-dialysis phosphate concentration was lower than the end-dialysis concentration, which seems unrealistic. This was considered as wrong phosphate concentration measurement; thus the phosphate % rebound calculation in HDF is from 12 patients. Similarly, the % rebound presented for HD-Ex is based on 12 patients, as one patient was not allowed to continue with the exercise due to poor baseline ejection fraction.

The blood temperature profiles during HD-Ex session are presented in Figure 4.5, where three peaks in arterial blood temperature can be observed. These three peaks correspond to three bouts of exercise. On the other hand, insignificant changes are seen in venous temperature. Small variations in venous temperature can be attributed to fluctuations in dialysate temperature. Notably for P6, the arterial temperature does not reflect in exact

three peaks, rather four small peaks can be observed. This is because patient completed the prescribed exercise protocol in four bouts. The venous temperature for the same patient P6 is also perturbed due to unexpected change in dialysate temperature. The difference between maximum and minimum arterial temperature was 0.96 ± 0.23 °C. The variation denotes the inter-patient variability, i.e. each patient hemodynamic response is different to exercise intervention. Also the intensity of exercise was not controlled, and patients exercised at their comfort levels.

The results for change in cardiac output and peripheral vascular resistance index for individual patients are presented in Figure 4.6. Although patients started the exercise bout at different times (Figure 4.5), it is assumed that all patients started their first exercise bout at 40 min during dialysis. This assumption is made to standardize the change in CO and resistance index for all patients. The mean increase in CO is 4.34 ± 1 L/min, while mean decrease in resistance index is 874 ± 272 dyn.s/cm^5. The mean maximum-percentage increase in CO is 106 ± 32%, with maximum and minimum increment being 147% and 61%, respectively. Similarly, the mean maximum-percentage decrease in resistance index is 94 ± 45%, with maximum and minimum reduction being 186% and 42%, respectively.

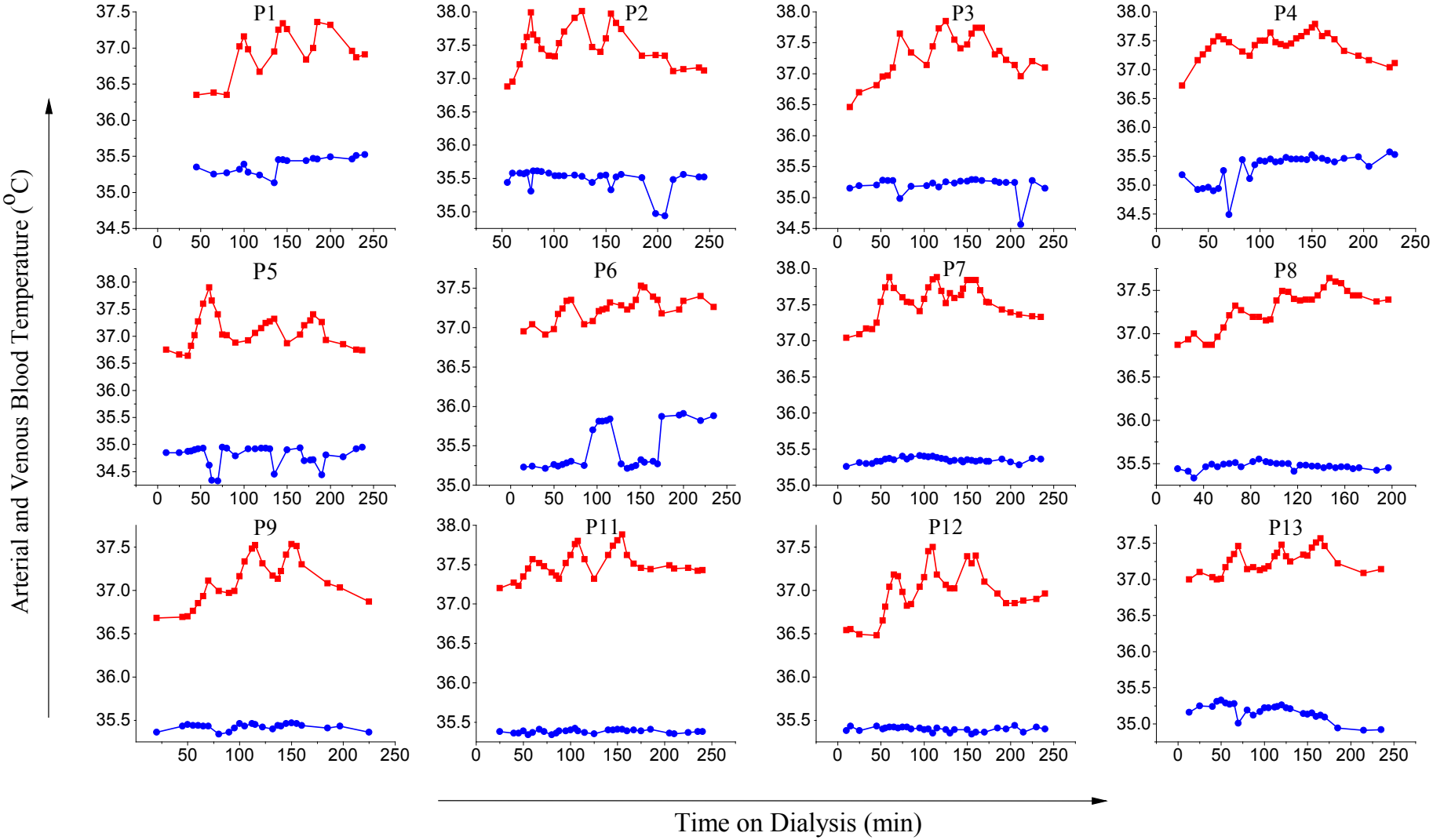

Figure 4.5: Arterial (red -■-) and Venous (blue -●-) blood temperature during HD-Ex session

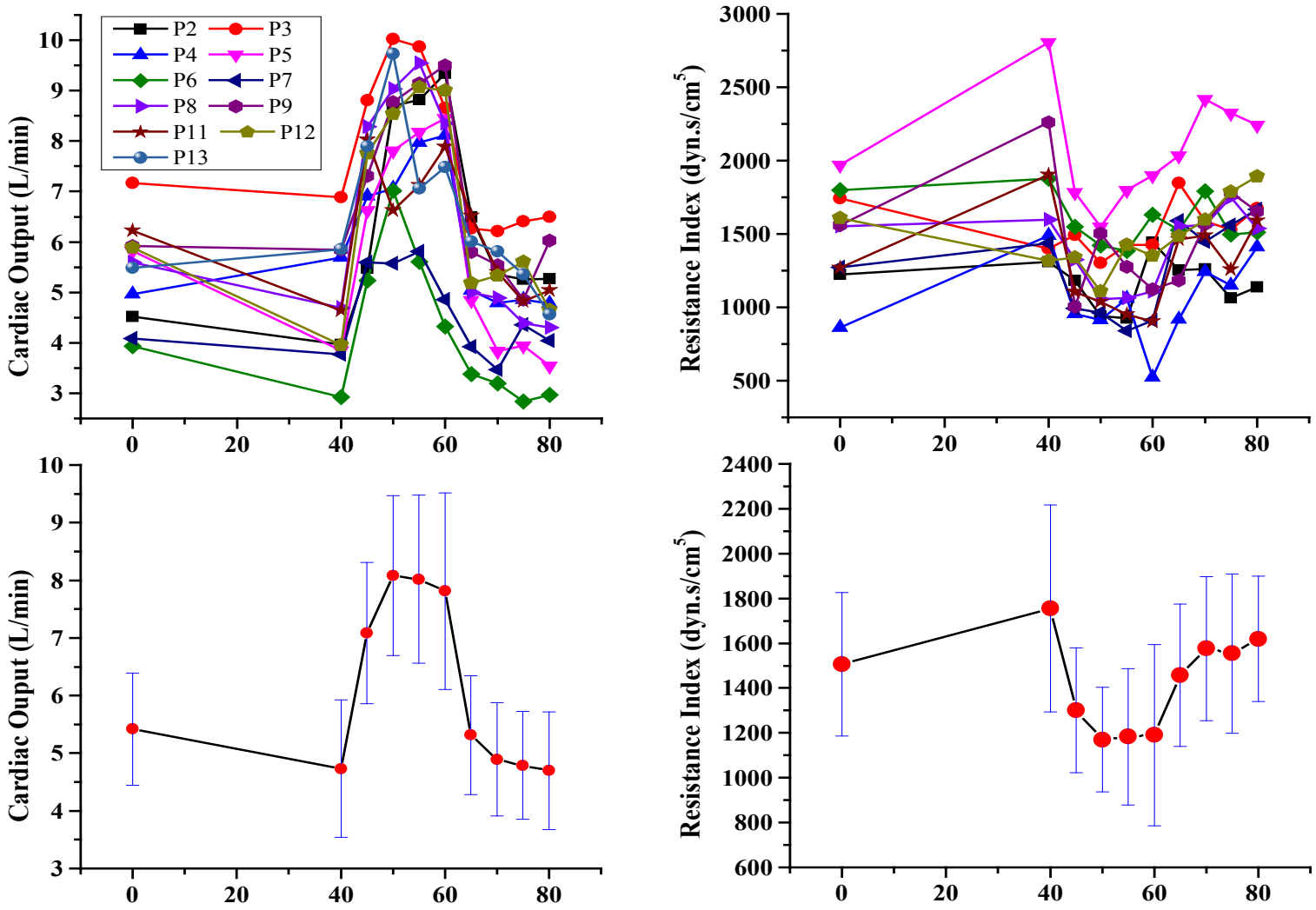

Figure 4.6: Patients' cardiac output and peripheral vascular resistance index during the first bout of exercise. In bottom panel, cardiac output and resistance index are presented as mean ± standard deviation.

4.6 Discussion

In this study, the toxin removal is adjudged by % rebound after dialysis. Comparison of % rebound in different dialysis protocols will prove the efficacy of one over another. It should be noted that magnitude of % rebound and time required for equilibration in body compartments can be different for different toxins, e.g. % rebound of large-sized toxins can be more pronounced due to slower diffusion of large-sized molecules. In this clinical study, it was assumed that toxins will equilibrate within two hours post-dialysis and rebound will recede thereafter. Comparing the urea rebound values in Table 4.2, it can be observed that mean % rebound is comparable among HD, HDF, and HD-Ex, except HDF results in slightly larger mean % rebound. These results suggest that urea removal is primarily controlled by diffusion and is not affected by convection, which is the augmented characteristic of HDF. The reason for slightly larger % urea rebound in HDF is unknown, but may be ascribed to interference between diffusion and convection [130]. Toxin removal via convection is dependent on fluid transport from blood to dialysate steam, i.e., it is independent of concentration gradient. Increased removal of fluid in HDF will plausibly move more urea into dialysate stream and decrease the urea concentration difference between blood and dialysate stream, and thus hamper the diffusive urea transport. The assumption in this argument is that there is sufficient amount of toxin in blood plasma compartment and there is no or insignificant resistance between physiological compartments. Urea conforms to this assumption because urea is small in size and inter-compartmental urea transport is boosted by urea transporters in cellular wall. For other small as well as large-sized uremic toxins, no such specific transporters exist on the cellular wall, and their removal is restricted by inter-compartmental resistance. This is evident from % rebound results for creatinine. The mean % rebound of creatinine is almost the same for both HD (22.7 %) and HDF (22.8 %), but is slightly

lower for HD-Ex (22.0 %). The similar creatinine rebound from HD and HDF points out to the similar contribution of diffusion and convection towards creatinine removal from blood to dialysate stream. However, physiological resistance still plays the dominant role, which is reduced by exercise. The slight drop in creatinine rebound in HD-Ex can be associated with increased blood flow to remote peripheral compartments during exercise and decreased peripheral resistance, quantified by resistance index (Figure 4.6).

The mean % rebound for β_2M is lowest in HDF (24.5 %), which suggest that removal of large-sized toxins is significantly contributed by convection. At the same time, the mean % rebound of β_2M in HD-Ex was 27.4 % which is lower than that obtained in HD (29.1%). This indicates that, even without convection (i.e., with diffusion alone), the % rebound can be reduced (i.e. toxin removal can be increased). These results suggests that exercise can not only augment the removal of small-sized toxins [120], but also has potential to increase the removal of large-sized uremic toxins. Comparing the toxin removal outcomes for urea, creatinine, and β_2M, it can be inferred that urea removal in dialyzer is influenced by diffusion alone, creatinine removal is influenced by both diffusion and convection, and β_2M removal is primarily influenced by convection.

Interestingly, the mean % rebound for phosphate is significantly pronounced in HD-Ex (52.1%) than that obtained in HD (37%) and HDF (23.5%). Vaithilingam *et al*. have found that intra-dialytic exercise increases the phosphate removal [99]. The unexpected high phosphate rebound in the present clinical study can only be explained by significantly delayed mobilization of phosphate from bones or remote intracellular compartments, which manifests much after completion of dialysis. It is important to note that in this study, the first exercise bout was implemented on or after 40 min from the start of dialysis, but in the study of Vaithilingam *et al*. the exercise intervention was before and/or during early phase of dialysis [99]. This suggests that exercise does increase

the phosphate removal, but delayed mobilization can be the root cause of pronounced rebound in this study. In other words, the post-dialytic wait of 2 hours is too small for complete equilibration of phosphate, i.e. the rebound of phosphate may be delayed by as much as 4 hours. In summary, to improve the phosphate removal, immediate pre-dialysis exercise intervention may be more helpful than the intra-dialytic exercise intervention. The important question then is whether this is true for all uremic toxins or only for phosphate whose kinetics is most complex among all studied uremic toxins [56, 69]?

At the same time, the % rebound for phosphate is lowest in HDF, but prolonged HDF interventions could not decrease the pre-dialysis phosphate concentration than that obtained in high-flux HD [110]. If HDF reduces the phosphate rebound to such great extent as observed in this pilot study then why it does not reflect in reduced pre-dialysis serum phosphate concentration? This can be attributed to the fact that the efficacy of HDF is primarily restricted to blood compartment only [74]. During 4h dialysis, the HDF will plausibly decrease the plasma phosphate concentration to very low levels. Post-dialysis, the phosphate rebound does occur but the 2h rebound period may be too small to see the significant phosphate rebound. To further strengthen the above mentioned claims, more clinical studies should be designed where patients should be asked to wait for 4h post-dialysis. However, this is difficult and inconvenient for many patients. The other method to adjudge the superiority of one dialysis protocol over another will be to collect the whole spent dialysis and analyze a representative sample for removal of total toxin mass.

Blood Temperature and Hemodynamic Response

This is the first clinical study to investigate the effect of exercise on body core temperature. As hypothesized, the intra-dialytic exercise results in increase in body core temperature which was inferred from measured arterial blood temperature. In Figure 4.5, three distinct peaks can be observed which correspond to three successive bouts of

exercise. Although all recruited patients were unconditioned to exercise, all of them were able to complete the 60 min exercise intervention without any adverse event requiring clinical intervention. The key reason for this is that the exercise protocol was performed at zero resistance, which was easily tolerated by this cohort of patients. The venous temperature is almost constant throughout the dialysis sessions (Figure 4.5), because inlet (arterial) blood comes in contact with dialysate which is at constant temperature. Within the length of dialyzer module, the heat transfer from inlet blood to dialysate stream will bring the outlet (venous) blood to the dialysate temperature. However, the venous blood temperature is always lower than the dialysate temperature. This is because, after exiting from the dialyzer, the venous blood circuit comes in contact with environmental temperature, which is much lower than the dialysate temperature. This environmental heat loss plausibly decreases the venous blood temperature below dialysate temperature.

During HD-Ex session, patient's cardiac output was also measured during the first bout of exercise using Doppler echocardiogram. As expected, the patient's CO peaks during exercise intervention (Figure 4.6). At the same time, the vascular resistance index reached the nadir during exercise. The decrease in peripheral resistance index can be attributed to increased CO as well as increased blood core temperature, which results in increased blood flow to remote compartments so that the excess heat can be removed via skin. It remains unclear that between CO and temperature which one is the dominant factor for decreasing the peripheral resistance. Nevertheless, without delving into the contribution from individual factors, it is ascertained that exercise increases the body core temperature (besides cardiac output) and decreases the inter-compartmental resistance which eventually results in enhanced toxin removal.

Notably, the baseline (t = 0) CO drops from 5.41 ± 0.97 L/min to 4.62 ± 1.19 L/min just before the start of exercise (t = 40 min), which is equivalent to ~15% decrease in CO.

This can be attributed to the reduced venous blood temperature, which is much lower than the arterial or systemic blood temperature (Figure 4.3). The systemic blood temperature decreases, when cooled venous blood mixes with the systemic circulation. To reconcile for this sudden decrease in blood temperature, the vasoconstriction occurs which reduces the blood flow to remote compartments or manifest in the form of decreased cardiac output. The vasoconstriction prevents the heat loss from skin or peripheral organs.

Although increased body core temperature may lead to incidence of intra-dialytic hypotension, increased core temperature induces the blood flow to remote peripheral compartments so that the body core temperature can be reduced. In the process, the central blood volume decreases which can potentially result in IDH episode. The same principle is used to achieve the hemodynamic stability via cool dialysate. Nevertheless, in the present clinical tests, no episode of IDH requiring clinical intervention was experienced. This can be credited to the inclusion-exclusion criteria which prevented the IDH prone patients to participate in the clinical study. The IDH prone patients were prevented to participate because the objective here was to compare the physiological changes and toxin removal, rather than to test the compliance of IDH prone patients on exercise intervention.

Is β_2-microglobulin an appropriate marker?

One should note that, among the four studied uremic toxins, % rebound is highest for phosphate. Although phosphate is much smaller in size than β_2M, its rebound is much more pronounced. This is because phosphate is distributed in both IC and EC, but β_2M is distributed in EC alone. Additionally, the phosphate mobilization can occur from pathologic stores of phosphate in bones. Following the model of Spalding *et al*. to explain phosphate kinetics [56], the phosphate mobilization need to overcome at least three

physiological resistances – the first resistance when phosphate mobilizes from bone matrix to cellular compartment, the second resistance by cellular membrane when phosphate mobilizes from IC to EC, and the third resistance by capillary endothelium when phosphate mobilizes from interstitial space to accessible blood compartment. On the other hand, β_2M, distributed in EC has to overcome only one resistance due to capillary endothelium. Multiple resistances delay the phosphate removal and eventually manifest in significantly high post-dialytic rebound. Although most uremic toxins do not behave like phosphate, these toxins are still distributed in both IC and EC, and experience at least two resistances by cellular membrane and by capillary endothelium. This questions the credibility of β_2M being designated as potential marker toxin instead of conventional marker urea. Urea cannot be the marker because its removal kinetics does not even coincide with other small-sized uremic toxins [67]. At the same time, caution should be exercised before β_2M is authoritatively accepted as the marker of toxin milieu. Historically, urea is considered as marker toxin because of its high plasma concentration and low cost of analysis, which seems to have played an important role in favoring urea as marker toxin [25]. Hence, not only the toxin distribution but also the cost of analysis should be considered while deciding a better representative of uremic toxins.

4.7 Summary

This is the first pilot clinical study to investigate the exercise induced physiological change(s) responsible for enhanced toxin removal. It is also perhaps the first one that compares the toxin removal outcome for both small and middle-sized toxins. The toxin removal outcomes are compared for HD, HDF, and HD-Ex. The urea rebound is higher in HDF, while creatinine rebound in HD-Ex is slightly lower than that obtained in HD or HDF. The β_2M rebound is lowest for HDF, but HD-Ex still results in lower rebound than HD. These results indicate that it is more important to focus on patient physiology i.e.

overcoming the inter-compartmental resistance rather than focusing on improvement of RRTs. The rebound for phosphate (true to its complex kinetics) was highest in HD-Ex, which is attributed to delayed mobilization of phosphate from remote bone matrix to blood compartment. Results demand for an optimal exercise intervention for enhancing the removal of phosphate as well as other uremic toxins. Note that the obtained results are based on single session study on patients unconditioned to exercise. With prolonged exercise intervention, it can be hypothesized that intra-dialytic exercise will culminate in improved physical function or improved performance towards exercise. Patients will be able to tolerate higher resistance exercise protocol which will further increase the toxin removal. Long term clinical studies comparing the toxin removal in HDF and HD-Ex are required to test the proposed hypotheses. With the obtained results, it can be proposed that exercise during HDF can improve the removal of both small and large uremic toxins.

The present clinical study also proves that exercise intervention not only increases the cardiac output but also increases the body core temperature which potentially decreases the vascular resistance. Note that the decrease in vascular resistance is only an indication towards reduced cellular resistance. It is impossible to measure the changes in inter-compartmental resistance. To quantify the decrease in compartmental resistance, previously discussed diffusion adjusted regional blood flow model (Chapter 3) can be employed. The increase in inter-compartmental clearance (K_{ip}, model parameter) can quantify the decrease in inter-compartmental resistance. This requires the precise estimation of K_{ip}, which requires appropriate experimental data. The next part of the thesis deals with experimental design aspects that lead to enhancing the precision of estimates model parameters.

Part 2

Model-based Design of Experiments

5. Multi-Objective Framework for Model-based Design of Experiment Techniques[§]

Conflict is the beginning of consciousness.

- Mary Esther Harding

In Part 1, a comprehensive toxin kinetic model for β_2-microglobulin was proposed. The model was subsequently employed to explain the effect of exercise and new hypotheses were proposed. To test the hypotheses, a pilot clinical study was carried out. The clinical study validated the hypotheses that exercise during dialysis increases the toxin removal by decreasing the inter-compartmental resistance. It also appears that decrease in inter-compartmental resistance is not only due to increased cardiac output which dilates the vasculature but also due to increased body core temperature which further dilates the vasculature. However, the clinical study did not quantify the decrease in inter-compartmental resistance. Quantifying the decrease in this resistance can provide a better understanding of exercise induced physiological changes and pave way for personalized prescription of intra-dialytic exercise. The model parameter K_{ip} that characterizes the inter-compartmental clearance can quantify the decrease in this compartmental resistance. To estimate K_{ip}, blood samples need to be collected. The important question addressed in Part 2 of this thesis is related to the timing of collection of those samples so that K_{ip} and other model parameters can be precisely estimated. Towards this end, model-based design of experiment (MBDOE) techniques can play an important role.

Before getting into the implementation details of MBDOE techniques for elucidating the optimal HD sampling protocol, the importance of experiments and MBDOE paradigm are

[§]The contents of this chapter have been published in: Vaibhav Maheshwari, Gade Pandu Rangaiah, Lakshminarayanan Samavedham, Multi-objective framework for model-based design of experiments to improve parameter precision and minimize parameter correlation, *Industrial and Engineering Chemistry Research,* 52, 8289-8304 (2013).

reviewed. It is observed that existing MBDOE techniques such as D-, A-, and E-optimal designs have inherent drawbacks, which can potentially lead to poor precision of model parameters and so defeats the objective of optimal experimental design. To overcome these drawbacks, a new strategy is proposed and evaluated on two case studies.

5.1 Mathematical Models and Experiment

Mathematical models for processes form the foundation for their performance improvement through optimization, control of product quality within pre-specified limits, developing soft sensors for predicting and monitoring "difficult to measure" states, *in silico* testing of new strategies, and/or for the development of new products/processes. Success of all these activities relies significantly on precise and accurate description of the system in the form of mathematical equations. Therefore, building a high-fidelity model is a crucial step before employing the model as a proxy to the real system.

Model building can be regarded as an iterative process: starting with the objective of model building, followed by *a priori* process knowledge in the form of physical, chemical, or biological laws governing the system, preliminary tests, and initial hypotheses; then a model structure in the form of algebraic equations (AEs), differential-algebraic equations (DAEs), or partial differential equations (PDEs), is decided. This will culminate in one or more model structures, which invariably contain adjustable model parameters. Selecting the most appropriate model out of all proposed models requires a maximally discriminating experiment; this aspect is studied under the category of experimental design for model discrimination. Once the appropriate model is selected, parameter estimation (also known as model calibration) is compulsory before using the model, because a mathematical model is only as good as its estimated parameters [131]. For estimating the model parameters, experiments need to be conducted. Experiments

require resources, time, and money. Hence it is imperative that intelligent experiments are designed for estimating the model parameters.

To obtain maximum information from limited resources, MBDOE techniques continues to play a pivotal role, and serve as a vital link between the modeling and experimental worlds. Informative data collected after such intelligent experiment(s) is used for model parameter estimation or for improving the precision of weakly known parameters. Subsequently, statistical validity of parameters must be checked, and if not satisfied, the DOE procedure is successively iterated. A schematic of the process of model development is shown in Figure 5.1, where two MBDOE perspectives, namely, design of experiments for model discrimination and design of experiments for precise parameter estimation are portrayed. In this work, the focus is on DOE for parameter estimation, and specifically on overcoming the drawbacks of traditional MBDOE techniques

Initially, MBDOE methodology was considered only for steady-state algebraic systems. Following this, researchers have successfully extended the concepts to dynamic systems, with applications in chemical kinetics [132], crystallization [133], systems biology [134-136], fermentation processes [137, 138], heat/mass transfer [139], etc. For more details and applications, readers are referred to the state-of-the-art review on MBDOE practices [140]. Along with these existing and emerging applications, research focus has been on improving the DOE methods by proposing new objectives [141] and new approaches [142].

All MBDOE problems culminate in an optimization problem; however, solving the optimization problems can be difficult in systems with significant parameter interactions. Often large correlation among model parameters is noticed, unless one resorts to properly designed experiments [140, 143, 144]. Reaction networks comprising sequential, parallel,

or consecutive steps are examples of kinetic models recognized as systems with highly correlated model parameters that pose challenges to successful experimental design and subsequent parameter identification [140, 145]. The objective of DOE techniques is to devise intelligent experiments such that the resulting experimental data can provide parameter estimates of improved statistical quality measured in terms of parameter precision and de-correlation [138, 146].

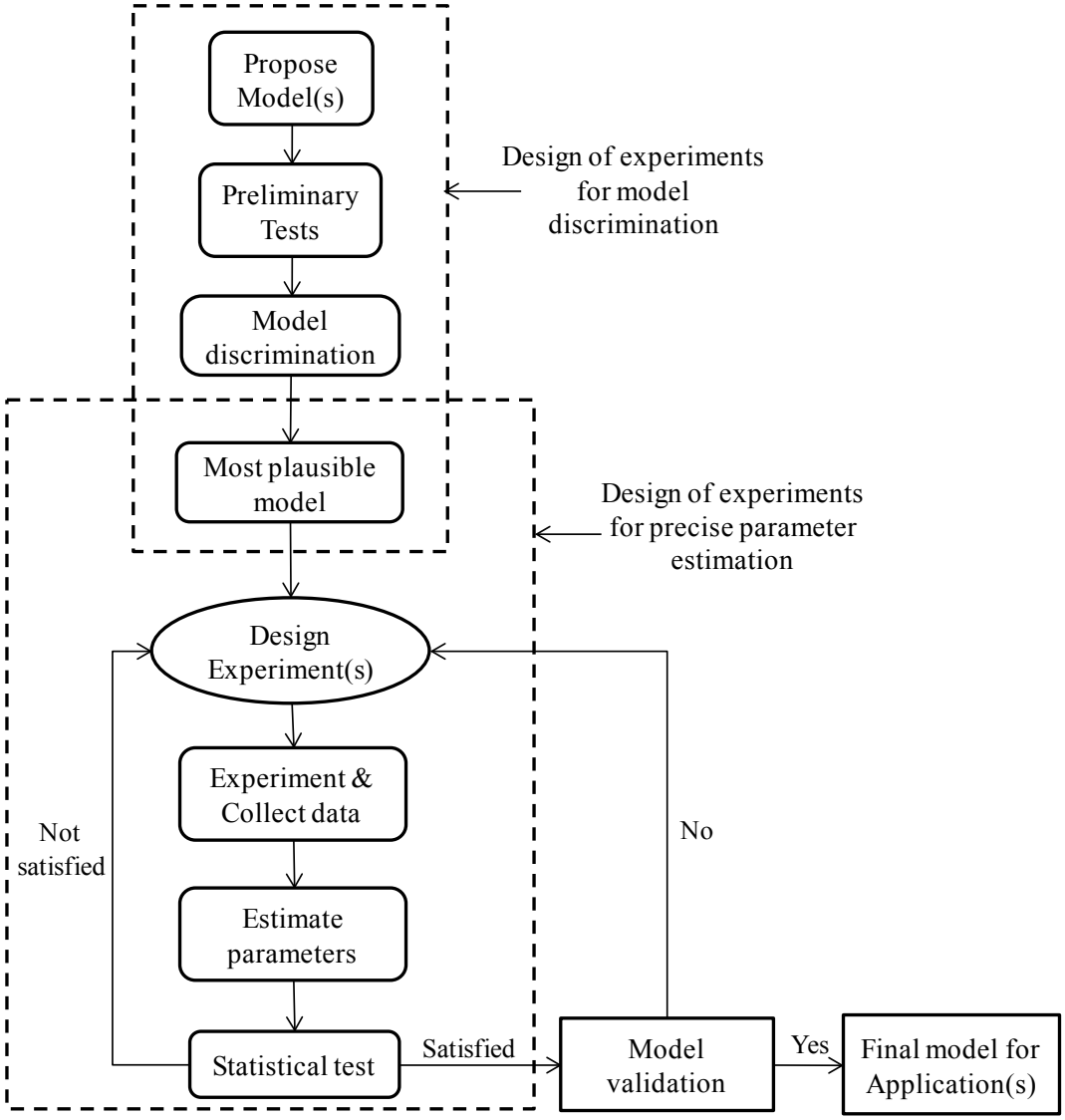

Figure 5.1: Schematic of model development following the principles of model-based design of experiments techniques

Existing MBDOE techniques that employ D-, A-, E-optimality criteria (discussed in Section 5.2) focus primarily on the first statistical quality i.e. improvement in parameter

precision, but overlook the parameter de-correlation. The increase in information content of the data often comes at the cost of increased correlation among parameters, which can lead to incorrect and imprecise point estimates of parameters; this violates the inherent objective of existing experiment design techniques [144, 147, 148]. To overcome the problem of correlated parameters, anti-correlation based formulations have been proposed and their successful applications have been reported [144, 149, 150].

This work here presents a distinct approach to overcome the correlation among parameters; essentially, we propose a multi-objective optimization (MOO) based DOE framework that considers two conflicting objectives: maximize the information measure and minimize the correlation among parameters. With this approach, a trade-off between conflicting objectives (in the form of Pareto-optimal front) is obtained; this can suggest the optimal experiment depending on the permissible trade-off. MOO based experimental design techniques have also been discussed earlier with the focus on reaping the benefit of multiple alphabetical designs, and overcoming their drawbacks [137, 146]. Here, we aim to overcome the drawback(s) of individual optimal experimental design technique by simultaneously de-correlating the parameters and maximizing the information for parameter estimation.

In the next section, a brief overview of various MBDOE techniques is presented. Subsequently, the correlation aspect among model parameters and the associated issues are also outlined in Section 5.3. The proposed MOO based formulations and the solution techniques employed are described in Sections 5.4 and 5.5, respectively. In Section 5.6, two case studies, namely, the modified Bergman Minimal model for Type 1 diabetes subjects and the Baker's yeast fermentation reactor model are employed to apply the proposed MOO based DOE techniques and to compare their performance against the

traditional alphabetical designs. The chapter ends with discussion and summary presented in Sections 5.7 and 5.8, respectively.

5.2 Mathematics of MBDOE

MBDOE techniques are formal and statistically well-founded procedures to select the best experimental settings corresponding to maximum information under pre-defined operational constraints. Their goal is to assist in rapid development, refinement, and statistical validation of process models. As the name suggests, a mathematical model structure with possibly imprecisely known parameters is an indispensable requirement of MBDOE techniques. In this work, a general deterministic, non-linear dynamic model, described by DAEs is considered. A DAE model can be described as follows:

$$\left.\begin{array}{c} \boldsymbol{f}\left(\dfrac{\boldsymbol{dx}(\mathrm{t})}{\boldsymbol{d}\mathrm{t}}, \boldsymbol{x}(\mathrm{t}), \boldsymbol{u}(\mathrm{t}), \theta, \mathrm{t}\right) = 0 \;;\; \boldsymbol{x}(\mathrm{t}_0) = \boldsymbol{x}(0) \\ \boldsymbol{y} = \boldsymbol{h}(\boldsymbol{x}(\mathrm{t})) \end{array}\right\} \tag{5.1}$$

In equation 5.1, $\boldsymbol{x}(\mathrm{t})$ is time-dependent state variables defining the system, $\dfrac{\boldsymbol{dx}(\mathrm{t})}{\boldsymbol{d}\mathrm{t}}$ is the time derivative of system states $\boldsymbol{x}(\mathrm{t})$, $\boldsymbol{u}(\mathrm{t})$ is the vector of time-varying control or manipulated variables in the process, θ is the *p*-dimensional vector of parameters to be estimated, $\boldsymbol{f}$ is the n_{eq}-dimensional set of DAEs, $\boldsymbol{y}$ is the vector of measured response variables that are function of state variables $\boldsymbol{x}(\mathrm{t})$, $\boldsymbol{h}(\boldsymbol{x}(\mathrm{t}))$ are the known functions that relates system states to the measured response variables. In most cases, $\boldsymbol{h}(\boldsymbol{x}(\mathrm{t}))$ is simply a selector function, i.e. some or all of the system states are measured. An experiment is defined by the vector of initial conditions $\boldsymbol{x}(\mathrm{t}_0) = \boldsymbol{x}(0)$, control moves and corresponding switch time for $\boldsymbol{u}(\mathrm{t})$, and sampling instances within the experiment duration.

At this stage, MBDOE techniques focus on identifying the experiment(s) which will result in maximally informative data for estimating unknown model parameters with high

degree of precision. Hence, before collecting the data, based on the current mathematical description of the process, *in silico* experiment(s) is/are designed, where the objective is to adjust the available manipulated inputs so as to minimize the effect of errors on estimated values of parameters, i.e. to make the output as 'sensitive' as possible to the parameters. Data collected from the implementation of such optimal experiment(s) is used for parameter estimation of process model under consideration. Factors such as the initial condition for various states in the process, the experiment duration, sampling instances, how and when the system should be perturbed, which manipulated variable(s) should be perturbed, the best sensor locations, etc. can be the decision variables that are decided based on the optimal solution of experimental design problem. All the decision variables are collected in a design vector $\boldsymbol{\phi}$, subjected to equality or inequality constraints defining the pre-specified operational restrictions in mathematical form. Each decision variable is bounded between the pre-set lower and upper bounds, constituting the design space ($\boldsymbol{\Phi}$). In addition to the operational constraints, an experiment may also involve system constraints which must be satisfied whilst designing the optimal experiment.

Characteristically, given the initial model structure and initial guess for its parameters, the aim of the classical DOE approaches is to minimize the parameter variance or minimize the parameter confidence interval i.e. to make the elements of parameter variance-covariance matrix small. A typical experiment design thus involves minimizing a metric of variance-covariance matrix ($\mathbf{V}$), or maximizing that of its inverse, the Fisher Information Matrix (FIM). Mathematically,

$$\Delta = min\, arg\left(\mathrm{V}\right) \equiv max\, arg\left(\mathrm{FIM}\right) \tag{5.2}$$

The FIM is ($p \times p$) symmetric matrix and is defined as,

$$\mathrm{FIM}(\hat{\theta}, \phi) = \sum_{i=1}^{n_y} \sum_{j=1}^{n_y} \sigma_{ij} G_i^{\mathrm{T}} G_j + \mathrm{FIM}_0 \tag{5.3}$$

where σ_{ij} is the $(i,j)^{th}$ element of inverse of variance-covariance matrix of experimental measurements, n_y is the number of measured states (outputs), FIM_0 is prior FIM from previous experiment(s), (used in sequential experiment design). $\mathbf{G_i}$ is s×p matrix of first order sensitivity coefficients at i^{th} measured state at n_{sp} sampling instances,

$$G_i = \left[\frac{\partial y_{is}}{\partial \theta_k} \right]; \; s = 1, 2, ..., n_{sp}; k = 1, 2, ..., p \tag{5.4}$$

Various real-valued functions are used to quantify the FIM or variance-covariance matrix into a scalar metric. All of them essentially focus on the eigenvalue(s) of FIM. The most common criteria include:

1. *D-optimality criterion* maximizes the determinant (product of eigenvalues) of FIM, or equivalently, minimizes the determinant of the variance-covariance matrix.
2. *A-optimality criterion* maximizes the trace (sum of eigenvalues) of FIM, or equivalently, minimizes the trace of variance-covariance matrix.
3. *E-optimality criterion* aims to maximize the smallest eigenvalue of FIM, or equivalently, minimizes the largest eigenvalue of variance-covariance matrix.

The geometrical interpretation of these criteria is provided in Figure 5.2. A distinct interpretation is that A- and D-optimal designs minimize the arithmetic and geometric mean of the identification errors, respectively, whereas the E-optimal design minimizes the largest error [146].

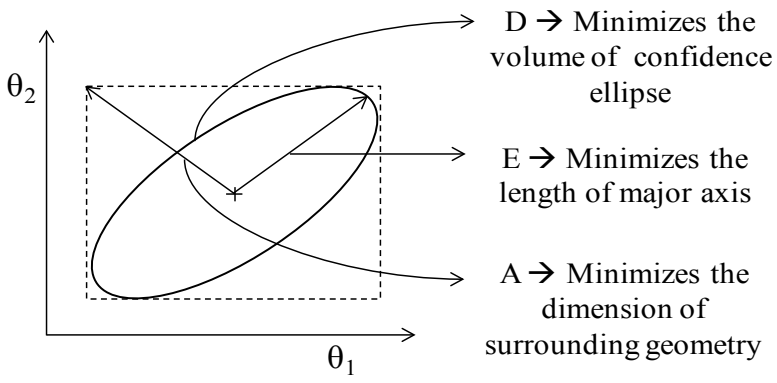

Figure 5.2: Geometrical interpretation of the D-, A-, and E-optimal design for two parameters

Though FIM based criteria are frequently discussed in the literature, their inherent limitations are also known. FIM is based on local first-order approximation, obtained from the Taylor series approximation of expectation function [140], and thus apply only approximately to non-linear systems and may not be applicable for highly non-linear systems [151]. Notwithstanding this, only the joint confidence region based on linear approximation of FIM is considered here, as is the common practice in MBDOE literature [135, 140, 141, 144]. Alternatively, other approaches like bootstrap, jackknife, or Monte Carlo simulations can be employed to characterize the uncertainty in estimated parameters, but with associated high computational costs [152].

5.3 Parameter correlation

As mentioned earlier, the purpose of MBDOE approaches is to devise the intelligent experiments such that the parameters estimates from the resulting experimental data are of improved statistical quality, measured in terms of precision and de-correlation of estimated parameters [139]. Traditional designs aim at maximizing the information content in experimental data, resulting in improved precision of parameter estimates, which is usually judged by a *t*-test [151]. However, the statistical quality of parameter estimates cannot be decided by precision measure alone; correlation among different model parameters should also be taken into consideration, as high parameter correlation

afflicts the inverse problem of parameter identification [140, 145]. Interestingly, the conventional objective of increasing the information measure alone inadvertently increases the parameter correlation [144, 147]. Correlation among parameters can potentially lead to convergence problems while estimating parameters [146]. Owing to the correlation, change in one parameter can be offset by the change in other(s), leading to the situation where various parameter combinations result in comparable values of the objective function [146, 152, 153]. This poses problems for optimization algorithms because no definite direction can be found in which the objective function value will improve, leading to premature convergence of the optimization algorithm [146]. This makes the unique identification of model parameters difficult, or even leads to inaccurate estimates of parameters [138]. Correlation can reduce parameter precision despite good experimental design and/or increased number of samples [147].

Correlation in parameters can manifest due to model structure (structural identifiability issue) and/or due to noisy/sparse experimental data (practical identifiability issue) [152]. A model is structurally identifiable when under the condition of noise-free infinite observations, one is able to uniquely identify the model parameters; otherwise, the model is structurally unidentifiable. Existing solutions to overcome the structural unidenfiability or structural correlation are model re-parameterization [147], parameter separation [154], or redefining the model structure. Structural identifiability of a model does not guarantee the unique identification of model parameters using real experimental data. The identifiability issue owing to experimental data is addressed under practical identifiability, which enables evaluation of the possibility of finding unique values of parameters from the available experimental data. Here, the application of MBDOE techniques can be very useful. Both identifiability aspects can be understood from the simple algebraic models (equation 5.5).

$$\begin{aligned} y_1 &= k_1 k_2 x \\ y_2 &= k_1 \left(1 - e^{-k_2 x}\right) \end{aligned} \tag{5.5}$$

In the first model, estimation of the parameter combination i.e. $k_1 k_2$ is possible from suitable experimental data, but individual estimation of k_1 and k_2 is impossible even with infinite samples. Hence, the model is structurally unidentifiable. On the other hand, in the second model, it seems that both the parameters can be estimated uniquely. However, for very small '$k_2 x$' values, $1 - e^{-k_2 x} \approx k_2 x$ and model 2 reduces to model 1, which we know to be structurally unidentifiable. Thus, to estimate both the parameters in model 2, samples should be collected for appropriate values of 'x'. This renders model 2 an example where parameter correlation issues can arise owing to poor experimental data. The issue can, however, be dealt with using intelligent experimental design. It may be relatively easier to detect the practical/structural correlation for algebraic systems, but such insights are difficult to obtain for dynamic systems [153].

Whilst researchers have discussed the issue of parameter correlation, only a few studies have investigated the problem in detail and proposed solutions. The D-optimal design can both reduce the parameter correlation and improve the parameter precision for two-parameter systems, but the approach cannot be extended to model systems with three or more parameters [140]. Modified E-optimal design, where the objective is to minimize the condition number (ratio of maximum and minimum eigenvalues of the FIM), has also been suggested for reducing parameter correlation [144]. Again, similar to the D-optimal criterion, the method is effective for two-parameter systems only. A promising solution to reduce the parameter correlation was proposed by Pritchard and Bacon [145], who instead of opting for traditional maximization of a metric of FIM, explicitly considered an objective function that minimizes a correlation measure [145],

$$\text{Min} \sum_{\substack{i,j \\ i \neq j}} \left\{ \frac{r_{ij}^2}{p^2 - p} \right\}^{1/2} \tag{5.6}$$

where r_{ij} corresponds to ij^{th} correlation element of correlation matrix. The approach was successful in reducing the parameter correlation, but at the expense of wider confidence interval for the individual parameters [147, 155]. Recently, Franceschini and Macchietto proposed a solution to this problem [144]; they introduced anti-correlation (AC) design criteria and proposed four different criteria. All four criteria considered an objective function either for minimizing correlation or for maximizing information in eigenvalue(s) of FIM, with constraints on eigenvalues or correlation elements, respectively [144]. An algorithm and *a priori* model analysis for implementing the AC design criteria were also suggested [150]. Subsequently, the AC criteria were validated on an experimental bio-diesel process [149]. In this work, we propose a distinct approach, namely, MOO based DOE framework, to overcome the correlation among parameters.

5.4 Multi-Objective Optimization based DOE framework

As mentioned earlier, traditional alphabetical designs may improve parameter precision, but could result in higher correlation among parameters. Hence, there is a trade-off between improvement in parameter precision and increase in parameter correlation. Acknowledging this fact, we propose an MOO framework by considering two objectives: maximize information for improving parameter estimation (as in traditional alphabetical designs) and minimize the correlation among parameters, simultaneously. For each alphabetical design, its complementary MOO based design is proposed. Essentially, three different MOO based designs – DMOO, AMOO, and EMOO are considered. In the proposed MOO framework, the correlation matrix (R) is calculated from variance-covariance matrix (V),

$$\mathrm{V} = \left(\mathrm{FIM}\right)^{-1} \frac{\mathrm{SSE}}{\mathrm{DOF}} = \begin{bmatrix} var(\theta_1) & covar(\theta_1,\theta_2) & . & covar(\theta_1,\theta_n) \\ covar(\theta_2,\theta_1) & var(\theta_2) & . & covar(\theta_2,\theta_n) \\ . & . & . & . \\ covar(\theta_n,\theta_1) & covar(\theta_n,\theta_2) & . & var(\theta_n) \end{bmatrix} \frac{\mathrm{SSE}}{\mathrm{DOF}} \quad (5.7)$$

$$r_{ij} = \frac{\mathrm{V}_{ij}}{\sqrt{\mathrm{V}_{ii}\mathrm{V}_{jj}}} \quad (5.8)$$

where V_{ij} and r_{ij} are the ij^{th} element of matrix V and R, characterizing the covariance and correlation between i^{th} and j^{th} parameters, respectively. For $i = j$, V_{ij} will be the diagonal element of variance-covariance matrix and corresponds to variance of i^{th} parameter. SSE is the sum of squared errors between model predictions and corresponding experimental data for obtained experimental design, and DOF corresponds to degrees of freedom, calculated as the difference between total number of data samples and number of estimated parameters.

The correlation matrix is symmetric with principal diagonal elements as one. The objective function for minimizing the correlation is denoted as $\|\mathrm{R}\|$. For a three parameter system, matrix R and $\|\mathrm{R}\|$ are shown for illustration (equation 5.9).

$$\mathrm{R} = \begin{bmatrix} 1 & r_{12} & r_{13} \\ r_{21} & 1 & r_{23} \\ r_{31} & r_{32} & 1 \end{bmatrix} \Rightarrow \|\mathrm{R}\| = \sqrt{r_{12}^{\,2} + r_{13}^{\,2} + r_{23}^{\,2}} \quad (5.9)$$

DMOO design

$$\begin{aligned} &\mathrm{obj1}: max\ |\mathrm{FIM}| \\ &\mathrm{obj2}: min\ \|\mathrm{R}\| \end{aligned} \quad (5.10)$$

AMOO design

$$\begin{aligned} &\mathrm{obj1}: max\ \mathrm{trace(FIM)} \\ &\mathrm{obj2}: min\ \|\mathrm{R}\| \end{aligned} \quad (5.11)$$

EMOO design

$$\begin{aligned} &\text{obj1}: max\ \ \lambda_{\min} \\ &\text{obj2}: min\ \ \|\mathrm{R}\| \end{aligned} \tag{5.12}$$

In equation 5.12, $\lambda_{\min}$ denotes the minimum eigenvalue of FIM. The second objective in the above MOO formulations (equations 5.10 to 5.12) is one of the many possible ways of minimizing parameter correlation. One other approach is to minimize specific correlation elements larger than a pre-specified limit [144]. However, care should be taken to ensure that minimizing one correlation element will not result in increasing other correlation(s). While the MOO framework can handle more than two objectives, scope of the present work is restricted to two objectives only.

5.5 Solution Approach (Genetic algorithm)

Non-dominated sorting genetic algorithm (NSGA-II) based solver (NGPM) available at MATLAB Central [156], is used for solving the formulated optimization problems. Genetic algorithm (GA) is a stochastic global optimization method that mimics the process of natural biological evolution. It repeatedly modifies a population of individual solutions. At each step, the GA selects individuals from the current population to be parents and uses them to produce children for the next generation. Three main rules are applied at each step for producing the improved population. (1) Selection rule to select better individuals that contribute to the population at the next generation. These individuals are also called Parents. (2) Crossover rule to combine two randomly chosen parents to form children. (3) Mutation rule that applies random change to the children, to form the population for the next generation. Over successive generations, the population advances towards an optimal solution [157]. NSGA-II is an adaptation of GA for multiple objectives. Solution of an MOO problem by this algorithm gives many equally good optimal solutions. Set of these non-dominated solutions is also known as the Pareto-

optimal solutions or front [158]. Selection of an optimal point from the obtained Pareto-optimal front depends on the desired trade-off between the conflicting objectives. In our case, each Pareto-optimal solution corresponds to trade-off between information and correlation measure, and an optimal experiment design.

A factor to note here is the computationally intensive nature of GA. Owing to the number of function evaluations, the GA requires longer time to reach to the optima. For large complex systems, the GA can be time-consuming. A simple approach to alleviate the problem is to use a hybrid approach that combines stochastic and deterministic algorithms [146]. Another plausible approach is to use appropriate termination criteria [158]. Since the primary focus of this work is on the benefits of MOO in DOE, we leave out further discussion on the computational aspects of GA.

5.6 Case Studies

To illustrate the effectiveness and applicability of the proposed MOO based DOE framework, two case studies are considered. In both the case studies, D-, A-, E-optimal designs, and their corresponding MOO based designs are compared. Experimental data are simulated using true values of parameters (known *a priori* as this is a simulation study) and inputs recommended by the chosen optimal experimental design. Normally distributed random errors with pre-specified error variance-covariance matrix are added to the simulated data to mimic, as close as possible, the characteristics of real data. The extreme point in the Pareto-optimal front, corresponding to maximum information–maximum correlation, belongs to alphabetical design, while the other extreme corresponding to minimum information–minimum correlation can be considered equivalent to Pritchard and Bacon criterion (equation 5.6). Between these two extremes, the experimenter can select the optimal trade-off (Figure 5.3). Approaches like net flow

method and rough set method can be employed for ranking Pareto optimal solutions and selection [159]; however, these methods require preferences from the decision maker (here, experimenter/modeler). Since the scope of this work is limited to illustration of conflicting objectives in traditional DOE techniques, a relatively simple way of Pareto-point selection is employed. In the case studies discussed, the optimal trade-off for MOO based design and corresponding design vector are selected after transforming the obtained Pareto-optimal front to 0 to 1 scaled Pareto-optimal front. The optimal trade-off is selected such that the percentage decrease in information measure is less than the percentage decrease in correlation measure. The trade-off selection is obvious when there is significant loss in correlation measure, but little loss in information measure, e.g. see Figure 5.8. On the other hand, for not so obvious cases, the selection is based on eyeballing the obtained Pareto-optimal front.

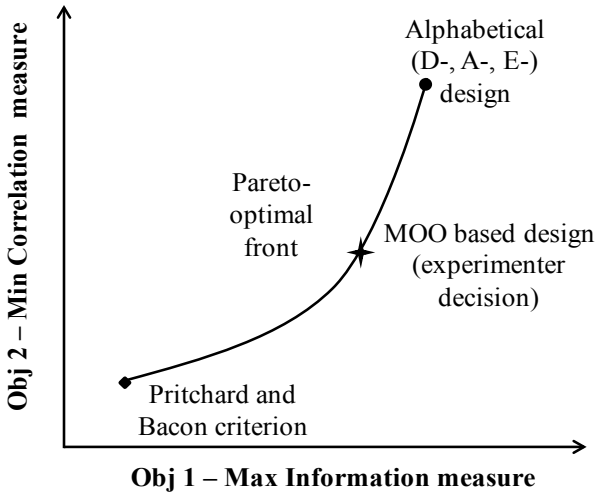

Figure 5.3: Schematic representation of trade-off between information measure and correlation measure. Between the two extremes of alphabetical (D-, A-, E-) design criterion and Pritchard and Bacon criterion, experimenter has freedom to select appropriate optimal experiment design from the Pareto-optimal front. Star is one chosen design for illustration.

After implementation of the selected experiment design, model parameters are estimated and their confidence intervals calculated. The *t*-value can indicate the reliable estimation [151]:

$$t_i = \frac{\hat{\theta}_i}{\sqrt{V_{ii}}} \tag{5.13}$$

The obtained *t*-value for individual parameters is tested against reference *t*-distribution for *n –p* DOF; a *t*-value higher than the reference indicates that the estimate is reliable. Figure 5.4 provides a detailed flow-sheet of the approach followed here.

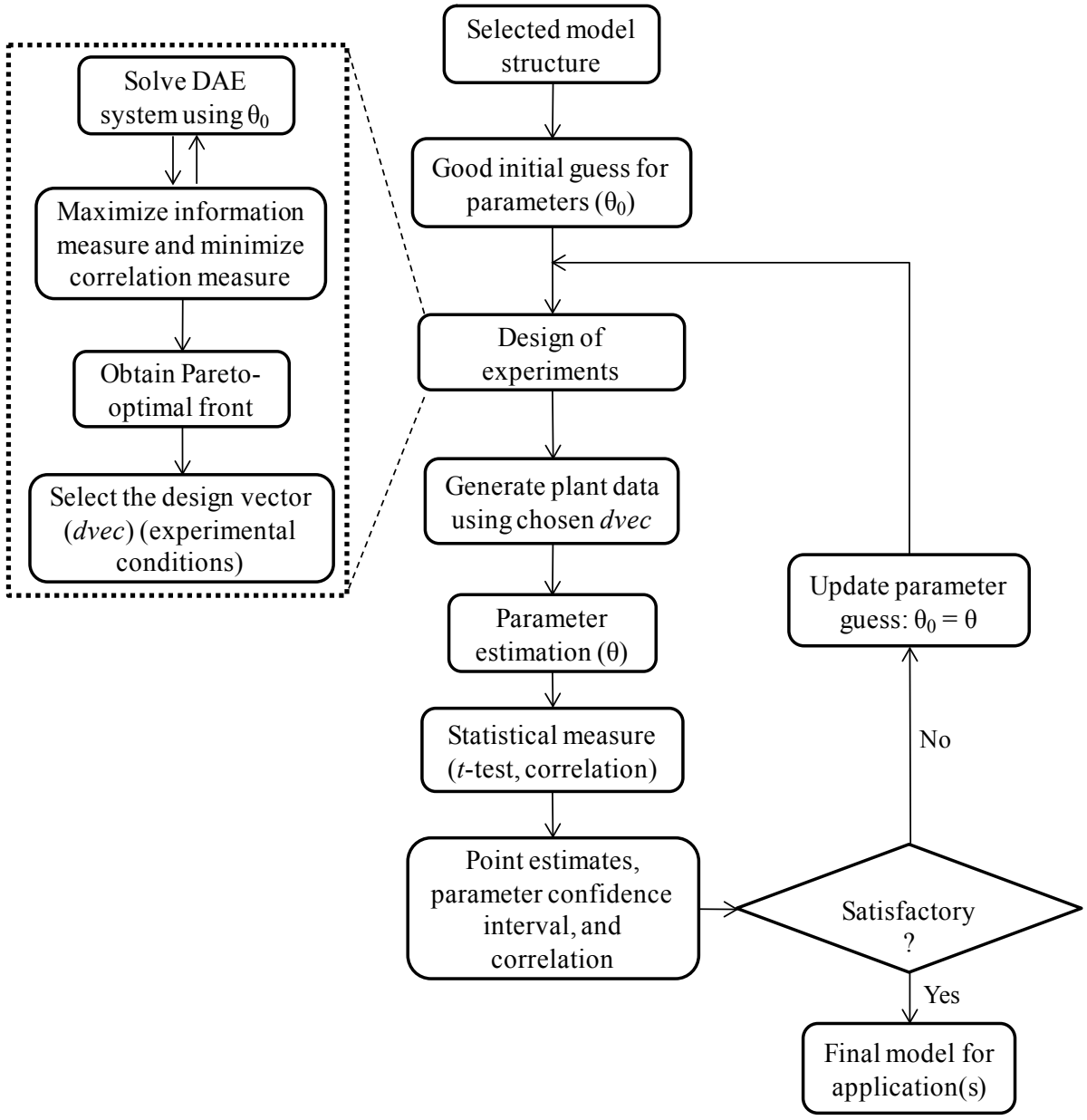

Figure 5.4: Schematic of the design procedure followed in the case studies

The procedure can be iterated until the obtained point estimates are close to those in the previous iteration, and satisfy the statistical quality tests of improved precision and

reduced correlation. Next, the case studies with their brief description, model equations, and corresponding results are presented. In both the case studies, the manipulated variable trajectory is parameterized as piecewise constant elements. The adopted piecewise constant trajectory has been found to give best experimental results, and also preferred from the operational point of view because it is easier to implement in practice [157].

5.6.1 Modified Bergman minimal model for Type 1 diabetes subjects

A model describing glucose-insulin kinetics in Type 1 diabetics is considered. Diabetes, a disease of endocrine malfunction, is one of the most prevalent lifestyle diseases resulting in significantly increased mortality and morbidities. A diabetic subject is either non-responsive to insulin secreted by the pancreatic cells or the insulin secretion is insufficient. Insulin deficient subjects are considered as Type 1 diabetes patients, and they depend on exogenous insulin infusion for maintaining the blood glucose at acceptable levels. In such patients, an optimal insulin infusion is required to maintain the glucose level within permissible limits. This can be obtained by employing an appropriate mathematical model that mimics the glucose-insulin dynamics in Type 1 diabetes patients [160]. In this work, the modified Bergman minimal model having three parameters is considered [161]. The model, earlier used in backoff based MBDOE [162], is given by the following set of ODEs:

$$\begin{aligned}\frac{\mathrm{d}G}{\mathrm{dt}} &= -\theta_1 G - X(G+G_\mathrm{b}) + \frac{D(\mathrm{t})}{V_\mathrm{G}} \\ \frac{\mathrm{d}X}{\mathrm{dt}} &= -\theta_2 X + \theta_3 I \\ \frac{\mathrm{d}I}{\mathrm{dt}} &= -n(I+I_\mathrm{b}) + \frac{u(\mathrm{t})}{V_\mathrm{I}}\end{aligned} \tag{5.14}$$

Here, G, X, and I represent the serum glucose concentration (mg/dL), the insulin concentration in non-accessible compartment (mU/L), and the serum insulin

concentration (mU/L) above their basal values, respectively. Basal glucose concentration (G_b = 81 mg/dL), basal insulin concentration (I_b = 15 mU/L), insulin distribution volume (V_I = 12 L), glucose distribution volume (V_G = 16 L), and disappearance rate of insulin (n = 5/54 min^{-1}) are constant parameters in the model; and $u(t)$ is the rate of infusion of exogenous insulin (mU/min). The unknown model parameters are θ_1, θ_2 and θ_3. In equation 5.14, $D(t)$ denotes meal absorption dynamics described by the following equation [163]:

$$D(t) = \frac{A\, f\, t\, e^{-\frac{t}{t_{max}}}}{t_{max}^2} \tag{5.15}$$

where 'A' is the amount of carbohydrates (CHO) in the meal (fixed at 75 g in this study), $t_{max} = 40\,min$ is the time required to reach the maximum glucose concentration in the accessible compartment, f is the dimensionless factor which represents the fraction of CHO being absorbed (here, f = 0.8). The meal model suggests that ingested meal does not alter the glucose concentration immediately; rather, there is a lag between food ingestion and subsequent manifestation of glucose concentration in the blood serum.

The exogenous insulin infusion, $u(t)$, is expressed as:

$$u(t) = u_{bolus} + u_{basal} \tag{5.16}$$

Here, u_{bolus} represents the subcutaneous bolus insulin kinetics for a bolus U_b (see equation 5.17), given at the start of experiment (at t = 0). This subcutaneous insulin dose compensates for CHO ingestion in a "feed-forward" manner. In this *in silico* experiment, the time of CHO intake is decided by the experimenter, and it can vary between 2 to 30 min after the bolus insulin dose [164]. The u_{bolus} kinetics is given by [165]:

$$u_{bolus} = \frac{t^{s-1} s T_{50}^s U_b}{(T_{50}^s + t^s)^2} \tag{5.17}$$

where T_{50} is the time required to reach 50% absorption of the bolus insulin. T_{50} is given by,

$$T_{50} = aU_b + b \tag{5.18}$$

In equations 5.17 and 5.18, the parameters a, b, and s depend on insulin type. For Humalog insulin, a, b, and s are 5.2 min/U, 41 min, and 1.6, respectively [166].

In equation 5.16, u_{basal} is time varying basal insulin infusion, approximated by a piecewise constant profile. The proposed clinical test is an adaptation of oral glucose tolerance test (OGTT), which is routinely conducted in clinical settings for measuing the glucose-insulin sensitivity of Type 1 diabetes subjects. In OGTT, following the measurement of fasting glucose concentration, the patient ingests 75g of CHO. Subsequently, glucose measurements at 60 min and 120 min are taken. This test is not informative enough to give data for estimation of unknown model parameters. Hence, a modified OGTT is proposed here, which is similar to the one proposed by Galvanin *et al*. [162], with the only difference being that the experimental duration is restricted to a maximum of 300 min. Also, only five piecewise constant moves are assumed for basal insulin infusion.

The experimental design objective is to suggest optimal basal insulin infusion profile, amount of bolus dose at t = 0, time of meal ingestion, and corresponding blood glucose measurement instances which will result in information-rich data for precise estimation of θ_1, θ_2, and θ_3, while ensuring that the correlation among estimated parameters is as low as possible. The experiment duration is decided based on the last sampling instance. Table 5.1 lists all the design variables with their lower and upper bounds, and initial guess.

Table 5.1: Design variables, their bounds, and initial guess for the proposed clinical test for Type 1 diabetes subjects

Design Variable	Symbol	Lower Bound	Upper bound	Initial guess
Bolus insulin dose (mU)	U_b	0	10000	1000
CHO ingestion time	A_t	2	30	5
Basal insulin (mU/min)	u_{basal}	16.67	300	[200, 100, 200, 0, 150]
Switch time for u_{basal}	t_{s1}	10	300	[20, 10, 30, 25]
Sampling instances (min)	t_{sp}	10	300	[20, 50, 70, 80, 95, 115, 140, 150, 162]

The lower bound for exogenous basal insulin is fixed at 16.67 mU/min such that the blood glucose concentration is maintained at its basal value (81 mg/dL). Several operational constraints considered in this work are mentioned below.

1. A total of 10 blood samples (including sample at t = 0) are taken for measuring glucose concentration [167].
2. Consecutive blood samples should have a minimum time interval of 10 min. The maximum allowed time interval between consecutive samples is 300 min, which is also the maximum allowed experiment duration. The last sampling instance decides the duration of clinical test.
3. Minimum 10 min interval is mandated between two consecutive switches of basal insulin infusion rates. Similar to the sampling constraints, the maximum switching time is also constrained to be within 300 min.

The proposed experimental design results in 20 decision variables and 22 linear constraints besides the model equations and physiological constraints, resulting in a fairly challenging optimization problem – a frequent situation for generic MBDOE implementation [141]. An intuitive approach of reducing the number of constraints is followed here – instead of considering the switching time instant or sampling instant as

design variables, we considered time intervals as design variables, each bounded in [10, 300]. This reduced the number of linear constraints from 22 in original optimization problem to just 2 in the modified optimization problem. Both optimization problems are essentially equivalent, but the latter is computationally more tractable than the original. The modification is schematically shown for basal insulin in Figure 5.5. Similar transformation is realized for sampling time instants.

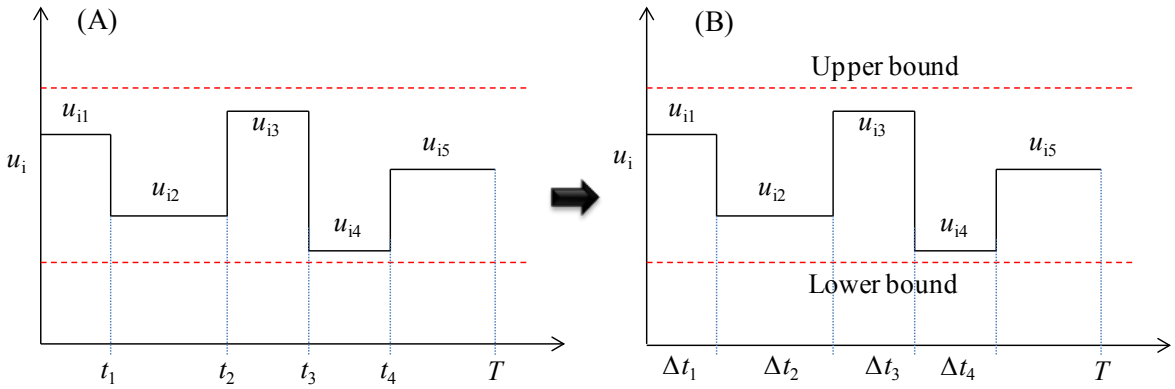

Figure 5.5: Transformation of exact time-instants into delta-time instants

The transformation of constraints into bounds is illustrated in Table 5.2. The 22 constraints in the original formulation are transformed into 2 constraints in the modified formulation. The switching constraint for last control move (u_{i5} in Figure 5.5B) is considered to ensure that it stays for at least 10 minutes (lower bound for each control move) within the experimental duration.

Table 5.2: Transformation of constraints into bounds

(A) Original Formulation

Switching constraints	Sampling constraints	Experiment duration bound
$\underbrace{\begin{matrix} t_j - t_i \geq 10 \\ t_j - t_i \leq 300 \end{matrix} ;\ i = 1,2,3; j = i+1}_{6\ constraints}$	$\underbrace{\begin{matrix} t_m - t_n \geq 10 \\ t_m - t_n \leq 300 \end{matrix} ;\ n = 1,2,...,8; m = n+1}_{16\ constraints}$	$t_{end} \leq 300$

(B) Modified Formulation

Switching bounds	Sampling bounds	Switching constraint for last control move	Duration constraint
$10 \leq \Delta t_i \leq 300; i = 1,2,3,4$	$10 \leq \Delta t_j \leq 300;\ j = 1,2,...9$	$\sum_{j=1}^{9} \Delta t_j - \sum_{i=1}^{4} \Delta t_i \geq 10$	$\sum_{j=1}^{9} \Delta t_j \leq 300$

The problem of designing the clinical test is further complicated due to additional physiological constraints. The function of insulin is to maintain the glucose concentration within the window of 60-120 mg/dL. However, in diabetic patients, the upper limit is relaxed to a value such as 160 mg/dL [168]. Patients are categorized as having experienced a hyperglycemic episode if they exceed 160 mg/dL glucose limit; in a similar fashion, a hypoglycemic episode is said to occur when the patient's blood glucose concentration goes below 60 mg/dL [168]. Hypoglycemia is more dangerous than hyperglycemia because it can result in coma or even death, thus the lower limit of 60 mg/dL may be considered as hard constraint and the upper limit of 160 mg/dL may be regarded as soft constraint. However, for simplicity, both are considered as hard constraints in the present simulation study. These physiological constraints are handled using penalty function method [158]. In this approach, first the constraints are scaled and constraint violation pertaining to hypo- and hyperglycemia for each experimental design is calculated. The total violation is multiplied with a large weight and then added to each objective. The penalty weight is decided based on the objective function value for experimental design corresponding to the initial guess in Table 5.1.

In the present simulation study, true parameters θ_{true} = [0.025, 0.015, 1.26×10^{-5}] are used in the patient model to generate the patient data for optimal experimental conditions. A constant relative variance of 0.01 is added to incorporate the real-world noise characteristics in glucose measurements. The initial parameter guess for designing the experiment is considered at 25% positive deviation from true parameter values. They were assumed equidistant from true parameter values so that obtained estimates and their precision characteristics cannot be attributed to better/worse initial guess [144]. Note that, the resulting experiment when implemented on real subjects can still violate the permissible glucose limits due to patient-model mismatch. To prevent such undesirable events, a conservative design approach has been considered in this work where the hypo- and hyperglycemia limits are set at 65 and 150 mg/dL, respectively. This conservative design may result in less information because functional value space is constrained; however, computationally intensive robust experimental design methods such as expected value criterion, min-max optimization [148] or backoff based technique for experiment design [162], can overcome this problem. The robust experimental design criteria can be incorporated in the proposed MOO based DOE framework, and will be explored in our future work.

Traditional vs. MOO based DOE: In the simulations below, the alphabetical design (D-, A-, and E-) and corresponding MOO based design are compared. The results for alphabetical design typically correspond to the extreme Pareto-optimal point for maximum information–maximum correlation, while MOO based design refers to a chosen experimental design from the obtained Pareto-optimal front. First, the comparison of D-optimal and DMOO design is presented – the Pareto-optimal front for DMOO based design (Figure 5.6), the schematic of D-optimal design and the chosen DMOO based experimental design (Figure 5.7), followed by the parameter estimates for both the

designs (Table 5.3). Similar sequence is followed for comparing simulation results for A-optimal vs. AMOO design and E-optimal vs. EMOO design. In the Pareto-optimal fronts for DMOO, AMOO, and EMOO designs (Figure 5.6, 5.8, and 5.10), the data-tip (X,Y) corresponds to the selected optimal trade-off for implementation.

Note that FIM is based on sensitivity coefficient (equation 5.4), which is dependent on initial guesses of parameters. The sensitivity coefficients based FIM may provide misleading experimental design due to order of magnitude difference in model parameters; hence, parameter-scaled sensitivity is considered for FIM calculation [169]. The parameter-scaled sensitivity ($G_{i,\theta}$) is defined as:

$$G_{i,\theta} = \frac{\partial y_{is}}{\partial \theta_j}\theta_j \tag{5.19}$$

In equation 5.19, i, j, and s are the indices of measured state (Glucose), parameters (j = 1, 2, 3), and sampling instances (s = 1, 2, 3…, 10), respectively.

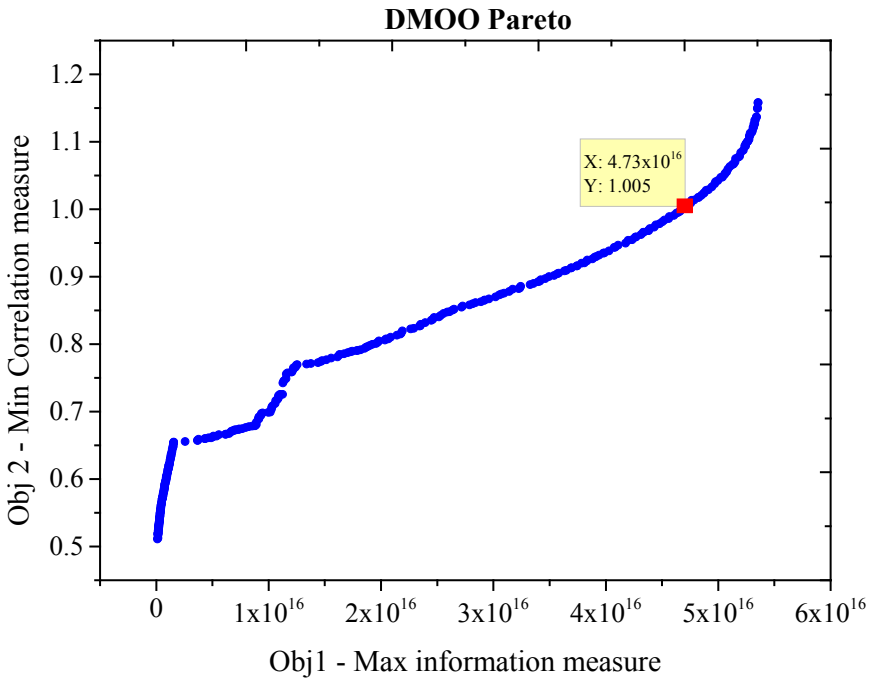

Figure 5.6: Pareto-optimal front for DMOO design

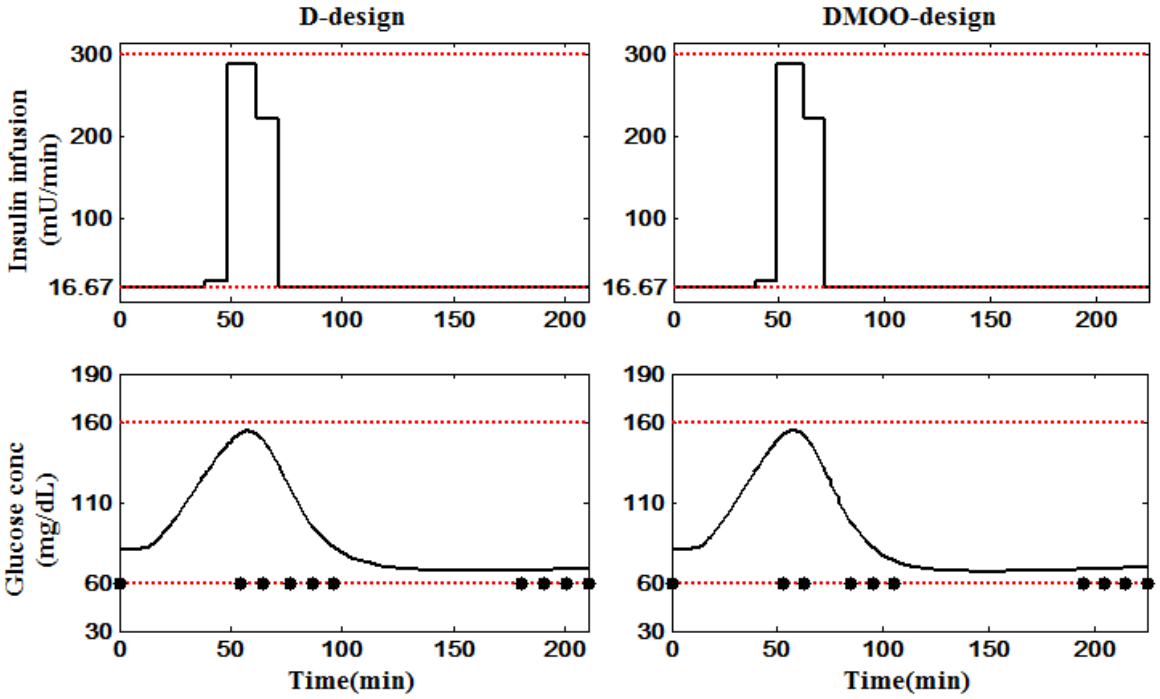

Figure 5.7: Time profiles of basal insulin infusion and blood glucose sampling instances (●) for D-optimal and DMOO design vectors and resulting glucose concentration profiles

Table 5.3: Parameter estimates and statistics for D-optimal and DMOO design

Design technique	Parameter (true value)	Estimates ± 95% confidence interval	*t*-test (t_{ref} = 2.36)	Correlation Matrix	$\|\mathbf{R}\|$
D-optimal design	θ_1 (0.025)	0.0282 ± 0.0026	25.90	$\begin{bmatrix} 1 & -0.57 & -0.65 \\ & 1 & 0.77 \\ & & 1 \end{bmatrix}$	1.158
	θ_2 (0.015)	0.0138 ± 0.0015	21.75		
	θ_3 (1.26×10^{-5})	$1.176\times10^{-5} \pm 0.09\times10^{-5}$	30.51		
DMOO-design	θ_1 (0.025)	0.0276 ± 0.0061	10.67	$\begin{bmatrix} 1 & -0.46 & -0.49 \\ & 1 & 0.75 \\ & & 1 \end{bmatrix}$	1.005
	θ_2 (0.015)	0.0145 ± 0.0033	10.45		
	θ_3 (1.26×10^{-5})	$1.228\times10^{-5} \pm 0.19\times10^{-5}$	14.72		

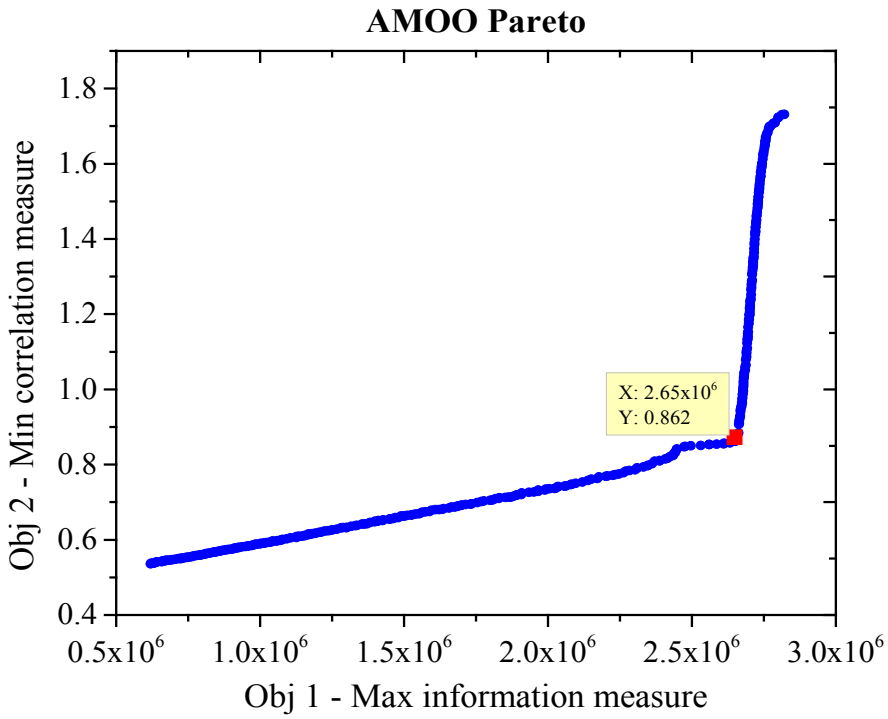

Figure 5.8: Pareto-optimal front for AMOO design

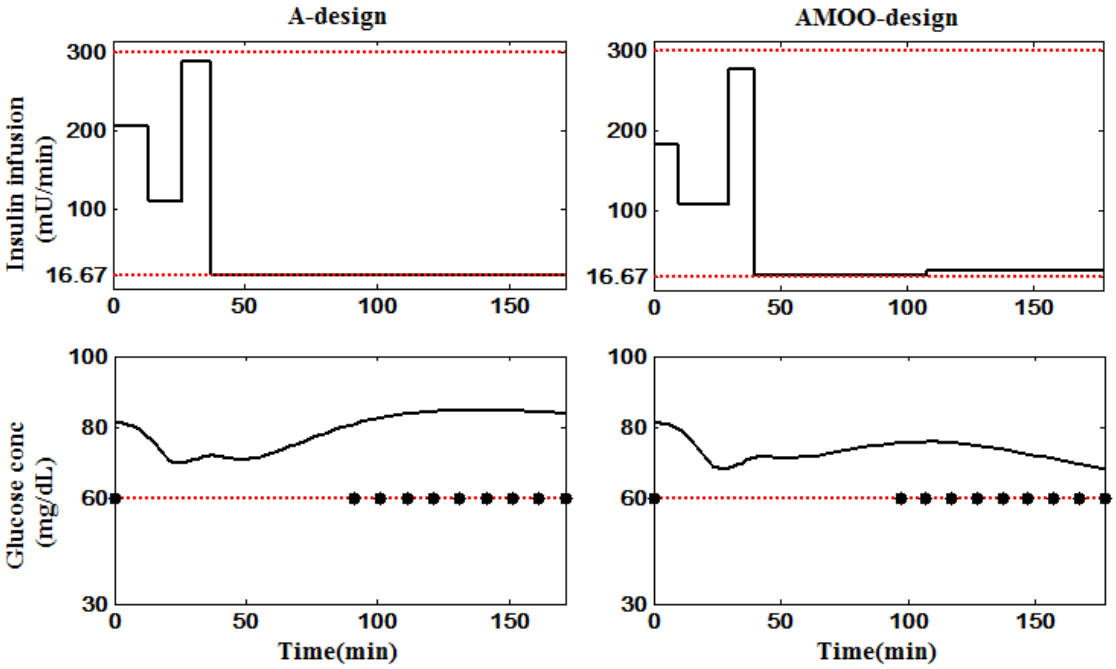

Figure 5.9: Time profiles of basal insulin infusion and blood glucose sampling instances (●) for A-optimal and AMOO design vectors and resulting glucose concentration profiles

Table 5.4: Parameter estimates and statistics for A-optimal and AMOO design

Design technique	Parameter (true value)	Estimates ± 95% confidence interval	*t*-test (t_{ref} = 2.36)	Correlation Matrix	$\|\mathbf{R}\|$
A-optimal design	θ_1 (0.025)	0.0770 ± 0.2371	0.77	$\begin{bmatrix} 1 & 0.999 & 0.999 \\ & 1 & 0.999 \\ & & 1 \end{bmatrix}$	1.731
	θ_2 (0.015)	0.0185 ± 0.0164	2.67		
	θ_3 (1.26×10^{-5})	$1.547\times10^{-5} \pm 1.41\times10^{-5}$	2.60		
AMOO-design	θ_1 (0.025)	0.0254 ± 0.0164	3.66	$\begin{bmatrix} 1 & -0.42 & -0.57 \\ & 1 & 0.50 \\ & & 1 \end{bmatrix}$	0.862
	θ_2 (0.015)	0.0143 ± 0.0016	21.54		
	θ_3 (1.26×10^{-5})	$1.218\times10^{-5} \pm 0.077\times10^{-5}$	37.27		

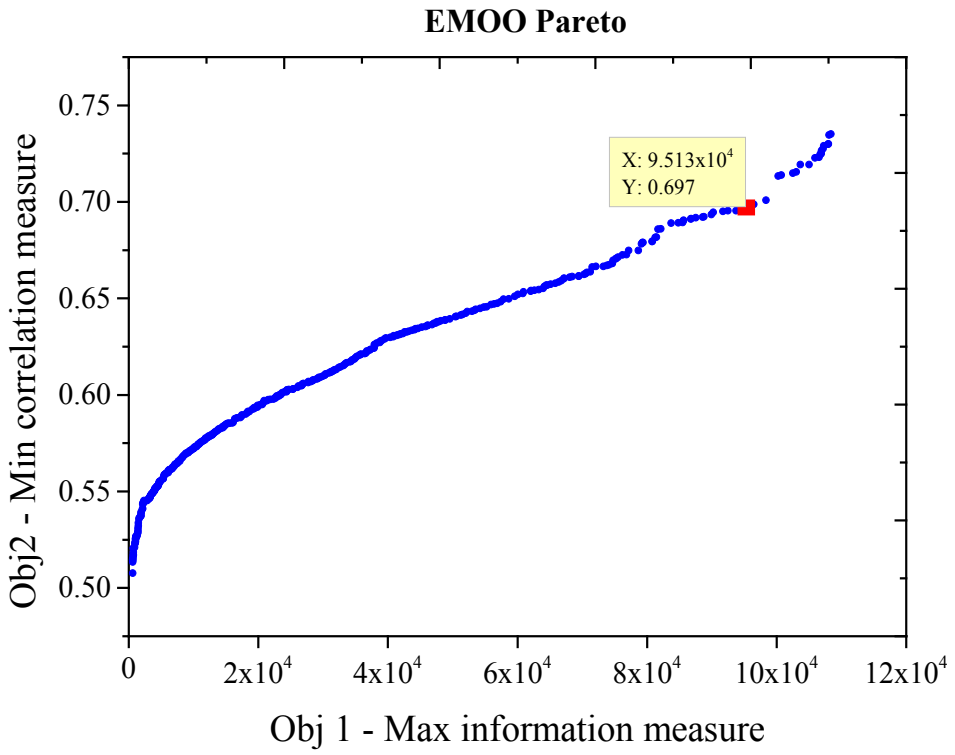

Figure 5.10: Pareto-optimal front for EMOO design

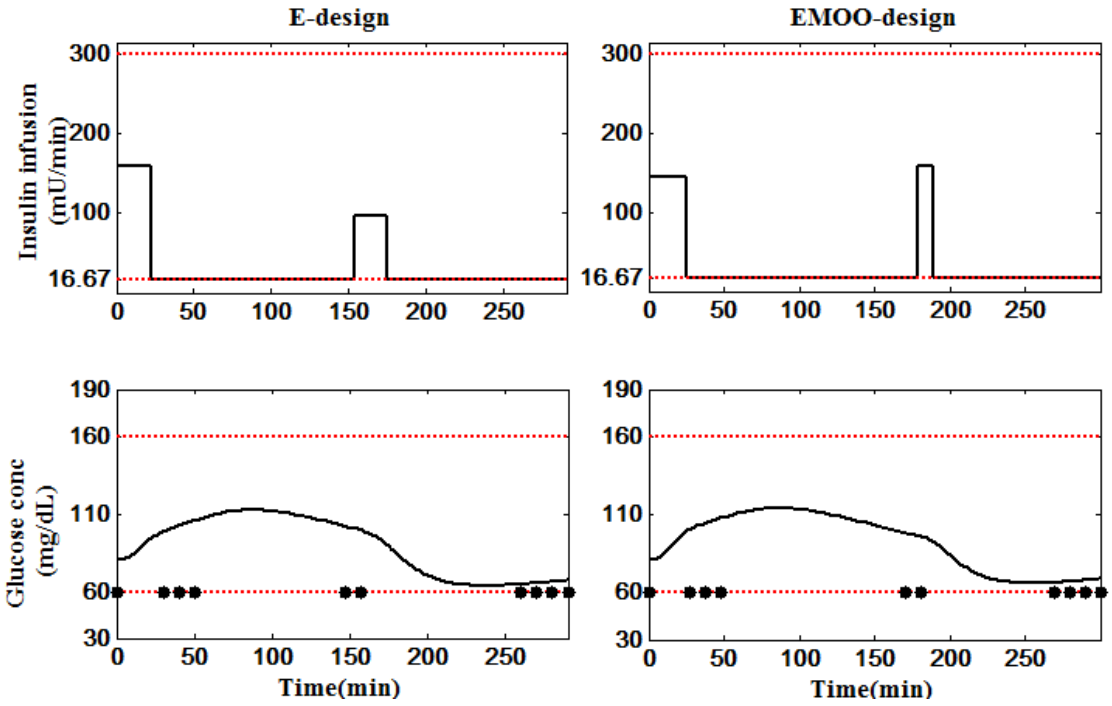

Figure 5.11: Time profiles of basal insulin infusion and blood glucose sampling instances (●) for E-optimal and EMOO design vectors and resulting glucose concentration profiles

Table 5.5: Parameter estimates and statistics for E-optimal and EMOO design

Design technique	Parameter (true value)	Estimates ± 95% confidence interval	*t*-test (t_{ref} = 2.36)	Correlation Matrix	$\|\mathbf{R}\|$
E-optimal design	θ_1 (0.025)	0.0263 ± 0.0043	14.41	$\begin{bmatrix} 1 & 0.11 & -0.13 \\ & 1 & 0.71 \\ & & 1 \end{bmatrix}$	0.735
	θ_2 (0.015)	0.0143 ± 0.0020	16.83		
	θ_3 (1.26×10^{-5})	1.228×10^{-5} ± 0.160×10^{-5}	18.17		
EMOO-design	θ_1 (0.025)	0.0261 ± 0.0047	13.11	$\begin{bmatrix} 1 & 0.10 & -0.12 \\ & 1 & 0.68 \\ & & 1 \end{bmatrix}$	0.697
	θ_2 (0.015)	0.0151 ± 0.0022	15.94		
	θ_3 (1.26×10^{-5})	1.220×10^{-5} ± 0.169×10^{-5}	17.03		

From the results in Tables 5.3 to 5.5, it can be observed that each MOO based experimental design performs better or equivalent to its alphabetical counterpart. For D vs. DMOO and E vs. EMOO scenarios, the decrease in correlation comes at a small cost of decreased parameter precision, but they give improved point estimates, which are

closer to true values of parameters. Both D-optimal and DMOO-designs result in similar basal insulin profiles, however, a closer inspection will indicate that the DMOO-design results in slightly longer experiment duration and different sampling instances (Figure 5.7). A-optimal design results in significantly high correlation among parameters, with all correlation elements close to 1. This results in poor point estimates as well as smaller *t*-value for parameters (Table 5.4). It is clear from Figure 5.8 that the selected AMOO experimental design provides a precipitous decrease in correlation measure with little loss in information measure. The resulting point estimates for individual parameters are closer to true values with significantly high *t*-values (Table 5.4).

The proximity of obtained parameter estimates is compared based on percentage normalized Euclidean distance (δ) between obtained parameter estimates and true parameters.

$$\delta = \sqrt{\sum_{i=1}^{n}\left(\frac{\theta_{i,true}-\theta_i}{\theta_{i,true}}\right)^2}\times 100\ ;\ n = \textit{number of parameters} \qquad (5.20)$$

The results are summarized in Table 5.6. In all three scenarios, the percentage normalized Euclidean distance is smaller for MOO based designs, which confirms that the resulting parameter estimates from MOO based designs are closer to the true values of model parameters when compared with the corresponding alphabetical designs**.**

Table 5.6: Percentage normalized Euclidean distance for alphabetical and MOO based designs for Type 1 diabetes model

Alphabetical vs. MOO design	$\delta_{traditional}$	δ_{MOO}
D vs. DMOO	16.62	11.12
A vs. AMOO	210.59	5.83
E vs. EMOO	7.29	5.57

5.6.2 Baker's Yeast Fermentation Reactor Model

This case study corresponds to fed-batch model for Baker's yeast fermentation [170]. This classical model has been widely employed for implementation of various DOE techniques such as D-optimal [171], E-optimal [142], SV-optimal [142], min-max robust optimal [148], P-optimal [141], and anti-correlation experimental design [150], and can be considered as a benchmark model in MBDOE literature. Assuming Monod kinetics for substrate consumption and biomass growth, the reactor model can be described by the following set of DAEs:

$$\begin{aligned} \frac{dy_1}{dt} &= (r - u_1 - \theta_4).y_1 \\ \frac{dy_2}{dt} &= -\frac{r.y_1}{\theta_3} + u_1(u_2 - y_2) \\ r &= \frac{\theta_1 y_2}{\theta_2 + y_2} \end{aligned} \tag{5.21}$$

where y_1 and y_2 are the biomass and substrate concentrations (g/L), respectively and *r* is the specific growth rate of bio-mass. The reactor system uses two piecewise constant manipulated variables u_1 (dilution factor, h^{-1}) and u_2 (feed substrate concentration, g/L). The reactor model has four unknown parameters, of which two are for the rate expression (θ_1, θ_2) and the rest two are yield coefficients (θ_3, θ_4). At t = 0, the substrate concentration y_2^0 equals 0.1 and biomass concentration denoted by y_1^0 is a design variable, i.e. $y_0 = [y_1^0, 0.1]$

The design variables comprise y_1^0, five manipulated variable moves for each of u_1 and u_2, four switching times for each manipulated variable, and ten sampling instances. In effect, the design space constitutes a total of 29 decision variables. All the design variables with their lower and upper bounds, and initial guess values are summarized in Table 5.7.

Table 5.7: Design variables, their bounds, and initial guess values for Baker's yeast fermentation reactor system

Design Variable	Symbol	Lower Bound	Upper bound	Initial guess
Initial amount of Biomass	y_1^0	1	10	5.5
Sampling instances (h)	t_{sp}	0.5	20	[2, 6, 9, 16, 21, 23, 27, 33, 36, 38]
Dilution factor (L^{-1})	u_1	0.05	0.2	[0.12, 0.12, 0.12, 0.12, 0.12]
Substrate in feed (g L^{-1})	u_2	5	35	[15, 15, 15, 15, 15]
Switch time for u_1	t_{s1}	0.5	20	[5, 15, 20, 30]
Switch time for u_2	t_{s2}	0.5	20	[5, 15, 20, 30]

The operational constraints considered in the design are as follows:

- Minimum and maximum duration between consecutive control switches is 0.5 and 20 hours, respectively.
- Two consecutive samples should be at least 0.5 hours apart and at most 20 hours apart [141].
- The first sample could only be taken after 0.5 hours of start of experiment.
- Maximum allowable experiment duration is 40 hours.

Based on the above constraints, a total of 30 linear constraints were obtained for experimental design, besides the model equations. These were reduced to 3 by employing the earlier mentioned approach of transforming the time instants to time intervals (Figure 5.5 and Table 5.2), each bounded between [0.5, 20]. Corresponding to measured states, y_1 and y_2, the error variance matrix $\sum$ is assumed to be diagonal and following a constant relative variance model [141]:

$$\sum = \begin{bmatrix} 0.04 & 0 \\ 0 & 0.04 \end{bmatrix} \tag{5.22}$$

The true parameter values for this system were, θ_{true} = [0.31, 0.18, 0.55, 0.05]. These values were used to obtain the "experimental data" from the model. For all the experimental designs, the initial parameter guess, θ = [0.5, 0.5, 0.5, 0.5] is used. In the parameter estimation stage, following upper and lower bounds on parameters were imposed [141]:

$$0.05 < \theta_1, \theta_2, \theta_3 < 0.98 \qquad 0.01 < \theta_4 < 0.98 \tag{5.23}$$

Traditional vs. MOO based DOE: Similar to the first case study, comparison of parameter estimates, correlation, and *t*-value for D-, A-, and E-optimal design with their respective MOO counterparts are tabulated in Tables 5.8, 5.9, and 5.10, respectively. Figures 5.12, 5.14, and 5.16 are Pareto-optimal fronts corresponding to DMOO, AMOO, and EMOO design, respectively; in these figures, the data-tip (X,Y) corresponds to the selected optimal trade-off for implementation. As in the first case study, parametric scaling of sensitivity coefficients is adopted. In addition, the sensitivity coefficients are also scaled with respect to states in order to remove the magnitude difference between different measured states. The modified scaled sensitivity is defined as response-ranged sensitivity ($G^{y}_{i,\theta}$) [169]:

$$G^{y}_{i,\theta} = \frac{\partial y_{is}}{\partial \theta_j} \frac{\theta_j}{y_{i,max} - y_{i,min}} \tag{5.24}$$

In this equation, ‘i’ is the index of measured state (both states y_1 and y_2 are measured), ‘s’ is the index for sampling instance (s = 1, 2,…,10), and ‘j’ is the index for parameters (j = 1, 2, 3, 4).

Figures 5.13, 5.15, and 5.17 show the optimal time profiles for dilution factor (u_1) and substrate in feed (u_2); all these figures show profiles for traditional designs and their

MOO design counterpart along with sampling instances, and the dotted lines in the figures denote the lower and upper bounds for manipulated variables u_1 and u_2.

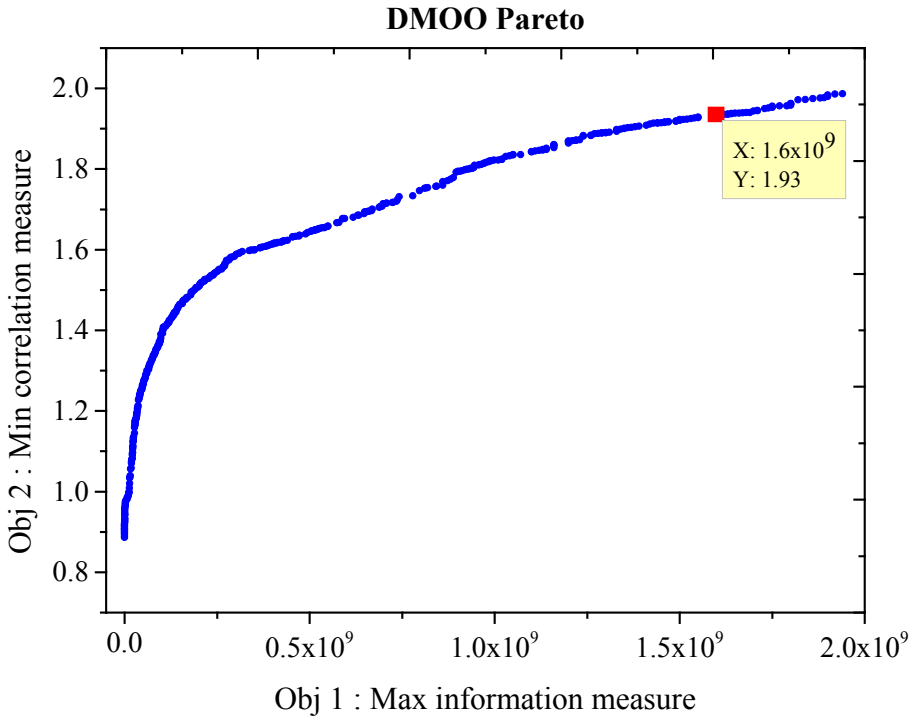

Figure 5.12: Pareto-optimal front for DMOO design

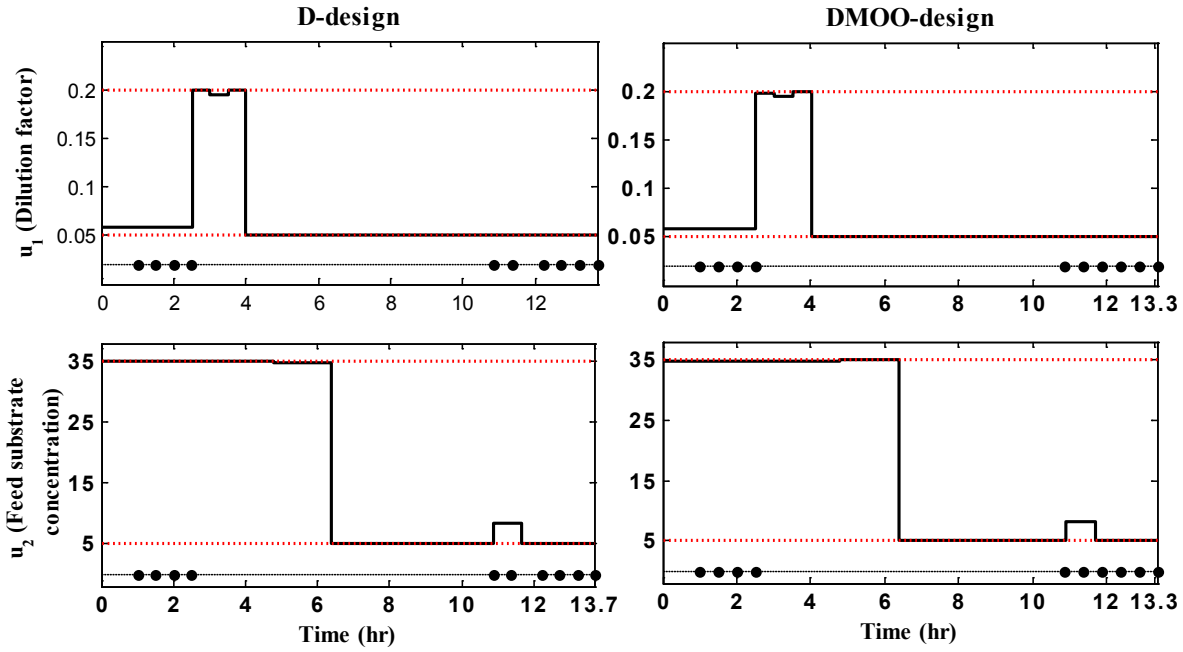

Figure 5.13: Time-profile of manipulated vairables (u_1 and u_2) and sampling instances (•) for D-optimal and DMOO design

Table 5.8: Parameter estimates and statistics for D-optimal design and DMOO design

Design technique	Parameter (true value)	Estimates ± 95% confidence interval	*t*-test (t_{ref} = 2.12)	Correlation Matrix	$\|\mathbf{R}\|$
D-optimal design	θ_1 (0.31)	0.275 ± 0.632	0.92*	$\begin{bmatrix} 1 & -0.60 & 0.95 & 0.997 \\ & 1 & -0.64 & -0.64 \\ & & 1 & 0.94 \\ & & & 1 \end{bmatrix}$	1.986
	θ_2 (0.18)	0.242 ± 1.031	0.50*		
	θ_3 (0.55)	0.602 ± 0.199	6.42		
	θ_4 (0.05)	0.061 ± 0.030	4.34		
DMOO-design	θ_1 (0.31)	0.407 ± 0.419	0.94*	$\begin{bmatrix} 1 & -0.54 & 0.94 & 0.997 \\ & 1 & -0.61 & -0.58 \\ & & 1 & 0.93 \\ & & & 1 \end{bmatrix}$	1.933
	θ_2 (0.18)	0.222 ± 0.415	0.69*		
	θ_3 (0.55)	0.537 ± 0.193	5.14		
	θ_4 (0.05)	0.049 ± 0.025	3.39		

* Statistically insignificant parameter(s)

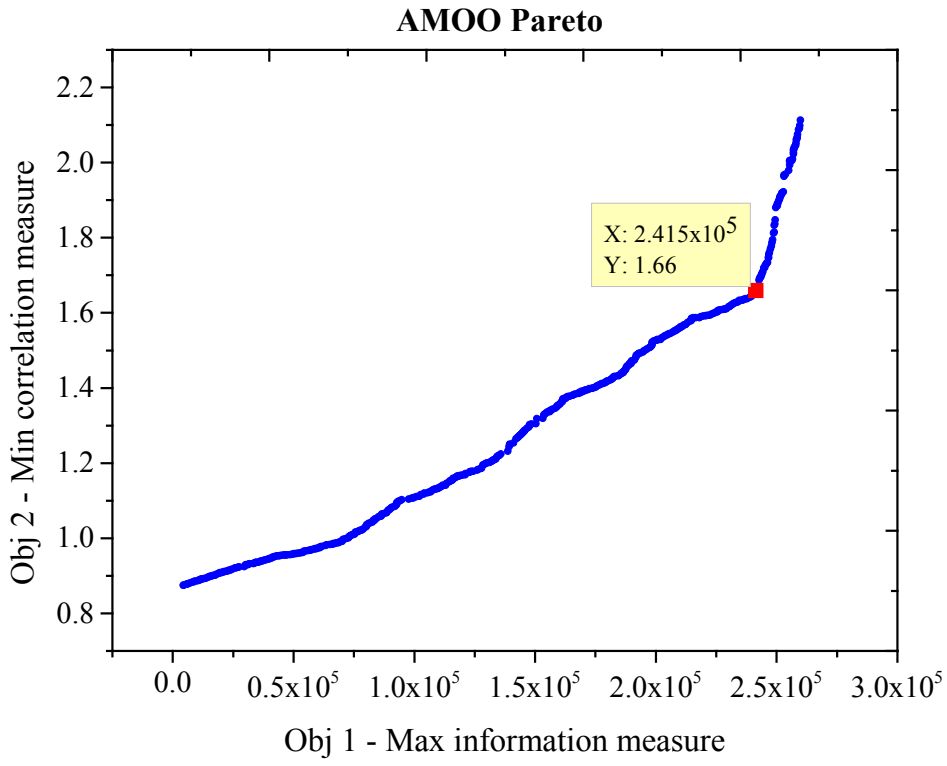

Figure 5.14: Pareto-optimal front for AMOO design

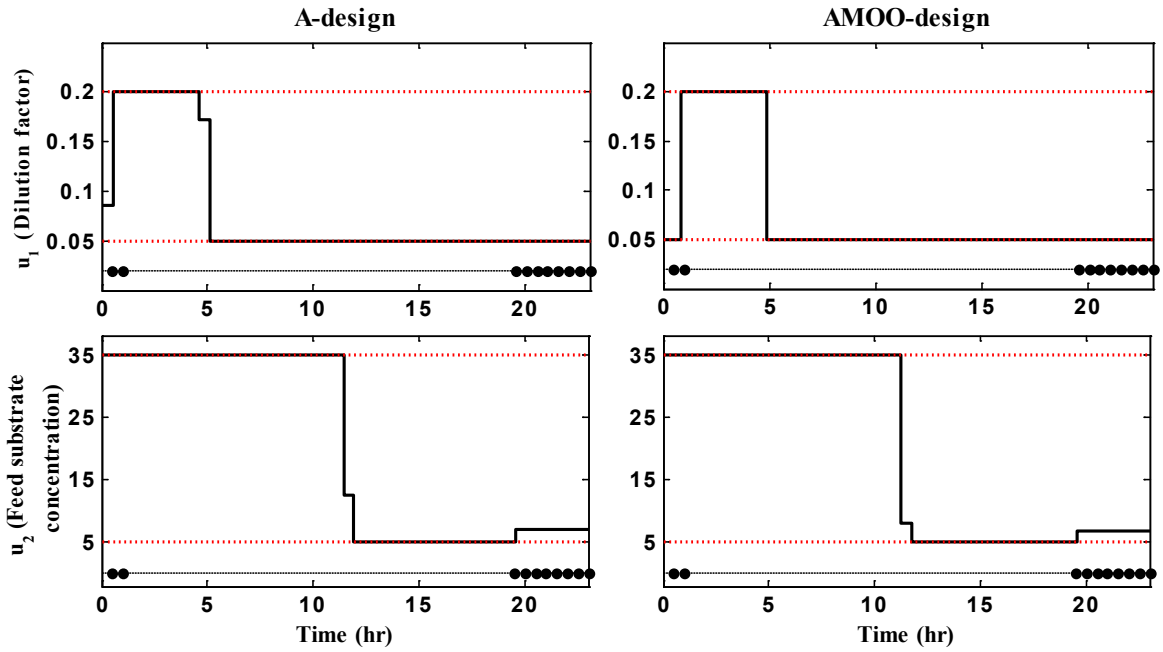

Figure 5.15: Time-profile of manipulated vairables (u_1 and u_2) and sampling instances (•) for A-optimal and AMOO design.

Table 5.9: Parameter estimates and statistics for A-optimal design and AMOO design

Design technique	Parameter (true value)	Estimates ± 95% confidence interval	*t*-test (t_{ref} = 2.12)	Correlation Matrix	$\|\mathbf{R}\|$
A-optimal design	θ_1 (0.31)	0.389 ± 0.152	5.42	$\begin{bmatrix} 1 & -0.69 & 0.99 & 0.999 \\ & 1 & -0.73 & -0.71 \\ & & 1 & 0.99 \\ & & & 1 \end{bmatrix}$	2.113
	θ_2 (0.18)	0.310 ± 0.246	2.66		
	θ_3 (0.55)	0.570 ± 0.203	5.95		
	θ_4 (0.05)	0.053 ± 0.023	4.92		
AMOO-design	θ_1 (0.31)	0.315 ± 0.176	3.80	$\begin{bmatrix} 1 & -0.12 & 0.94 & 0.993 \\ & 1 & 0.04 & -0.23 \\ & & 1 & 0.90 \\ & & & 1 \end{bmatrix}$	1.660
	θ_2 (0.18)	0.210 ± 0.189	2.35		
	θ_3 (0.55)	0.620 ± 0.256	5.14		
	θ_4 (0.05)	0.060 ± 0.027	4.68		

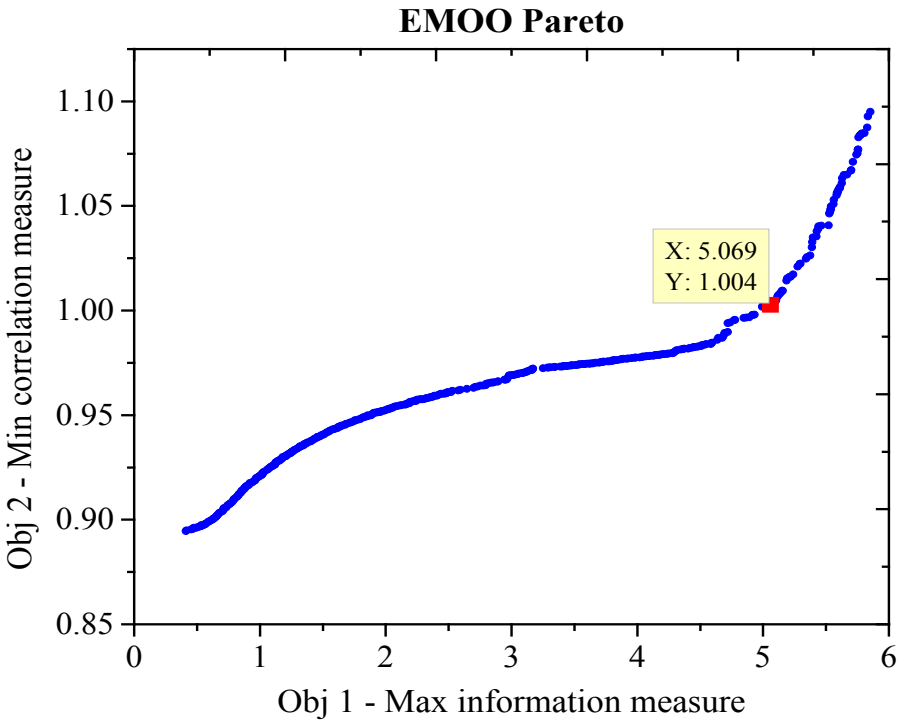

Figure 5.16: Pareto-optimal front for EMOO design

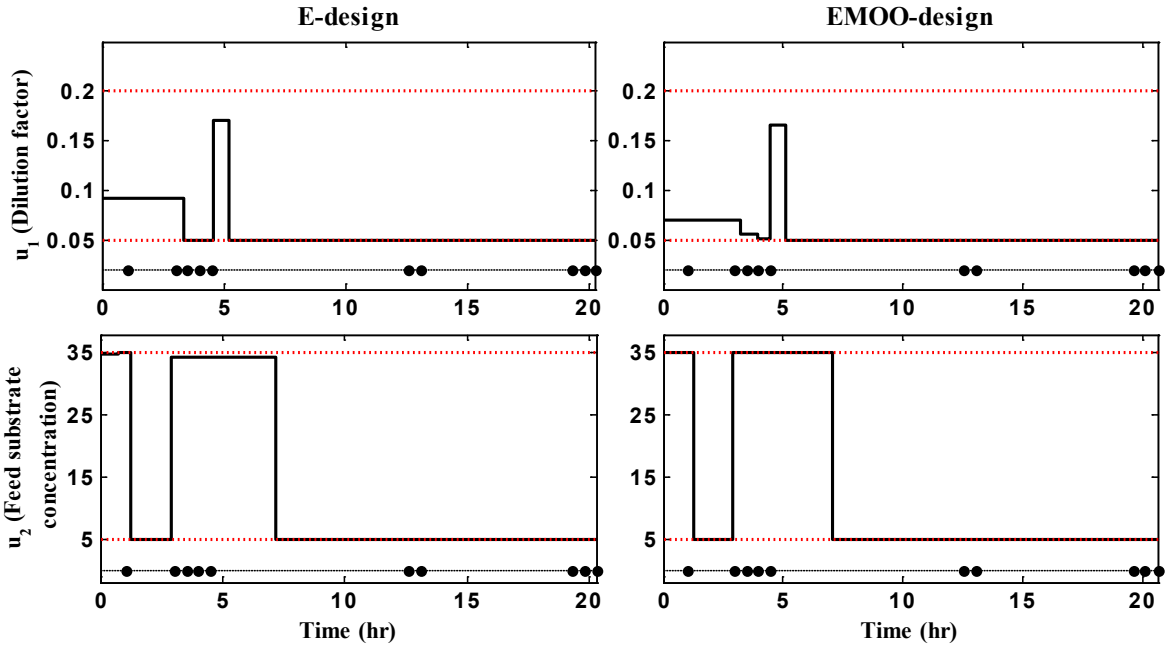

Figure 5.17: Time-profile of manipulated vairables (u_1 and u_2) and sampling instances (•) for E-optimal and EMOO design.

Table 5.10: Parameter estimates and statistics for E-optimal design and EMOO design

Design technique	Parameter (true value)	Estimates ± 95% confidence interval	*t*-test (t_{ref} = 2.12)	Correlation Matrix	$\|\mathbf{R}\|$
E-optimal design	θ_1 (0.31)	0.230 ± 0.117	4.17	$\begin{bmatrix} 1 & 0.09 & 0.31 & 0.97 \\ & 1 & -0.25 & -0.11 \\ & & 1 & 0.27 \\ & & & 1 \end{bmatrix}$	1.095
	θ_2 (0.18)	0.176 ± 0.203	1.84*		
	θ_3 (0.55)	0.483 ± 0.131	7.84		
	θ_4 (0.05)	0.042 ± 0.016	5.46		
EMOO-design	θ_1 (0.31)	0.275 ± 0.167	3.49	$\begin{bmatrix} 1 & 0.08 & 0.18 & 0.97 \\ & 1 & -0.06 & -0.14 \\ & & 1 & 0.08 \\ & & & 1 \end{bmatrix}$	1.004
	θ_2 (0.18)	0.173 ± 0.177	2.08*		
	θ_3 (0.55)	0.547 ± 0.172	6.75		
	θ_4 (0.05)	0.050 ± 0.019	5.49		

* Statistically insignificant parameter(s)

In all the three MOO based designs, point estimates of parameters are close to true parameter values (Table 5.8, 5.9, and 5.10). The proximity of these to true parameter values are compared based on percentage normalized Euclidean distance (δ), defined in equation 5.20. The results are summarized in Tables 5.6 and 5.11. Considering D- vs. DMOO designs, only a small decrease in correlation measure can be obtained for a somewhat large decrease in information measure (Figure 5.12). This is reflected in obtained parameter estimates for both designs, which are similar with two parameters turning out to be statistically insignificant (Table 5.8). D-optimal design results in more precise parameters, while DMOO design results in slightly better point estimates. This suggests that based on one's requirement, the alphabetical design or MOO based design can be preferred. If the parameter precision is more important, then one should opt for D-design, and if focus is on accurate point estimates then one should opt for DMOO design. Similarly, the AMOO design outperforms A-optimal design while considering point estimates, but result in slightly poor *t*-values or wider confidence interval (Table 5.9).

Similar results are obtained for E-EMOO pair where improved point estimates are obtained at the cost of wider confidence interval (Table 5.10).

Table 5.11: Percentage normalized Euclidean distance for alphabetical and MOO based designs for Baker's yeast fermentation reactor model

Alphabetical vs. MOO design	$\delta_{traditional}$	δ_{MOO}
D vs. DMOO	43.30	39.07
A vs. AMOO	76.87	28.40
E vs. EMOO	32.59	11.84

5.7 Discussion

The foremost advantage of the proposed MOO based DOE framework is that it results in multiple optimal experiment designs in the form of a Pareto-optimal front. The two extremes of Pareto-optimal front can be considered equivalent to single objective designs: one extreme corresponds to maximum information–maximum correlation which is equivalent to the traditional alphabetical design, while the other extreme refers to minimum information–minimum correlation, equivalent to the design for Pritchard and Bacon criterion [145]. Between these two extremes, there exist a number of optimal trade-offs between information and correlation measures. This offers the experimenter the freedom to choose an optimal experiment design according to the desired trade-off. From the results on the two case studies, it can be concluded that MOO based designs result in better point estimates than the traditional alphabetical designs. The improved point estimates are obtained at the cost of slightly decreased precision in MOO based designs. The decreased precision is expected owing to the fact that MOO based experimental design opts for decreased information measure. This decreased information contributes towards poor precision of estimated parameters. Note that the comparison of results is based on the chosen optimal trade-off between information and correlation measure and the respective alphabetical design.

Interestingly, the AMOO-design results for Type 1 diabetes model clearly outperforms those from the A-optimal design, both in the context of point estimates as well as parameter precision (Table 5.4). Even in the Baker's yeast fermentation reactor case study, the A-optimal design results in poorer point estimates (Table 5.9); this is also evident from Table 5.11, where the worst percentage normalized Euclidean distance (δ) is obtained for A-optimal design. Earlier, it has been recommended that A-optimal criterion should not be employed for experimental design since it may lead to non-informative experiments due to high correlation in parameters [140]. Results of the present simulation study show that AMOO design can overcome the problems associated with A-optimal design and results in better parameter estimates. Among the discussed alphabetical designs, E-optimal design performs better for the two case studies, but EMOO-design performs even better than E-optimal design, as can be observed from percentage normalized Euclidean distance (δ) in Tables 5.6 and 5.11. The lower value of δ indicates that the obtained point estimates for parameters are closer to true parameter values.

Further, comparison of the obtained Pareto-optimal fronts for DMOO, AMOO, and EMOO designs shows that the point corresponding to minimum correlation measure is very similar in all the designs (Figures 5.6, 5.8, and 5.10 for Type 1 diabetes model, and Figures 5.12, 5.14, and 5.16 for Baker's yeast fermentation reactor model). The minor discrepancy could be attributed to the stochastic nature of genetic algorithm employed. Notably, the other extreme corresponding to maximum information–maximum correlation i.e. alphabetical design shows the least value for EMOO Pareto-optimal front, when compared with corresponding DMOO and AMOO Pareto-optimal fronts. This suggests that this particular extreme point in EMOO Pareto-optimal front or E-optimal design can also reduce parameter correlation. In other words, among the alphabetical designs, E-optimal design can better handle the correlation among parameters.

Results of the case studies show that the obtained Pareto-optimal fronts for the two case studies are different for the same design. Also, for each case study, the Pareto-optimal front is different for different designs. This suggests that shape of the Pareto-optimal front depends on model equations, number of parameters, and the choice of design criteria. The other plausible factors affecting the shape of the Pareto-optimal front are number of measured states, number of samples, and input perturbation allowed. Generally, the correlation among parameters increases with increase in information, but the actual trade-off needs to be established for each scenario by MOO.

5.8 Summary

An MOO based DOE framework, which provides an optimal trade-off between information for parameter estimation and correlation among parameters, is proposed. Two case studies, namely, a 3-parameter modified Bergman minimal model for Type 1 diabetes patients and a 4-parameter Baker's Yeast fermentation model are used to illustrate the effectiveness of the proposed approach. The results highlight the potential of MOO based DOE formulations to perform better than the traditional alphabetical designs. Specifically, the proposed approach can provide point estimates closer to the true values than those obtained by the traditional alphabetical designs; the AMOO design overcomes the problems associated with A-optimal design. Among the alphabetical designs, the E-optimal design is superior in reducing the correlation among parameters, but EMOO design performs even better.

6. Optimal Sampling Protocol for Toxin Kinetic Modeling

If your experiment needs statistics, you ought to have done a better experiment.

- Ernest Rutherford

Part 2 of the thesis started with the premise that, if better estimates of inter-compartmental clearance (K_{ip}) and/or other model parameters are obtained, then exercise induced physiological changes can be better quantified. To obtain precise estimates of the model parameters, an intelligent experiment design is a pre-requisite. Towards this end, the previous chapter proposed a novel MOO based DOE framework for experimental design. The proposed DOE framework was tested on two case studies. It was shown that though traditional MBDOE techniques maximize the information content for precise parameter estimation, they also increase the correlation among model parameters. In this chapter, the same framework will be used on the proposed toxin kinetic model (TKM) in Chapter 3. The objective here is not to compare the performance of alphabetical and MOO based DOE, but to provide the optimal sampling protocol for TKM. Hence, only D-optimal design and its MOO based counterpart will be studied. The D-optimal design is chosen because it is the most popular experimental design criterion [140].

6.1 Sampling protocols in TKM

To improve the existing dialysis care i.e. obtaining enhanced toxin removal, TKM can play an important role [69]. For details of TKM and related literature, see Chapter 2 where a review of TKM has been presented. Briefly, TKM relates to the mathematical approximation of physiology. A number of mathematical representations such as single-pool model, two-pool model, regional blood flow model, and diffusion-adjusted regional blood flow model are available to approximate the physiology. Irrespective of the type of model employed, all of them have unknown model parameters whose estimation is necessary before the model can be employed to understand the toxin kinetics and to

decipher how the dialysis adequacy can be increased for pathophysiologically important toxins. A better understanding of the toxin kinetic behavior not only provides a rational for choosing dialysis dose [172], but also gives important insights about physiological resistance responsible for inadequate toxin removal [173]. The aspects related to physiological resistance were detailed in Chapter 3, and change in this resistance as a result of intra-dialytic exercise was presented in Chapter 4. The physiological changes related to inter-compartmental toxin transfer are lumped in a model parameter K_{ip}, which is inversely proportional to inter-compartmental resistance. The precise estimation of K_{ip} can not only quantify the exercise induced physiological changes, but also provide a better estimate of toxin removal. Apart from K_{ip}, estimation of other model parameters can facilitate a better understanding of patient physiology [29, 173].

Parameter estimation necessitates toxin concentration measurement, and number of blood samples are collected during and post-dialysis phase. The importance of intelligent sampling is paramount considering the significance of TKM [69]. Numerous sampling practices exist in the TKM literature (Table 6.1); but an important question remains unanswered: Which sampling protocol is superior (to others)? Specifically, when and how many samples should be collected such that precise estimates for physiologically important model parameters can be obtained? MBDOE techniques can potentially play an important role in this regard, because a good physiological representation in the form of DA-RBF model already exists (Chapter 3). The MBDOE paradigm has already been realized in engineering, systems biology domain [140], and also in biomedical fields such as diabetes care [167]. Despite this, there is no mention or use of MBDOE in TKM literature. This chapter intends to fill this gap.

Table 6.1: Existing sampling protocols for various uremic toxins

Reference	Solute	Dialysis regimen	Kinetic modeling approach	Sampling instances during dialysis	Sampling instances post-dialytic	Total samples
Eloot *et al*.[67]	Urea, Guanidino compounds	HD	Two-pool model	0, 5, 15, 30, 120, end dialysis	No sample	6
Schneditz *et al*.[51]*	Urea, Creatinine	HD	DA-RBF model	0, 5, 15, 30, 120, end dialysis	No sample	6
Yashiro *et al*.[87]	Urea	HD	RBF model	0, 15, 30, 45, 60, 90, 120, 180, 240	60	10
Liberati *et al*.[174]	Urea	HD	Bi- and Tri-compartment model	0, 5, 10, 30, 100, 240	5, 10, 30 ,60	10
DeSoi *et al*.[55]**	Phosphate	HD	Two-pool model	0, 15, 30, 45, 60, 90, 120, 150, 180, 210, 240	15, 30, 45, 60, 90, 120, 150, 180, 210, 240	21
Spalding *et al*.[56]	Phosphate	HD/HDF	Four-pool model	0, 40, 80, 120, 160, 200, 240	2, 15, 30, 60	11
Ursino *et al*.[63]	K^+, Na^+, Cl^-, Urea, HCO_3^-, H^+	Profiled HD	Two-pool model	0, 20, 40, 60, 80, 100, 120, 140, 160, 180, 200, 220, 240	No sample	13
Leypoldt *et al*.[72]	β_2-microglobulin	HD	Two-pool model	0, 60, 120, 180, 210	20 sec, 2, 10, 20, 30, 60	11
Stiller *et al*.[73]	β_2-microglobulin	HD	Two-pool model	0, 30, 60, 120, 180, 240	10, 20, 30, 40, 50, 60	12
Ward *et al*.[74]	β_2-microglobulin	HDF	Two-pool model	0, 60, 120, 240	20 sec, 5, 10 ,30 ,60, 90 120, 240	12
Maheshwari *et al*.[173]***	β_2-microglobulin	HDF	DA-RBF model	0, 60, 120, 240	20 sec, 5, 10 ,30 ,60, 90 120, 240	12

* Urea and creatinine concentrations reported by Eloot *et al*.[67] were used for the study.

** Recruited study subjects dialyzed for different durations. The sampling protocol presented here reflects 4 hour dialysis.

*** β_2-microglobulin concentrations reported by Ward *et al*.[74] were used for the study.

As mentioned earlier, different sampling protocols exist in the context of TKM. However, no definite consensus exists for sampling during and post-dialysis period (Table 6.1). Also, how many samples should be collected for precise estimation of model parameters remains an unstudied problem. Different clinical studies follow different sampling protocols, without accounting for the fact that those sampling protocols may be expensive due to too many samples and/or uninformative due to sampling decisions based on intuition. The objective of this work is to provide an optimal sampling protocol for precise estimation of DA-RBF model parameters. In the next section, experimental design details are presented. Obtained sampling protocols and results from MBDOE paradigm are presented in Section 6.3. A discussion on the obtained results is presented in Section 6.4. The last section summarizes the important insights developed from this investigation.

6.2 Materials and Methods

Toxin Kinetic Model

The foremost requirement for MBDOE techniques is a mathematical model with some *a priori* knowledge of values for unknown model parameters. In this work, the DA-RBF model, which arguably is the most comprehensive TKM available at present, is employed for elucidating the optimal sampling protocol. The toxin considered is β_2-microglobulin, a marker of middle-sized uremic toxins and also an independent marker of mortality and morbidity in maintenance HD patients [75]. The model description, equations, and related details can be found in Chapter 3. The original model comprised seven parameters, which were reduced to three parameters using *a priori* identifiability analysis (Section 3.3). The three model parameters that need to be estimated are K_{ip}, V_d, and f_P. The measured state is arterial serum concentration (C_{art}).

As mentioned in the previous chapter, central to the MBDOE techniques is the Fisher Information Matrix (FIM) which is calculated from sensitivity coefficients. In this particular model, the corresponding sensitivity coefficient defined at each sampling instant (t_j) is:

$$Z_{ij} = \frac{\partial C_{art,j}}{\partial \theta_i}; \text{where i} = 1,2,3 \; and \; \text{j} = sampling\ instance \qquad (6.1)$$

Note that Z_{ij} corresponds to ij^{th} element of sensitivity coefficient matrix (Z), whose size depends on the number of samples; e.g., if 10 samples are collected for estimating 3 parameters, then the size of Z matrix is 10×3.

Experimental Design Information

The flowchart of employed MBDOE methodology is shown in a previous chapter (Figure 5.4), which starts with model selection and initialization of model parameters. The model structure corresponds to the DA-RBF model. The initial guess for parameters can be obtained from the literature or from an understanding of patient physiology; e.g., β_2-microglobulin distribution volume (V_d) corresponds to extracellular fluid volume which is typically 33% of total body water. In this simulation study, the true value of patient parameters is known and the design objective is to obtain the output samples at optimal times that will result in point estimates closer to the true values. The true values of model parameters were taken as the mean estimates from Chapter 3. The initial guess for K_{ip}, V_d, and f_P were chosen at 50%, 20%, and 20% negative deviation from known true values. The inter-compartmental clearance is considered to have a larger deviation because it cannot be measured, while the V_d and f_P can be inferred from patient physiology. The true parameter values along with their initial guess values (for MBDOE purposes) are presented in Table 6.2.

Table 6.2: Model parameters with their known true values and initial guesses used for model-based design of experiment techniques

Parameter	True Value [173]	Initial guess (% deviation from true values)	
K_{ip}	44 mL/min	22 mL/min	(-50%)
V_d	14 L	11.2 L	(-20%)
f_P	0.39	0.31	(-20%)

Two important considerations in the experimental design for TKM are the experiment duration and the number of samples. From Table 6.1, it can be noted that different TKM studies have followed different criteria for both these aspects. First, for the experiment duration, it can be suggested that smaller the experiment duration the more convenient it is for the patients; however, it cannot be less than 240 min dialysis duration and so the decision variable with clinician/experimenter is the post-dialysis wait. In Table 6.1, the post-dialysis ranges from 0 to 240 min. To ascertain the optimal duration of experiment, different experiment duration (including post-dialysis wait), namely, 240 min, 300 min, 360 min, and 480 min are studied independently. The second important aspect for TKM experiment design is the total number of samples. Again, from Table 6.1, it is clear that a wide variety of sampling protocol exists. The important question is: should all the samples be collected in intra-dialytic phase, or more samples should be collected during intra-dialytic phase and less in post-dialysis phase, or vice-versa? Here, four different scenarios for total number of samples are considered (Table 6.3). The MBDOE will automatically decide the distribution of sampling instances in intra-dialysis phase as well as post-dialysis phase. For each of the experiment duration, individual sampling scenario is considered. In effect, total 16 scenarios as mentioned in Table 6.3 are considered. Note that, in design procedure, the pre-dialysis sample (at t = 0) and end-dialysis sample (t = 240 min) are mandatory because these are conventionally required for estimation of

$K_D t / V_{urea}$ or toxin reduction ratio. To account for this, the decision variables in Table 6.3 exclude the sample at t = 0, but sample at t = 240 is decided by MBDOE itself. If MBDOE does not result in t = 240 min in the final sampling protocol, then sampling t = 240 is included for final parameter estimation. Few operational constraints were also incorporated in the experimental design: a minimum gap of 5 minutes is maintained between two consecutive samples. At the same time, maximum time interval between two consecutive samples is restricted to 120 min.

Table 6.3: Two factors – Experiment duration and number of decision variables, each at 4 levels

	Number of decision variables (dv)			
Experiment duration	240 min 6 dv	240 min 8 dv	240 min 10 dv	240 min 12 dv
	300 min 6 dv	300 min 8 dv	300 min 10 dv	300 min 12 dv
	360 min 6 dv	360 min 8 dv	360 min 10 dv	360 min 12 dv
	480 min 6 dv	480 min 8 dv	480 min 10 dv	480 min 12 dv

Here, the objective is to suggest the optimal sampling instances for TKM, based on D-optimal design. At the same time, the DMOO design is also studied. In all the 16 scenarios, the arterial serum toxin concentration is obtained at these optimal sampling instances using the model with true parameter values. To incorporate the characteristics of real-time data, 10% relative noise was added to all the samples. In clinical setting, the data will be obtained from actual measurement during intra- and post-dialysis. This data is used for parameter estimation and subsequent calculation of parameter confidence interval. The entire procedure highlighted above was repeated for all the 16 scenarios shown in Table 6.3. In all the scenarios, it is assumed that post-dialysis fluid intake is at constant rate (α), while there is no fluid intake during dialysis.

6.3 Results

The MBDOE and parameter estimation procedure was repeated for each scenario. The sampling instances for each experiment scenario are shown in Table 6.4. In Table 6.5, only optimal sampling instances are shown. The mandatory samples at t = 0 and t = 240 min are not shown. In some scenarios, t = 240 is the sampling instance from optimizer itself, and hence included in Table 6.5. For DMOO-design, the presented sampling instances correspond to chosen trade-off solution from the Pareto-optimal front. For each of the 16 scenarios, one Pareto-optimal front was obtained. For illustration, only four of these Pareto-optimal fronts for the case of 8 decision variables, one each for experimental duration, are presented in Figures 6.1 to 6.4. The data-tip in each of these figures corresponds to the chosen experimental design.

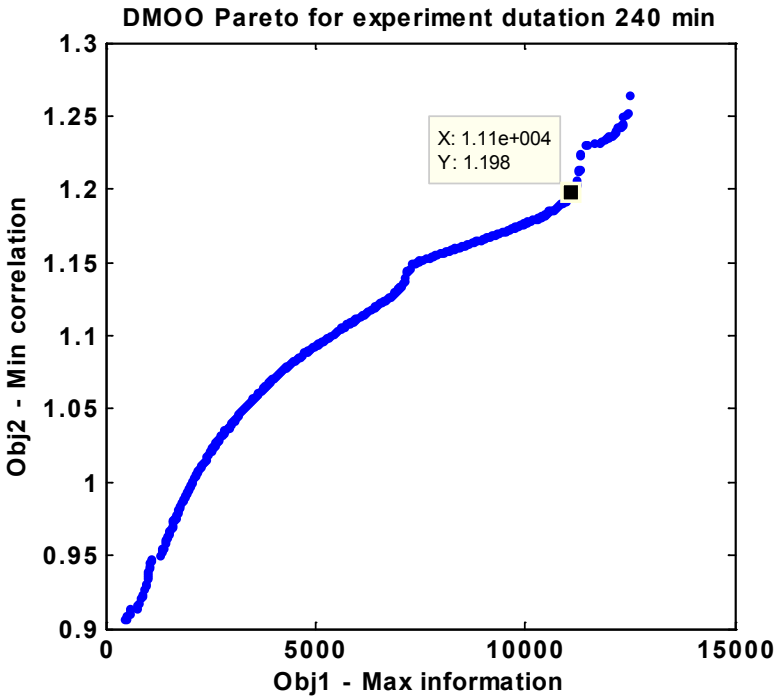

Figure 6.1: Pareto-optimal front for 240 min experiment duration and 8 decision variables

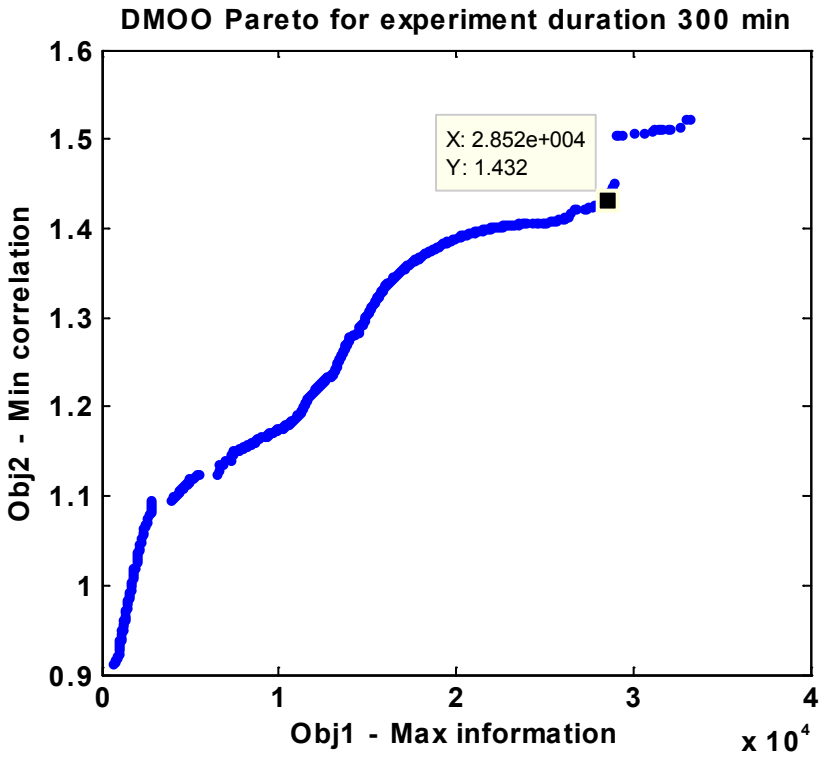

Figure 6.2: Pareto-optimal front for 300 min experiment duration and 8 decision variables

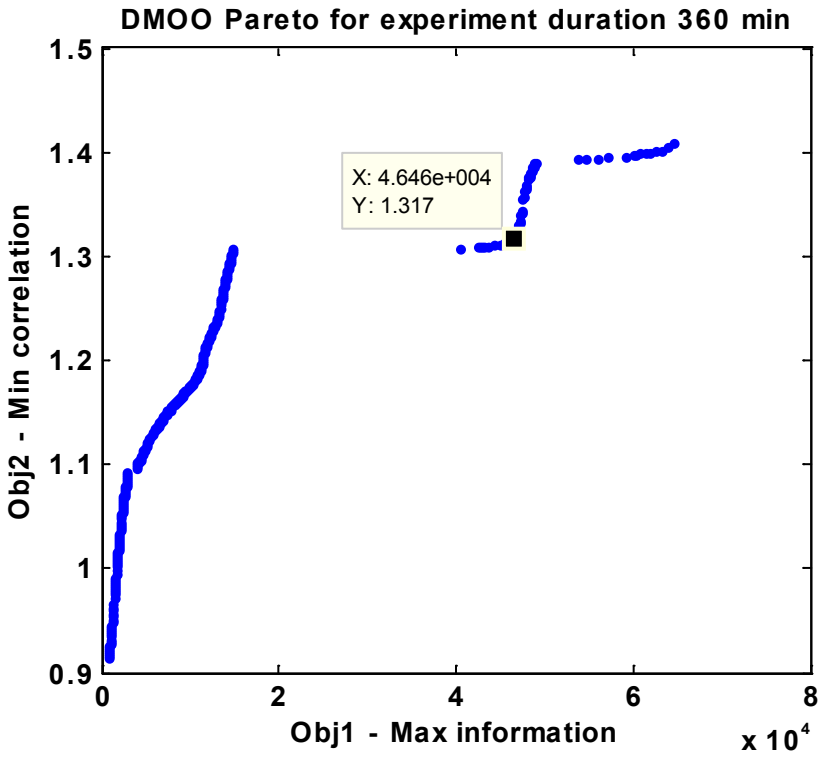

Figure 6.3: Pareto-optimal front for 360 min experiment duration and 8 decision variables

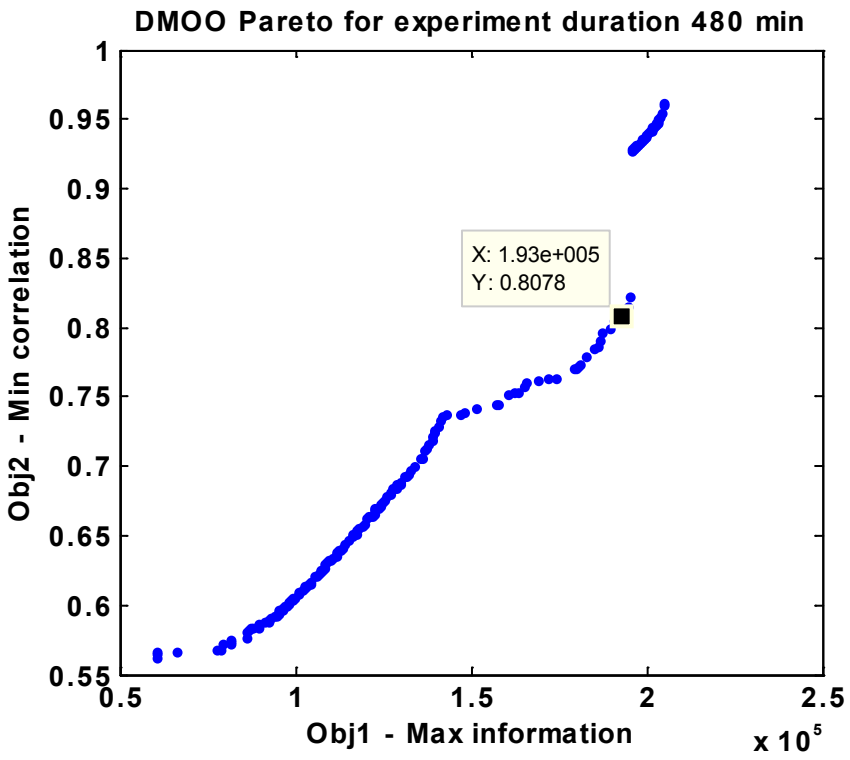

Figure 6.4: Pareto-optimal front for 480 min experiment duration and 8 decision variables

As mentioned earlier, in this simulation study, the patient model with known true parameter values is assumed as proxy to the patient, and it is simulated to obtain the toxin concentration at the optimal sampling instances. The obtained data was used to estimate the unknown model parameters K_{ip}, V_d, and f_P. To evaluate the individual parameter precision, the *t*-value for individual parameter is calculated. At the same time, the point estimates were compared using percentage normalized Euclidean distance (δ) between obtained parameter estimates and true parameters (equation 5.20). In Table 6.5, obtained point estimates with *t*-value and the δ are shown for comparative analysis. Larger *t*-value for individual parameter indicates improved precision while smaller value of δ denotes superior point estimates.

Table 6.4: Decision variables (d.v.) or optimal sampling instances in different experiment duration (during dialysis + post-dialysis). Sampling instances during dialysis (normal text) and post-dialysis (bold text), respectively.

	240 min				300 min				360 min				480 min			
	6 d.v.	**8 d.v.**	**10 d.v.**	**12 d.v.**	**6 d.v.**	**8 d.v.**	**10 d.v.**	**12 d.v.**	**6 d.v.**	**8 d.v.**	**10 d.v.**	**12 d.v.**	**6 d.v.**	**8 d.v.**	**10 d.v.**	**12 d.v.**
D-optimal design	25	22	22	19	25	25	21	19	23	23	20	20	29	27	31	28
	30	27	28	24	30	30	26	24	28	28	25	25	34	32	36	33
	101	32	33	29	105	107	31	29	110	108	30	30	154	105	41	38
	115	98	94	34	120	115	97	34	151	113	106	98	**274**	172	161	95
	235	110	99	41	240	120	102	95	**271**	118	111	103	**370**	**292**	**281**	170
	240	115	105	94	**300**	240	107	100	**360**	240	117	108	**480**	**355**	**298**	**290**
		235	110	99		**294**	120	105		**355**	240	120		**475**	**350**	**304**
		240	230	105		**300**	240	110		**360**	**350**	131		**480**	**470**	**330**
			235	110			**295**	170			**355**	230			**475**	**450**
			240	229			**300**	**290**			**360**	**350**			**480**	**470**
				235				**295**				**355**				**475**
				240				**300**				**360**				**480**
DMOO design	25	22	23	21	21	20	18	19	22	22	20	20	32	27	27	24
	93	27	28	26	26	25	23	24	27	27	25	25	152	32	32	29
	98	90	90	31	101	30	28	29	107	101	30	30	**272**	148	109	34
	115	95	95	78	120	97	97	34	120	107	100	93	**355**	**267**	168	112
	235	101	100	88	240	102	102	95	240	112	107	99	**475**	**350**	**288**	165
	240	115	105	93	**300**	120	107	100	**360**	120	112	104	**480**	**470**	**345**	**285**
		235	110	98		240	120	105		240	117	110		**475**	**465**	**339**
		240	230	105		**300**	240	110		**360**	235	115		**480**	**470**	**459**
			235	110			**295**	120			**355**	120			**475**	**465**
			240	230			**300**	240			**360**	240			**480**	**470**
				235				**295**				**355**				**475**
				240				**300**				**360**				**480**

Table 6.5: Point estimates (θ), *t*-value, and Percentage normalized Euclidean distance (δ) from true parameter for each scenario

			240 min			300 min			360 min			480 min		
			θ	***t*-value**	**δ**	**θ**	***t*-value**	**δ**	**θ**	***t*-value**	**δ**	**θ**	***t*-value**	**δ**
6 decision Variables	**D-design**	K_{ip}	26.1	2.47		28	3.02		30.5	1.95		29.5	3.36	
		V_d	14.39	3.8	42.7	15.86	2.69	40.17	16.11	2.32	35.68	14.52	9.63	33.77
		f_P	0.44	4.7		0.35	3.31		0.35	3.2		0.42	13.86	
	DMOO design	K_{ip}	26.8	1.71		28.4	3.05		30.8	1.14		31.8	3.04	
		V_d	14.49	3.46	43.2	15.74	2.83	39.18	16.05	1.97	33.53	15.36	11.2	33.37
		f_P	0.46	4.9		0.35	3.52		0.40	2.96		0.45	13.8	
8 decision Variables	**D-design**	K_{ip}	44.8	2.12		32.2	2.14		33.3	2.16		55.3	3.32	
		V_d	16.74	2.05	35.69	14.15	3.4	27.46	14.72	5.43	25	14.26	16.22	27.81
		f_P	0.27	2.29		0.37	5.15		0.40	9.73		0.35	6.91	
	DMOO design	K_{ip}	43	2.01		33	1.87		36	2.05		53.7	3.02	
		V_d	16.92	1.92	35.46	13.37	4.29	26.41	14.28	7.47	22.85	14.35	14.6	24.77
		f_P	0.28	2.17		0.42	5.75		0.44	8.34		0.35	6.55	
10 decision variables	**D-design**	K_{ip}	32.4	2.27		50.7	3.04		37.7	3.07		48.6	2.74	
		V_d	16.66	2.56	32.74	13.1	11.65	16.86	15.39	8.94	17.35	13.7	19.98	19.29
		f_P	0.38	3.20		0.38	8.2		0.33	15.14		0.45	8.2	
	DMOO design	K_{ip}	31.6	1.84		50.3	2.99		40	2.85		47.4	2.77	
		V_d	15.08	3.25	30.34	13.1	11.32	15.86	14.29	7.49	15.44	13.77	19.76	17.74
		f_P	0.42	4.38		0.38	8		0.34	8.61		0.45	7.14	
12 decision Variables	**D-design**	K_{ip}	31.9	1.84		50.4	4		49.5	3.48		46.9	3.91	
		V_d	15.19	3.01	30.88	13.43	14.64	15.64	13.72	20.27	14.56	13.62	25.1	11.46
		f_P	0.43	3.74		0.37	12.23		0.42	9.02		0.42	10.66	
	DMOO design	K_{ip}	38	1.46		45.7	3.19		46.3	3.91		48.8	3.56	
		V_d	13.32	4.86	24.96	13.36	14.09	14.88	14.93	11.1	14.52	13.64	19.98	11.56
		f_P	0.47	4.72		0.44	10.9		0.34	10		0.4	8.57	

6.4 Discussion and Sampling Recommendation

The importance of TKM has been widely recognized in dialysis community and recently elucidated in an editorial review titled "What can the dialysis physician learn from kinetic modeling beyond Kt/V_{urea}?" by Eloot *et al*. [69]. The review recommends further clinical research for kinetic studies especially for the toxins whose impact on patient outcome is well established. A number of clinical studies have been performed to improve HD care through improved understanding of toxin kinetics via TKM. The information from clinical trials completely depends on the blood samples collected. These blood samples are used to estimate the unknown model parameters in the TKM. From a preliminary study of 2 patients, Eloot *et al*. determined that 14 samples during dialysis can characterize the toxin kinetics [67]. A number of TKM studies prescribe the sampling at equal time-intervals during dialysis, and frequent sampling after dialysis [73, 74]. There is no consensus among medical professionals or modelers about the sampling instances and sampling for TKM remains an intuition driven strategy. To the best of our knowledge, there is no simulation/clinical study which explores the optimal sampling protocol for TKM in maintenance HD subjects. Acknowledging the importance of sampling in TKM, an MBDOE based approach was employed in this work to elucidate the optimal sampling instances. Specifically, the D-optimal design was employed to suggest the optimal sampling instances. The foremost and important observation from the optimal sampling instances reported in Table 6.4 is that more samples should be collected during early phase of dialysis when maximum change in arterial serum toxin concentration takes place. The discussion below details the important outcome of MBDOE based sampling in comparison with existing literature.

Intra-dialytic sampling: Sampling during dialysis is important because plasma toxin/solute concentration decreases exponentially during the initial phase of dialysis.

Eloot *et al*. have qualitatively highlighted the importance of intra-dialytic sampling protocol and suggested that logarithmic sampling intervals should be observed rather than a linear sampling interval protocol [69]. In other words, unlike sampling at regular intervals, more samples should be collected in the early phase of dialysis. The MBDOE based sampling results presented in Table 6.4 corroborate the logarithmic sampling protocol in intra-dialytic phase. The prescribed sampling in the intra-dialytic phase typically manifest in pairs or triplets, e.g. in 240 min experiment duration with 6 decision variables scenario, sampling at 25 min is followed by sampling at 30 min (Table 6.4). The 5 min interval between successive samples is due to the inherent constraint that the minimum difference between consecutive samples should be 5 min. This minimum interval can be adjusted based on the available resources. It is recommended that minimum sampling interval should not be decreased beyond 5 min because when samples are too close the effect of noise can be more pronounced, e.g. toxin concentration at t = 30 min should be less that at t = 25 min. If noise is high or samples are too close then owing to randomized nature of noise it may so happen that concentration at t = 30 min is higher than that at t = 25 min. The intra-dialytic sampling results from MBDOE are different from the sampling protocols in the existing TKM studies [55, 67, 73, 174] (see Table 6.1). Also, the sampling instance results in all scenarios suggest that there is no need for sampling during the first 20 min of dialysis.

Post-dialysis sampling: Though intra-dialytic samples are important, steep change of toxin concentration in post-dialysis phase renders the post-dialysis sampling important as well. This is evident from the point estimates for 240 min experiment duration (Table 6.5), where irrespective of the number of samples, it is not possible to estimate all model parameters accurately as well as precisely. The results here also advocate the importance of post-dialysis samples.

In the simulation here, the post-dialysis sampling is restricted to 4 hours maximum i.e. patient waits for 4 hours post-dialysis. Three different scenarios are considered – 60 min, 120 min, and 240 min post-dialysis wait. It can be understood that, the shorter the post-dialysis wait, the more convenient it is for patients. The important question is what post-dialysis wait is optimal for precise and accurate estimation of model parameters?

Firstly, the post-dialysis sampling results suggested by MBDOE are in contrast with existing literature. From Table 6.1, it can be observed that post-dialysis sampling should be frequent [55, 56, 73, 74, 174], which is based on the assumption that there is significant change in toxin concentration. This is due to the fact that during dialysis the high dialyzer clearance causes faster removal of toxins from blood compartment. The rapid decrease in serum toxin concentration leads to a considerably wider gap between the IC and the EC toxin concentrations, since only a small proportion of toxins pass over from the IC to the EC space during dialysis. This results in a rapid increase of plasma concentration after dialysis. This increase is referred to as *rebound*. The argument in favor of post-dialytic sampling is that the magnitude of rebound is higher when K_{ip} is low (as in case of middle-sized toxins). However, similar argument can be proposed for concentration change during dialysis, i.e. when K_{ip} is low, then a steep decline in serum toxin concentration is observed (again as in case of middle-sized marker toxins or intracellular toxins). The MBDOE results appear to favor the second argument and suggest that more samples should be collected during intra-dialytic phase rather than during rebound (Table 6.4 – see 300 and 360 min experiment duration). Popovich *et al*. have also suggested that steep decline in serum toxin concentration can be used to calculate the cell membrane mass transfer coefficient (K_{ip}) [175]. The post-dialysis sampling results here corroborate the above argument and recommends that very few

sample(s) is/are required which should be collected towards the end of experiment duration.

Secondly, as the experiment duration increases, the point estimates improve. The best point estimates both in terms of accuracy and precision are obtained for 480 min duration with 12 decision variables. Nevertheless, 60 min post-dialysis wait (i.e. 300 min experiment duration) is adequate for estimating all three parameters of DA-RBF model. It is interesting to note that unlike the MBDOE results for 300 min and 360 min experimental duration, the MBDOE results for 480 min experiment duration recommends more samples in post-dialysis phase and less during the dialysis phase itself. The plausible reason behind this exception can be that 4 hours post-dialysis wait is sufficient time for toxin equilibration or to characterize the K_{ip}. Frequent sampling during this phase will capture the role of inter-compartmental resistance in delayed toxin transfer from IC to EC. On the other hand, MBDOE results for 300 min or 360 min experiment duration suggest frequent sampling in intra-dialytic phase where sharp change in toxin concentration takes place. One major problem of note in longer experiment duration is the fluid intake by patient. The fluid intake will affect the bodily fluid volume which will change the toxin distribution volume (V_d). A patient cannot restrict his/her thirst, but for shorter experiment duration the frequency of fluid intake will be less than that in longer experiment. This further recommends the 300 min experiment.

Total number of samples: Irrespective of experiment duration, sampling at 6 time points are too little to obtain good quality estimates of model parameters. It can be anticipated that as the number samples increases, the parameter precision will improve. This is evident from the results in Table 6.5 – for the same experiment duration, as the number of samples increases, the *t*-value for individual parameter i.e. parameter precision improves.

It appears that 10 decision variables is the optimal number of samples. Further increasing the decision variables will inevitably increase the cost of laboratory analysis with little improvement in the precision of estimates. In effect, the experiment duration of 300 min with 10 decision variables will suffice for precise as well as accurate point estimates.

D-optimal vs. DMOO design: The DMOO design clearly outperforms the D-optimal design. In almost all the scenarios, the percentage normalized Euclidean distance (δ) is smaller for DMOO design, i.e. the DMOO based sampling protocol results in slightly superior point estimates than those obtained by D-optimal design. The improved point estimates are obtained at some cost – the parameter precision becomes poorer. This can be anticipated because DMOO design compromises between information and correlation. In a few instances, DMOO based experimental design results in better precision than that obtained by D-optimal design; e.g., the *t*-values for V_d and f_P in experiment duration of 240 min with 12 decision variables are larger in DMOO design. However, DMOO design does not improve the precision of **all** parameters. This indicates that MOO based design provides a better distribution of information for estimation of model parameters. The sampling instances and corresponding parameter estimates in D- vs. DMOO design can be found in Tables 6.4 and 6.5, respectively. Unlike the case studies discussed in Chapter 5, the HD experimental design does not involve any manipulated variable which can be used to perturb the system. The only design variables are sampling instances. This may be one of the reasons why D- and DMOO designs provide similar point estimates for model parameters.

6.5 Summary

MBDOE techniques can provide optimal moves for available manipulated variables and optimal sampling instances for measurements, so that the uncertainty in parameter

estimates can be minimized. Hence, an MBDOE based sampling protocol for TKM was studied for the first time. Conventional sampling protocols recommend sampling during intra-dialytic and post-dialysis phase; however, different TKM studies used different sampling times. In this study, four distinct experiment durations, namely 240 min, 300 min, 360 min, and 480 min were considered. For each of these durations, distinct experimental protocols with 6, 8, 10, or 12 decision variables were investigated using DA-RBF model as basis for MBDOE. The results indicate that, irrespective of the number of measurement samples, the 240 min experiment is inadequate for precise and accurate estimation of model parameters. Similarly, irrespective of experiment duration, sampling at 6 time points are too little to obtain good quality estimates of model parameters. Among 300 min, 360 min, and 480 min experiment duration, the point estimates from 480 min outperform the rest. The sampling instances in 480 min experiment duration are primarily in the post-dialysis phase, while for 300 and 360 min experiment duration, the sampling instances are primarily in the intra-dialytic phase. Though the point estimates from 300 min and 360 min experiment are inferior to those obtained in 480 min experiment, they are reasonably good when compared based on percentage normalized Euclidean distance. Also, the 480 min experiment duration can be too long and logistically expensive. Considering these aspects, this work recommends a sampling protocol of 11 samples collected over 300 min experiment duration, as adequate for both precise and accurate point estimates.

7. Conclusions and Recommendations for Future Works

The important thing is not to stop questioning. Curiosity has its own reason for existing.

- *Albert Einstein*

Hemodialysis, a method to detoxify blood, is an established life-saving treatment for ESRD patients. Remarkable improvements in HD care in the last five decades has rendered HD as the most sought after renal replacement therapy [4]. For more than 2.3 million patients worldwide, HD is part of life [12]. Nevertheless, patients on HD still have poor quality of life, high morbidity and mortality. The pertinent question is "what can be done to improve the existing HD care?" Improvement can be achieved via several ways. The direction followed in this thesis is to suggest approaches to enhance the toxin removal, which is the chief aim of HD. Improvement in toxin removal can be studied via experimental studies and/or computer simulations. The experimental focus can be on aspects such as clinical testing of more efficient dialyzer for enhanced toxin removal, comparing the performance of daily dialysis vs. conventional 3 times × 4 hours dialysis, etc. One should note that conducting experiments without sound hypotheses rarely provides good outcomes, and one may end up wasting useful resources. Indeed, a good understanding of system is the foremost requirement to form sound hypotheses, and clinicians can provide that understanding. The system understanding can also be obtained via computer simulation, which is a common Process System Engineering (PSE) technique. The PSE approach represents the underlying system as a mathematical model which can be simulated beyond the conventional settings. These simulations can form the basis of generating new hypotheses and thus suggesting new clinical studies. This research work has followed this combined approach of modeling as well as clinical testing of model generated hypotheses. As the mathematical model forms the foundation

for simulations and subsequent clinical studies, the aspects pertaining to model improvement are also explored. The approach for model improvement is based on improved estimates of model parameters, which are obtained via MBDOE approach.

The salient contributions from this thesis work are highlighted in Section 7.1. This thesis work has also led to more research questions which need to be addressed in future. The potential future works are presented in Section 7.2.

7.1 Contributions

The contributions from this thesis work are highlighted in the order of their occurrence in the preceding chapters. Since the thesis focuses on two different aspects – the first on TKM and clinical testing of model generated hypothesis, and the second on improvement of TKM itself via MBDOE for improvement of model parameter estimates, the contributions pertaining to each aspect are discussed separately in Sub-sections 7.1.1 and 7.1.2.

7.1.1 Toxin Kinetic Modeling and Clinical Study

TKM and clinical study constituted Part 1 of this thesis. Chapter 2 provided the foundation for TKM paradigm in HD care. Starting with the toxin classification and concept of marker toxin(s), the importance of TKM was elucidated and related literature was reviewed. The evolution of TKM starting from single-pool model assumption to the two-pool model and physiological RBF model to the present state-of-the-art DA-RBF model was presented. An overview of TKM studies for a number of uremic toxins such as urea, creatinine, guanidino compounds, phosphate, and β_2-microglobulin, was also provided. It was noted that the DA-RBF model, despite being a fairly comprehensive representation of physiology, is limited to characterizing the kinetics of small-sized uremic toxins urea and creatinine only. Cognizant of this gap in the TKM literature, the

Chapter 3 of this thesis explored the extension of DA-RBF model for middle-sized marker toxin, β_2-microglobulin.

DA-RBF model for β_2-microglobulin and model application: In this research contribution, a comprehensive model of middle-sized marker toxin β_2-microglobulin was presented. The model is an adaptation and refinement of existing DA-RBF model [51], which was proposed for urea. However, this model by Schneditz *et al*. suffers from the drawback of having too many model parameters. This has limited the acceptability of DA-RBF by dialysis research community [69, 86]. Also, the model was never validated with real clinical data. To overcome the mentioned drawbacks, first *a priori* identifiability analysis was employed to elucidate the estimable subset of model parameters. This step reduced the number of unknown parameter from seven to three. Subsequently, the model was validated with the clinical data of 10 patients obtained from Dr. Richard Ward (of University of Louisville). The parameter estimates for proposed DA-RBF model were better representative of HD patient physiology than those obtained from the existing two-pool model parameter estimates [74].

Note that the model application is not restricted to explain the underlying HD process; rather it should be further employed to study aspects which can improve the toxin removal. Accordingly, this research contribution simulated the effect of exercise on toxin removal. Based on the simulation results, a new hypothesis is proposed to explain the effect of intra-dialytic exercise toxin removal. It was suggested that exercise not only increases the cardiac output (CO), but also decreases the peripheral vascular resistance. More importantly, the simulation results suggest that decrease in inter-compartmental resistance is the dominant factor contributing towards enhanced toxin removal. This work on DA-RBF model for β_2-microglobulin and its application has been published [173]; this

has been reviewed post-publication by Dr. Daniel Schneditz, who designated this research contribution as a recommended read in Faculty of 1000 [176]. To advance further, clinical studies are required to test the proposed hypotheses.

Clinical study to investigate the effect of exercise on physiological changes: Exercise during dialysis has been shown to improve the removal of small-sized toxins, but no such study exists for middle-sized uremic toxins. In Chapter 3, it was hypothesized that intra-dialytic exercise not only increases the perfusion of remote peripheral compartments but also decrease the inter-compartmental resistance, which is often designated as major barrier for toxin removal [74]. To test this hypothesis and to understand the exercise physiology, a pilot clinical study was designed. The study obtained prior ethics approval from the National Healthcare Group, Singapore, and was registered in www.clinicaltrials.gov with trial identifier NCT01674153. In this self-controlled, open label, randomized prospective clinical study, a total of 15 subjects satisfying the pre-defined inclusion-exclusion criteria were enrolled. Each study subject underwent three study sessions - HD, HDF, and HD-Ex. Here, HDF is also studied because HDF is widely proclaimed as superior to HD. Out of these 15 subjects, 12 completed all three sessions, one subject completed HD and HDF, while two subjects withdrew prior to their initiation into study sessions. The questions asked in this clinical study were as follows: (1) what physiological changes are responsible for decrease the inter-compartmental resistance? (2) will those physiological changes be sufficient to increase the removal of middle-sized uremic toxins? and (3) can intra-dialytic exercise provide the similar quantum of toxin removal as that obtained in HDF?

It is known that exercise increases the CO which mobilizes the toxins from remote peripheral compartments [85, 98]. However, the factors responsible for decreased inter-

compartmental resistance are not explicitly known as yet. It was hypothesized that exercise increases the body core temperature thereby decreasing the peripheral resistance. To test this hypothesis, the arterial and venous blood temperatures were measured using BTM. The clinical results confirmed that intra-dialytic exercise increase the body core temperature. The change in core temperature from baseline was as much as 0.96 ± 0.23 °C. To quantify the corresponding physiological changes, the Doppler Ultrasound Echocardiography was employed. Echocardiography provided information about the increase in CO and decrease in peripheral vascular resistance index, which can be associated with increase in body core temperature. The maximum mean percentage increase in CO is 106 ± 32%, while the maximum mean percentage reduction in peripheral vascular resistance index was 94 ± 45%. This answers the first question and elucidates the factors responsible for increased toxin removal.

To answer the next questions, the quantum of toxin removed was assessed via % toxin rebound. A lower % toxin rebound indicates higher toxin removal. The studied toxins space was not restricted to β_2-microglobulin. Other uremic toxins namely, urea, creatinine, and phosphate were also studied. For β_2-microglobulin, it was observed that HD-Ex outperformed that HD and resulted in lower post-dialytic rebound, but HDF still outperformed HD-Ex and resulted in still lower post-dialytic rebound. Nevertheless, one should note that the patients were unconditioned to exercise and exercise intensity was minimum (set at zero resistance). It can be hypothesized that prolonged intra-dialytic exercise intervention can lead to equivalent or even more toxin removal than that obtained in HDF. For urea and creatinine, all three study sessions (i.e. HD, HDF, and HD-Ex) gave similar results for post-dialytic rebound. Interestingly, for phosphate, the HD-Ex resulted in significantly higher toxin rebound than that obtained in HD and HDF. It is hypothesized that this happens due to the delayed mobilization of phosphate from

bone matrix. This hypothesis is further strengthened due to the existing studies where pre-dialysis exercise has shown its potential to decrease the serum phosphate concentration [99]. Only long term clinical studies can prove the validity of above mentioned hypothesis. The clinical study related content is presented in Chapter 4 of the thesis. A portion of this chapter has been published in [177].

7.1.2 Model-based Design of Experiments

Part 1 of the thesis focused on the DA-RBF model for β_2-microglobulin, its application, and testing of model generated hypotheses. It is the model simulations that helped in explaining the effect of intra-dialytic exercise. This culminated in the clinical study where the effect of exercise on physiological changes and toxin removal was investigated. A good model is the foremost requirement for model-based hypotheses testing and clinical studies. It is known that a model is as good as its estimated parameters [131]. Hence, Part 2 of the thesis contributed toward improvement of the DA-RBF model parameters proposed in this thesis. To improve or estimate the model parameters, appropriate data needs to be collected. The important question is: what is the best experiment and sampling protocol? In this context, MBDOE techniques have become an essential tool to plan and conduct experiments that provide high information for a given experimental effort. However, an inherent drawback in existing MBDOE techniques was observed. These techniques not only maximize the system information for improvement of parameter precision but also result in increased correlation among model parameters which corrupt the final point estimates. Second part of the thesis contributed to the scientific literature by proposing a novel MOO based experimental design solution which appropriately addressed the correlation issue (Chapter 5). Subsequently, the sampling protocol for newly proposed DA-RBF model was elucidated (Chapter 6).

Multi-objective optimization based MBDOE framework:

To obtain the maximum system information from limited experimental work, MBDOE techniques have played a pivotal role serving as a vital link between the modeling and experimental worlds. The purpose of MBDOE techniques is to devise intelligent experiments such that the parameter estimates from the resulting experimental data are of "best" statistical quality. However, it was noted that existing MBDOE techniques, such as D-, A-, and E-optimal designs suffer from inherent drawback of maximizing the correlation among model parameters; this can deteriorate the point estimates and/or reduce the parameter precision. To overcome this drawback, a novel MOO based MBDOE framework was proposed. The proposed framework incorporates the traditional alphabetical design objective to maximize the information measure and another objective to minimize the correlation measure (between parameters), thus resulting in DMOO, AMOO, and EMOO designs, which are counterparts of D-, A-, and E-optimal designs, respectively. The MOO based designs result in a Pareto-optimal front from which an appropriate trade-off solution can be chosen as MOO based experimental design. The proposed framework was tested for two case studies, namely, a three parameter Type 1 diabetes model and a four parameter Baker's yeast fermentation reactor model. The results show that proposed MOO designs outperform the existing single objective alphabetical designs. This research contribution has already been published [178].

Optimal sampling protocol for TKM:

The aim of this research contribution was to elucidate the sampling protocol for TKM. The TKM literature is rich in modeling studies for a number of uremic toxins, but the important question – "when should one collect the blood samples so that TKM parameters can be better estimated?" remains unanswered. A good estimation of these

parameters can lead to new hypotheses and ideas for further clinical studies. In the existing TKM literature, there is no mention of optimal sampling protocol, except a qualitative recommendation from Eloot *et al*. who suggested logarithmic sampling i.e. frequent sampling in early phase of dialysis [69]. However, there is no recommendation for post-dialytic sampling. Also, there is no definite consensus for sampling, as different TKM studies have followed different sampling protocols (see Table 6.1). This research contribution provided the optimal sampling protocol for "best" or precise estimation of DA-RBF model parameters. The results suggested that 300 min experiment duration with 10 samples (excluding sample at t = 0) interspersed in dialysis as well as post-dialytic phase is sufficient to obtain precise estimates for model parameters. The obtained results are important because it specifies the optimal post-dialytic wait and restricts it to 60 min. The suggested optimal sampling instances have potential to encourage nephrologists and TKM researchers to explore kinetic studies for other uremic toxins. The characterization of TKM can also pave ways for identifying global marker(s) for uremia in the future.

7.2 Recommendations for Future Works

This section highlights the important topics that may be studied by interested researchers in future.

7.2.1 One TKM for All Marker Toxins

Currently there appears to be little or no investigation on the kinetic behavior for both small and large-sized uremic toxins in a single clinical study, i.e. when the marker toxins are measured and analyzed within the same experiment. Eloot *et al*. have explored the kinetics of number of guanidino compounds in same experiment [29, 67], but all the studied toxins are small-sized molecules and are found in both IC and EC. Also, their objective was to test the hypothesis that kinetic behavior of other small-sized uremic

toxins is different from urea. It does not answer the question "which model is better for majority of uremic toxins?" Studying both small (urea, creatinine) and large-sized marker toxins (β_2-microglobulin) in a single session can provide this information based on the estimates of respective toxin distribution volume (V_d). The urea or creatinine distribution volume will correspond to total fluid volume, while the β_2-microglobulin distribution volume corresponds to extracellular fluid volume. These distribution volume estimates can be compared with those obtained from anthropometric formulae [96] or bioelectrical impedance method [97]. A global TKM study of this kind can provide insight of fluid distribution in HD patients and a better understanding of physiology. More importantly, it can highlight the relative superiority of DA-RBF and the two-compartment models. One TKM (with toxin specific parameters) can provide guidelines for removal of a wide-spectrum of uremic toxins.

7.2.2 Clinical Study: HDF vs. HD-Ex

HDF has been proclaimed as more efficient than the conventional HD. The convection augmented toxin removal is supposed to enhance the toxin removal in HDF, but long term clinical outcomes with regard to pre-dialysis toxin concentration remained similar in both HD and HDF [109-111, 179]. On the other hand, a randomized clinical study comparing HDF and HD has shown that HDF potentially improves the cardiovascular status of ESRD patients but could not reduce mortality rate [109]. The debate on the superiority of HDF over conventional HD is still on. A pro-con debate about HDF controversy in the recent ERA-EDTA conference (http://www.era-edta2013.org/en-US/industry-symposium-15) further suggest that, before HDF is universally accepted, more research on HDF is required.

As of now, it is understood that the efficacy of HDF is restricted by inter-compartmental resistance [20, 74, 117]. The clinical study results in presented in Chapter 4 indicated that this resistance can be overcome by intra-dialytic exercise (HD-Ex). This leads to the following questions:

1. Will this decrease in resistance translate into reduced pre-dialysis toxin concentration?
2. Will prolonged HD-Ex result in lower pre-dialysis toxin concentration than HDF?

The clinical study performed as part of this doctoral thesis research was a single session study and was not designed to answer the above questions. To answer these questions, a long-term clinical study could be designed so as to compare HDF and HD-Ex.

Based on the existing evidence, it can be hypothesized that HD-Ex can perform similar or better in terms of toxin removal compared to HDF. This hypothesis is based on the clinical study results where HD-Ex performed much better than HD for β_2-microglobulin removal, but HD-Ex still performed poorer that HDF. This may be due to the fact that recruited patients were unconditioned to exercise. Prolonged HD-Ex may not only enhance the toxin removal but also the patient's quality of life, which is one the major goals for HD patients. Intra-dialytic exercise prescription is reported to be useful for treatment of depression in ESRD patients [180]. Can HDF also alleviate the depression? All these hypotheses should be tested via randomized prospective clinical study.

7.2.3 Clinical Study: Cool vs. Warm Dialysate

The focus of this research has been on enhancing the toxin removal. The notion is that increased toxin removal will culminate in improved patient outcome in long term. While this may be the case, short-term outcomes are also important. One of the common short-

term complications for HD patients is the intra-dialytic hypotension (IDH) which affects almost 30% of dialysis patients [181]. Though short-term in nature, IDH has been suggested as one of the most important cause of mortality and morbidity in dialysis patients [60]. It occurs when patient's cardiovascular responses cannot compensate for large fluid losses that can occur with high UF. IDH can also occur when UF rate is more than the plasma refilling rate and persists for long enough to reach a critical threshold in the reduction of blood volume. The decrease in blood volume results in sudden drop in blood pressure which results in severe cramps, dizziness, headache, etc. The easy solution to this approach is to decrease the UF rate thereby preventing further reduction in blood volume. The downside of this approach is that patient is left "fluid overloaded", which results in chronic hypertension and associated complications.

The other important maneuver is the reduction in dialysate temperature. The conventional dialysate temperature is set at 36°C. The cool dialysate is recommended at 35 or 35.5°C. The cool dialysate decreases the blood temperature. When this cool blood mixes with the systemic circulation the body core temperature decreases. To adjust for the reduced body core temperature, vasoconstriction takes place preventing the blood flow to remote peripheral compartments and the central fluid volume is ultimately stabilized. The results presented in Chapter 4 of this thesis pointed out that increase in body core temperature leads to increased toxin removal. This implies that cool dialysate will potentially inhibit the toxin removal. The effect of cool dialysate on urea removal has been studied in 1995 and 1998, and it was found that urea removal remains unaffected with cool dialysate [125, 182]. Nevertheless, it has been mentioned repeatedly in this thesis that urea removal does not ensure the removal of other uremic toxins, because urea is small in size and urea exchange between compartments is facilitated by urea transporters on the cell wall. This explains why cool dialysate could not inhibit the urea removal. The question is – will cool

dialysate not inhibit the removal of other small and large-sized uremic toxins? To answer this question, clinical studies could be conducted to study the effect of cool vs. warm dialysate (37°C). A pilot clinical study funded by National Kidney Foundation, Singapore (NKFRC/2012/01/08) is currently under progress. This study is designed to answer the above mentioned question.

7.2.4 Model Predictive Controller and Dialysate Temperature

The previous section highlighted the importance of cool dialysate for hemodynamic stability and also its unfortunate side-effect of reduced toxin removal. Therefore, a clinical study comparing cool and warm dialysate was proposed. If the above mentioned hypothesis is indeed correct, then warm dialysate should result in improved toxin removal but poor hemodynamic stability. This would lead to the temperature induced trade-off between toxin removal and hemodynamic stability. As future work, one could explore intelligent control of dialysate temperature. The Model Predictive Controller (MPC) technique could use the current hemodynamic response and a model to predict the future hemodynamic responses. Based on this information, the MPC can take appropriate corrective actions and either increase or decrease the dialysate temperature to elicit the enhanced toxin removal and hemodynamic stability and avoid IDH.

7.2.5 Exploring Synergies between Exercise Regimen and Dialysate Temperature

Experimental results in Chapter 4 indicate that intra-dialytic exercise leads to increase in body core temperature. For three bouts of exercise, three distinct peaks in arterial blood temperature were observed (Figure 4.5). On the other hand, it is also known that increased body core temperature can potentially lead to incidence of IDH (see Sub-section 7.2.3) [60, 183]. This implies the possible hemodynamic instability due to intra-dialytic exercise. In summary, intra-dialytic exercise and dialysate temperature can

change the body core temperature. A synergy of these two aspects can further maximize the toxin removal and minimize the hemodynamic instability. In other words, exercise time, duration, intensity, and the dialysate temperature are primary handles to attain the improved patient outcomes. Careful experimentation and modeling of these aspects can help to decrease the mortality and morbidity in HD patients, and they are recommended as future work.

7.2.6 MOO based DOE for Larger Systems

In Chapter 5 of the thesis, the MOO based DOE framework was proposed. The framework was tested on two case studies, namely, the three-parameter type 1 diabetes model and the four-parameter Baker's yeast fermentation reactor model. Those case studies were used to illustrate the effect of correlation on parameter estimates and to demonstrate that the proposed MOO based DOE performs better than the basic alphabetical experimental designs. Future work could study the performance of proposed framework on systems characterized by large number of parameters. Another important aspect in proposed DOE framework is the Pareto-optimal point selection. This aspect could be explored in this future work.

REFERENCES

[1] W.M. Saltzman, *Biomedical engineering: bridging medicine and technology*: Cambridge University Press, 2009.

[2] C. Cobelli and E. Carson, *Introduction to modeling in physiology and medicine*: Academic Press, 2007.

[3] J. Levy, E. Brown, C. Daley, and A. Lawrence, *Oxford handbook of dialysis*: Oxford University Press, 2009.

[4] J. Himmelfarb and T.A. Ikizler, "Hemodialysis," *New England Journal of Medicine*, vol. 363, (no. 19), pp. 1833-1845, 2010.

[5] R. Sam, M. Vaseemuddin, W.H. Leong, B.E. Rogers, C.M. Kjellstrand, and T.S. Ing, "Composition and clinical use of hemodialysates," *Hemodialysis International*, vol. 10, (no. 1), pp. 15-28, 2006.

[6] "Chronic kidney failure," in: http://www.mayoclinic.com/health/medical/IM00801 Mayo Clinic, 2013, [25 July 2013].

[7] "Your Health," in: http://www.aurorahealthcare.org/yourhealth/healthgate/images/si55551793.jpg Aurora Health Care, [25 Jul 2013].

[8] S.P. McDonald, M.R. Marshall, D.W. Johnson, and K.R. Polkinghorne, "Relationship between dialysis modality and mortality," *Journal of the American Society of Nephrology*, vol. 20, (no. 1), pp. 155-163, 2009.

[9] N. Di Paolo and G. Sacchi, "Peritoneal vascular changes in continuous ambulatory peritoneal dialysis (CAPD): an in vivo model for the study of diabetic microangiopathy," *Peritoneal Dialysis International*, vol. 9, (no. 1), pp. 41-45, 1989.

[10] E.F. Vonesh, J.J. Snyder, R.N. Foley, and A.J. Collins, "Mortality studies comparing peritoneal dialysis and hemodialysis: What do they tell us?," *Kidney International*, vol. 70, (no. S103), pp. S3-S11, 2006.

[11] "U S Renal Data System, USRDS 2012 Annual Data Report: Atlas of Chronic Kidney Disease and End-Stage Renal Disease in the United States " National Institutes of Health, National Institute of Diabetes and Digestive and Kidney Diseases, Bethesda, MD2012.

[12] "ESRD patients in 2012: A Global Perspective," in http://www.vision-fmc.com/I/pazienti-esrd.html *ESRD patients*, Bad Homburg, Germany:Fresenius Medical Care, 2012, [01 May 2013].

[13] D.E. Weiner, H. Tighiouart, M.G. Amin, P.C. Stark, B. MacLeod, J.L. Griffith, D.N. Salem, A.S. Levey, and M.J. Sarnak, "Chronic Kidney Disease as a Risk Factor for Cardiovascular Disease and All-Cause Mortality: A Pooled Analysis of Community-Based Studies," *Journal of the American Society of Nephrology*, vol. 15, (no. 5), pp. 1307-1315, 2004.

[14] A. Yavuz, C. Tetta, F.F. Ersoy, V. D'intini, R. Ratanarat, M.D. Cal, M. Bonello, V. Bordoni, G. Salvatori, E. Andrikos, G. Yakupoglu, N.W. Levin, and C. Ronco, "Uremic toxins: A new focus on an old subject," *Seminars in Dialysis*, vol. 18, (no. 3), pp. 203-211, 2005.

[15] G.A. Block, P.S. Klassen, J.M. Lazarus, N. Ofsthun, E.G. Lowrie, and G.M. Chertow, "Mineral metabolism, mortality, and morbidity in maintenance hemodialysis," *Journal of the American Society of Nephrology*, vol. 15, (no. 8), pp. 2208-2218, 2004.

[16] J. Himmelfarb, P. Stenvinkel, T.A. Ikizler, and R.M. Hakim, "The elephant in uremia: oxidant stress as a unifying concept of cardiovascular disease in uremia," *Kidney International*, vol. 62, (no. 5), pp. 1524-1538, 2002.

[17] R. Vanholder, "The ultimate salt war? Uraemic toxins are all that count in dialysis patients," *Nephrology Dialysis Transplantation*, vol. 27, (no. 1), pp. 62-66, 2012.

[18] R. Fissell, G. Schulman, M. Pfister, L. Zhang, and A.M. Hung, "Novel Dialysis Modalities Do We Need New Metrics to Optimize Treatment?," *The Journal of Clinical Pharmacology*, vol. 52, (no. 1 suppl), pp. 72S-78S, 2012.

[19] P. Blankestijn, "Has the Time Now Come to More Widely Accept Hemodiafiltration in the United States?," *Journal of the American Society of Nephrology*, vol. 24, (no. 3), pp. 332-334, 2013.

[20] R.A. Ward, B. Schmidt, J. Hullin, G.F. Hillebrand, and W. Samtleben, "A comparison of on-line hemodiafiltration and high-flux hemodialysis: A prospective clinical study," *Journal of the American Society of Nephrology*, vol. 11, (no. 12), pp. 2344-2350, 2000.

[21] C. Almeras and À. Argilés, "Progress in Uremic Toxin Research: The General Picture of Uremia," *Seminars in Dialysis*, vol. 22, (no. 4), pp. 329-333, 2009.

[22] S. Massry, "Parathyroid hormone: a uremic toxin," *Advances in experimental medicine and biology*, vol. 223, pp. 1, 1987.

[23] R. Vanholder, U. Baurmeister, P. Brunet, G. Cohen, G. Glorieux, and J. Jankowski, "A bench to bedside view of uremic toxins," *Journal of the American Society of Nephrology*, vol. 19, (no. 5), pp. 863-870, 2008.

[24] R. Vanholder, R. De Smet, G. Glorieux, A. Argiles, U. Baurmeister, P. Brunet, W. Clark, G. Cohen, P.P. De Deyn, R. Deppisch, B. Descamps-Latscha, T. Henle, A. Jorres, H.D. Lemke, Z.A. Massy, J. Passlick-Deetjen, M. Rodriguez, B. Stegmayr, P. Stenvinkel, C. Tetta, C. Wanner, and W. Zidek, "Review on uremic toxins: Classification, concentration, and interindividual variability," *Kidney International*, vol. 63, (no. 5), pp. 1934-1943, 2003.

[25] R.J. Glassock and S.G. Massry, "Uremic Toxins: An Integrated Overview of Definition and Classification," in Uremic Toxins: John Wiley & Sons, Inc., 2012, pp. 1-12.

[26] W.J. Johnson, W.W. Hagge, R.D. Wagoner, R.P. Dinapoli, and J.W. Rosevear, "Effects of urea loading in patients with far-advanced renal failure," *Mayo Clinic proceedings. Mayo Clinic*, vol. 47, (no. 1), pp. 21-29, 1972.

[27] R. Vanholder, A. Argiles, U. Baumeister, P. Brunet, W. Clark, G. Cohen, P. De Deyn, R. Deppisch, B. Descamps-Latscha, and T. Henle, "Uremic toxicity: present state of the art," *International Journal of Artificial Organs*, vol. 24, (no. 10), pp. 695-725, 2001.

[28] P.P. De Deyn, B. Marescau, R. D'Hooge, I. Possemiers, J. Nagler, and C. Mahler, "Guanidino compound levels in brain regions of non-dialyzed uremic patients," *Neurochemistry international*, vol. 27, (no. 3), pp. 227-237, 1995.

[29] S. Eloot, A. Torremans, R. De Smet, B. Marescau, P.P. De Deyn, P. Verdonck, and R. Vanholder, "Complex compartmental behavior of small water-soluble uremic retention solutes: Evaluation by direct measurements in plasma and erythrocytes," *American Journal of Kidney Diseases*, vol. 50, (no. 2), pp. 279-288, 2007.

[30] R.A. Campbell, "Polyamines and uremia," *Advances in experimental medicine and biology*, vol. 223, pp. 47, 1987.

[31] G. Lesaffer, R. De Smet, N. Lameire, A. Dhondt, P. Duym, and R. Vanholder, "Intradialytic removal of protein-bound uraemic toxins: role of solute characteristics and of dialyser membrane," *Nephrology Dialysis Transplantation*, vol. 15, (no. 1), pp. 50-57, 2000.

[32] N. Jourde-Chiche, L. Dou, C. Cerini, F. Dignat-George, R. Vanholder, and P. Brunet, "PROGRESS IN UREMIC TOXIN RESEARCH: Protein-Bound Toxins—Update 2009," *Seminars in Dialysis*, vol. 22, (no. 4), pp. 334-339, 2009.

[33] B. Bammens, P. Evenepoel, H. Keuleers, K. Verbeke, and Y. Vanrenterghem, "Free serum concentrations of the protein-bound retention solute p-cresol predict mortality in hemodialysis patients," *Kidney International*, vol. 69, (no. 6), pp. 1081-1087, 2006.

[34] F.C. Barreto, D.V. Barreto, S. Liabeuf, N. Meert, G. Glorieux, M. Temmar, G. Choukroun, R. Vanholder, and Z.A. Massy, "Serum indoxyl sulfate is associated with vascular disease and mortality in chronic kidney disease patients," *Clinical Journal of the American Society of Nephrology*, vol. 4, (no. 10), pp. 1551-1558, 2009.

[35] G. Stein, S. Franke, A. Mahiout, S. Schneider, H. Sperschneider, S. Borst, and J. Vienken, "Influence of dialysis modalities on serum AGE levels in end-stage renal disease patients," *Nephrology Dialysis Transplantation*, vol. 16, (no. 5), pp. 999-1008, 2001.

[36] Z.A. Massy, "Importance of homocysteine, lipoprotein (a) and non-classical cardiovascular risk factors (fibrinogen and advanced glycation end-products) for atherogenesis in uraemic patients," *Nephrology Dialysis Transplantation*, vol. 15, (no. suppl 5), pp. 81-91, 2000.

[37] B. Canaud, M. Morena, J.P. Cristol, and D. Krieter, "Beta2-microglobulin, a uremic toxin with a double meaning," *Kidney International*, vol. 69, (no. 8), pp. 1297-1299, 2006.

[38] S. Okuno, E. Ishimura, K. Kohno, Y. Fujino-Katoh, Y. Maeno, T. Yamakawa, M. Inaba, and Y. Nishizawa, "Serum beta2-microglobulin level is a significant predictor of mortality in maintenance haemodialysis patients," *Nephrology Dialysis Transplantation*, vol. 24, (no. 2), pp. 571-577, 2009.

[39] T. Yamamoto, J.J. Carrero, B. Lindholm, P. Stenvinkel, and J. Axelsson, "PROGRESS IN UREMIC TAXIN RESEARCH: Leptin and Uremic Protein-Energy Wasting—The Axis of Eating," *Seminars in Dialysis*, vol. 22, (no. 4), pp. 387-390, 2009.

[40] R. Vanholder, S. Van Laecke, and G. Glorieux, "The middle-molecule hypothesis 30 years after: lost and rediscovered in the universe of uremic toxicity?," *Journal of nephrology*, vol. 21, (no. 2), pp. 146-160, 2008.

[41] F.A. Gotch, J.A. Sargent, M.L. Keen, and M. Lee, "Individualized, quantified dialysis therapy of uremia," *Proceedings of the Clinical Dialysis and Transplant Forum*, (no. 4), pp. 27-35, 1974.

[42] F. Gotch and M. Keen, "Kinetic modeling in hemodialysis," in Clinical dialysis: Appleton and Lange, 1995, pp. 156–188.

[43] F. Gotch, "A quantitative evaluation of small and middle molecule toxicity in therapy of uremia," *Dialysis & Transplantation*, vol. 9, pp. 183-192, 1980.

[44] F.A. Gotch, J.A. Sargent, and M.L. Keen, "Hydrogen-ion balance in dialysis therapy," *Artificial Organs*, vol. 6, (no. 4), pp. 388-395, 1982.

[45] F.A. Gotch and J.A. Sargent, "A mechanistic analysis of the National Cooperative Dialysis Study (NCDS)," *Kidney International*, vol. 28, (no. 3), pp. 526-534, 1985.

[46] K.B.G. Sprenger, W. Kratz, A.E. Lewis, and U. Stadtmuller, "Kinetic modeling of hemodialysis, hemofiltration, and hemodiafiltration," *Kidney International*, vol. 24, (no. 2), pp. 143-151, 1983.

[47] R. Star, J. Hootkins, J. Thompson, T. Poole, and R. Toto, "Variability and stability of two pool urea mass transfer coefficient," *Journal of the American Society of Nephrology*, vol. 3, pp. 395, 1992.

[48] D. Schneditz, J.C. Van Stone, and J.T. Daugirdas, "A Regional blood circulation alternative to in-series two compartment urea kinetic modeling," *ASAIO Journal*, vol. 39, (no. 3), pp. M573–M577, 1993.

[49] D. Schneditz and J.T. Daugirdas, "Formal Analytical Solution to a Regional Blood Flow and Diffusion Based Urea Kinetic Model," *ASAIO Journal*, vol. 40, (no. 3), pp. M667-M673, 1994.

[50] D. Schneditz, B. Fariyike, R. Osheroff, and N.W. Levin, "Is intercompartmental urea clearance during hemodialysis a perfusion term - A comparison of 2 pool urea kinetic models," *Journal of the American Society of Nephrology*, vol. 6, (no. 5), pp. 1360-1370, 1995.

[51] D. Schneditz, D. Platzer, and J.T. Daugirdas, "A diffusion-adjusted regional blood flow model to predict solute kinetics during haemodialysis," *Nephrology Dialysis Transplantation*, vol. 24, (no. 7), pp. 2218-24, 2009.

[52] W.E. Bloembergen, D.C. Stannard, F.K. Port, R.A. Wolfe, J.A. Pugh, C.A. Jones, J.W. Greer, T.A. Golper, and P.J. Held, "Relationship of dose of hemodialysis and cause-specific mortality," *Kidney International*, vol. 50, (no. 2), pp. 557-565, 1996.

[53] G. Eknoyan, G.J. Beck, A.K. Cheung, J.T. Daugirdas, T. Greene, J.W. Kusek, M. Allon, J. Bailey, J.A. Delmez, and T.A. Depner, "Effect of dialysis dose and membrane flux in maintenance hemodialysis," *New England Journal of Medicine*, vol. 347, (no. 25), pp. 2010-2019, 2002.

[54] T. Haas, D. Hillion, and G. Dongradi, "Phosphate kinetics in dialysis patients," *Nephrology Dialysis Transplantation*, vol. 6, (no. suppl 2), pp. S108-S13, 1991.

[55] C.A. DeSoi and J.G. Umans, "Phosphate kinetics during high-flux hemodialysis," *Journal of the American Society of Nephrology*, vol. 4, (no. 5), pp. 1214-1218, 1993.

[56] E.M. Spalding, P.W. Chamney, and K. Farrington, "Phosphate kinetics during hemodialysis: evidence for biphasic regulation," *Kidney International*, vol. 61, (no. 2), pp. 655-667, 2002.

[57] I. Mucsi, G. Hercz, R. Uldall, M. Ouwendyk, R. Francoeur, and A. Pierratos, "Control of serum phosphate without any phosphate binders in patients treated with nocturnal hemodialysis," *Kidney International*, vol. 53, (no. 5), pp. 1399-1404, 1998.

[58] E. Ritz, R. Dikow, C. Morath, and V. Schwenger, "Salt–A Potential 'Uremic Toxin'?," *Blood Purification*, vol. 24, (no. 1), pp. 63-66, 2006.

[59] E. Ok and E.J.D. Mees, "Unpleasant truths about salt restriction," *Seminars in Dialysis*, vol. 23, (no. 1), pp. 1-3, 2010.

[60] M.J. Damasiewicz and K.R. Polkinghorne, "Intra-dialytic hypotension and blood volume and blood temperature monitoring," *Nephrology*, vol. 16, (no. 1), pp. 13-18, 2011.

[61] S. George Lam Sui, K. Carl, U. Ray, and M.K. Carl, "Sodium ramping in hemodialysis: A study of beneficial and adverse effects," *American Journal of Kidney Diseases*, vol. 29, (no. 5), pp. 669-677, 1997.

[62] L. Coli, M. Ursino, V. Dalmastri, F. Volpe, G. La Manna, G. Avanzolini, S. Stefoni, and V. Bonomini, "A simple mathematical model applied to selection of the sodium profile during profiled haemodialysis," *Nephrology Dialysis Transplantation*, vol. 13, (no. 2), pp. 402-414, 1998.

[63] M. Ursino, L. Colí, C. Brighenti, L. Chiari, A. De Pascalis, and G. Avanzolini, "Prediction of Solute Kinetics, Acid-Base Status, and Blood Volume Changes During Profiled Hemodialysis," *Annals of Biomedical Engineering*, vol. 28, (no. 2), pp. 204-216, 2000.

[64] M. Gerrish and J. Little, "The effect of profiling dialysate sodium and ultrafiltration on patient comfort and cardiovascular stability during haemodialysis," *EDTNA-ERCA Journal*, vol. 29, (no. 2), pp. 61-72, 2012.

[65] P.P. De Deyn, R. Vanholder, S. Eloot, and G. Glorieux, "PROGRESS IN UREMIC TOXIN RESEARCH: Guanidino Compounds as Uremic (Neuro)Toxins," *Seminars in Dialysis*, vol. 22, (no. 4), pp. 340-345, 2009.

[66] B. Marescau, G. Nagels, I. Possemiers, M.E. De Broe, I. Becaus, J.-M. Billiouw, W. Lornoy, and P.P. De Deyn, "Guanidino compounds in serum and urine of nondialyzed patients with chronic renal insufficiency," *Metabolism*, vol. 46, (no. 9), pp. 1024-1031, 1997.

[67] S. Eloot, A. Torremans, R. De Smet, B. Marescau, D. De Wachter, P.P. De Deyn, N. Lameire, P. Verdonck, and R. Vanholder, "Kinetic behavior of urea is different from that of other water-soluble compounds: The case of the guanidino compounds," *Kidney International*, vol. 67, (no. 4), pp. 1566-1575, 2005.

[68] R. Vanholder, S. Eloot, and W. Van Biesen, "Do we need new indicators of dialysis adequacy based on middle-molecule removal?," *Nature Clinical Practice Nephrology*, vol. 4, (no. 4), pp. 174-175, 2008.

[69] S. Eloot, D. Schneditz, and R. Vanholder, "What can the dialysis physician learn from kinetic modelling beyond Kt/Vurea?," *Nephrology Dialysis Transplantation*, vol. 27, (no. 11), pp. 4021-4029, 2012.

[70] A.K. Cheung, T. Greene, J.K. Leypoldt, G. Yan, M. Allon, J. Delmez, A.S. Levey, N.W. Levin, M.V. Rocco, G. Schulman, G. Eknoyan, and for HEMO Study Group, "Association between serum 2-microglobulin level and Infectious mortality in hemodialysis patients," *Clinical Journal of the American Society of Nephrology*, vol. 3, (no. 1), pp. 69-77, 2008.

[71] K. Maeda, T. Shinzato, T. Ota, H. Kobayakawa, I. Takai, Y. Fujita, and H. Morita, "Beta-2-microglobulin generation rate and clearance rate in maintenance hemodialysis patients," *Nephron*, vol. 56, (no. 2), pp. 118-125, 1990.

[72] J.K. Leypoldt, A.K. Cheung, and R.B. Deeter, "Rebound kinetics of beta2-microglobulin after hemodialysis," *Kidney International*, vol. 56, (no. 4), pp. 1571-1577, 1999.

[73] S. Stiller, X.Q. Xu, N. Gruner, J. Vienken, and H. Mann, "Validation of a two-pool model for the kinetics of Beta 2-microglobulin," *International Journal of Artificial Organs*, vol. 25, (no. 5), pp. 411-420, 2002.

[74] R.A. Ward, T. Greene, B. Hartmann, and W. Samtleben, "Resistance to intercompartmental mass transfer limits beta(2)-microglobulin removal by post-dilution hemodiafiltration," *Kidney International*, vol. 69, (no. 8), pp. 1431-1437, 2006.

[75] A.K. Cheung, M.V. Rocco, G. Yan, J.K. Leypoldt, N.W. Levin, T. Greene, L. Agodoa, J. Bailey, G.J. Beck, W. Clark, A.S. Levey, D.B. Ornt, G. Schulman, S. Schwab, B. Teehan, and G. Eknoyan, "Serum beta-2 microglobulin levels predict

mortality in dialysis patients: Results of the HEMO study," *Journal of the American Society of Nephrology*, vol. 17, (no. 2), pp. 546-555, 2006.

[76] T.B. Drueke, "{beta}2-Microglobulin and amyloidosis," *Nephrology Dialysis Transplantation*, vol. 15, (no. suppl 1), pp. 17-24, 2000.

[77] J. Farrell and B. Bastani, "Beta 2-microglobulin amyloidosis in chronic dialysis patients: a case report and review of the literature," *Journal of the American Society of Nephrology*, vol. 8, (no. 3), pp. 509-514, 1997.

[78] T. Miyata, M. Jadoul, K. Kurokawa, and C. Van Ypersele de Strihou, "Beta-2 microglobulin in renal disease," *Journal of the American Society of Nephrology*, vol. 9, (no. 9), pp. 1723-1735, 1998.

[79] M. Ziolko, J.A. Pietrzyk, and J. Grabska-Chrzastowska, "Accuracy of hemodialysis modeling," *Kidney International*, vol. 57, (no. 3), pp. 1152-1163, 2000.

[80] J.K. Leypoldt, "Kinetics of β2-Microglobulin and Phosphate during Hemodialysis: Effects of Treatment Frequency and Duration," *Seminars in Dialysis*, vol. 18, (no. 5), pp. 401-408, 2005.

[81] S. Eloot, A. Dhondt, E. Hoste, A. Verstraete, J. De Waele, K. Colpaert, H. Hoeksema, F. Tromp, and R. Vanholder, "How to remove accumulated iodine in burn-injured patients," *Nephrology Dialysis Transplantation*, vol. 25, (no. 5), pp. 1614-1620, 2010.

[82] S. Eloot, W. van Biesen, A. Dhondt, R. de Smet, B. Marescau, P.P. De Deyn, P. Verdonck, and R. Vanholder, "Impact of increasing haemodialysis frequency versus haemodialysis duration on removal of urea and guanidino compounds: A kinetic analysis," *Nephrology Dialysis Transplantation*, vol. 24, (no. 7), pp. 2225-2232, 2009.

[83] A.S. Goldfarb-Rumyantzev, A.K. Cheung, and J.K. Leypoldt, "Computer simulation of small-solute and middle-molecule removal during short daily and long thrice-weekly hemodialysis," *American Journal of Kidney Diseases*, vol. 40, (no. 6), pp. 1211-1218, 2002.

[84] T.O. George, A. Priester-Coary, G. Dunea, D. Schneditz, N. Tarif, and J.T. Daugirdas, "Cardiac output and urea kinetics in dialysis patients: Evidence supporting the regional blood flow model," *Kidney International*, vol. 50, (no. 4), pp. 1273-1277, 1996.

[85] S. Smye, E. Lindley, and E. Will, "Simulating the effect of exercise on urea clearance in hemodialysis," *Journal of the American Society of Nephrology*, vol. 9, (no. 1), pp. 128-132, 1998.

[86] P. Korohoda, "Flow based two-compartment models - A comparative computational study," in Book Flow based two-compartment models - A comparative computational study, vol. 25/7, *Series Flow based two-compartment models - A comparative computational study*, Editor ed.^eds., City: Springer Berlin Heidelberg, 2009, pp. 838-841.

[87] M. Yashiro, H. Watanabe, and E. Muso, "Simulation of post-dialysis urea rebound using regional flow model," *Clinical and Experimental Nephrology*, vol. 8, (no. 2), pp. 139-145, 2004.

[88] K.Z. Yao, B.M. Shaw, B. Kou, K.B. McAuley, and D.W. Bacon, "Modeling ethylene/butene copolymerization with multi-site catalysts: Parameter estimability and experimental design," *Polymer Reaction Engineering*, vol. 11, (no. 3), pp. 563-588, 2003.

[89] T. Kanamori and K. Sakai, "An estimate of [beta]2-microglobulin deposition rate in uremic patients on hemodialysis using a mathematical kinetic model," *Kidney International*, vol. 47, (no. 5), pp. 1453-1457, 1995.

[90] M. Debowska, B. Lindholm, and J. Waniewski, "Adequacy Indices for Dialysis in Acute Renal Failure: Kinetic Modeling," *Artificial Organs*, vol. 34, (no. 5), pp. 412-419, 2010.

[91] M. Debowska, J. Waniewski, and B. Lindholm, "Bimodal dialysis: theoretical and computational investigations of adequacy indices for combined use of peritoneal dialysis and hemodialysis," *ASAIO Journal*, vol. 53, (no. 5), pp. 566-575, 2007.

[92] D. Schneditz, A.M. Kaufman, H.D. Polaschegg, N.W. Levin, and J.T. Daugirdas, "Cardiopulmonary recirculation during hemodialysis," *Kidney International*, vol. 42, (no. 6), pp. 1450-1456, 1992.

[93] N.M. Krivitski and T.A. Depner, "Cardiac output and central blood volume during hemodialysis: Methodology," *Advances in renal replacement therapy*, vol. 6, (no. 3), pp. 225-232, 1999.

[94] S.J. Harper, C.R.V. Tomson, and D.O. Bates, "Human uremic plasma increases microvascular permeability to water and proteins in vivo," *Kidney International*, vol. 61, (no. 4), pp. 1416-1422, 2002.

[95] J. Daugirdas, D. Schneditz, and D. Leehey, "Effect of access recirculation on the modeled urea distribution volume," *American Journal of Kidney Diseases*, vol. 27, (no. 4), pp. 512-518, 1996.

[96] P. Watson, I. Watson, and R. Batt, "Total body water volumes for adult males and females estimated from simple anthropometric measurements," *The American Journal of Clinical Nutrition*, vol. 33, (no. 1), pp. 27-39, 1980.

[97] S. Ishibe and A.J. Peixoto, "Methods of assessment of volume status and intercompartmental fluid shifts in hemodialysis patients: Implications in clinical practice," *Seminars in Dialysis*, vol. 17, (no. 1), pp. 37-43, 2004.

[98] T.L. Parsons, E.B. Toffelmire, and C.E. King-Van Vlack, "Exercise training during hemodialysis improves dialysis efficacy and physical performance," *Anglais*, vol. 87, (no. 5), pp. 680–687, 2006.

[99] I. Vaithilingam, K.R. Polkinghorne, R.C. Atkins, and P.G. Kerr, "Time and exercise improve phosphate removal in hemodialysis patients," *American Journal of Kidney Diseases*, vol. 43, (no. 1), pp. 85-89, 2004.

[100] C.H. Kong, J.E. Tattersall, R.N. Greenwood, and K. Farrington, "The effect of exercise during haemodialysis on solute removal," *Nephrology Dialysis Transplantation*, vol. 14, (no. 12), pp. 2927-2931, 1999.

[101] A.K. Cheung, N.W. Levin, T. Greene, L. Agodoa, J. Bailey, G. Beck, W. Clark, A.S. Levey, J.K. Leypoldt, and D.B. Ornt, "Effects of high-flux hemodialysis on clinical outcomes: results of the HEMO study," *Journal of the American Society of Nephrology*, vol. 14, (no. 12), pp. 3251-3263, 2003.

[102] F. Locatelli, A. Martin-Malo, T. Hannedouche, A. Loureiro, M. Papadimitriou, V. Wizemann, S.H. Jacobson, S. Czekalski, C. Ronco, and R. Vanholder, "Effect of membrane permeability on survival of hemodialysis patients," *Journal of the American Society of Nephrology*, vol. 20, (no. 3), pp. 645-654, 2009.

[103] R.E. Treybal, *Mass-transfer operations*: McGraw-Hill New York, 1980.

[104] B. Canaud, Q. Nguyen, C. Polito, F. Stec, and C. Mion, "Hemodiafiltration with on-line production of bicarbonate infusate. A new standard for high-efficiency, low-cost dialysis in elderly and uncompliant patients," *Contributions to nephrology*, vol. 74, pp. 91-100, 1989.

[105] B. Canaud, "Online Hemodiafiltration," in Hemodiafiltration, vol. 158, C. B. Ronco C, Aljama P ed., Basel: Karger, 2007, pp. 110-122.

[106] G. Krick and C. Ronco, *On-line Hemodiafiltration: The Journey and the Vision*: S Karger Ag, 2011.

[107] H. Schiffl, "Prospective randomized cross-over long-term comparison of online haemodiafiltration and ultrapure high-flux haemodialysis," *European journal of medical research*, vol. 12, (no. 1), pp. 26-33, 2007.

[108] L.A. Pedrini, V. De Cristofaro, M. Comelli, F.G. Casino, M. Prencipe, A. Baroni, G. Campolo, C. Manzoni, L. Colì, and P. Ruggiero, "Long-term effects of high-efficiency on-line haemodiafiltration on uraemic toxicity. A multicentre prospective randomized study," *Nephrology Dialysis Transplantation*, vol. 26, (no. 8), pp. 2617-2624, 2011.

[109] M.P. Grooteman, M.A. van den Dorpel, M.L. Bots, E.L. Penne, N.C. van der Weerd, A.H. Mazairac, C.H. den Hoedt, I. van der Tweel, R. Lévesque, and M.J. Nubé, "Effect of online hemodiafiltration on all-cause mortality and cardiovascular outcomes," *Journal of the American Society of Nephrology*, vol. 23, (no. 6), pp. 1087-1096, 2012.

[110] E. Ok, G. Asci, H. Toz, E.S. Ok, F. Kircelli, M. Yilmaz, E. Hur, M.S. Demirci, C. Demirci, S. Duman, A. Basci, S.M. Adam, I.O. Isik, M. Zengin, G. Suleymanlar, M.E. Yilmaz, M. Ozkahya, and O.b.o.t.T.O.H. Study', "Mortality and cardiovascular events in online haemodiafiltration (OL-HDF) compared with high-flux dialysis: results from the Turkish OL-HDF Study," *Nephrology Dialysis Transplantation*, vol. 28, (no. 1), pp. 192-202, 2013.

[111] F. Maduell, F. Moreso, M. Pons, R. Ramos, J. Mora-Macià, J. Carreras, J. Soler, F. Torres, J.M. Campistol, and A. Martinez-Castelao, "High-Efficiency

Postdilution Online Hemodiafiltration Reduces All-Cause Mortality in Hemodialysis Patients," *Journal of the American Society of Nephrology*, 2013.

[112] G. Thomas and B.L. Jaber, "Convective therapies for removal of middle molecular weight uremic toxins in end-stage renal disease: a review of the evidence," *Seminars in Dialysis*, vol. 22, (no. 6), pp. 610-614, 2009.

[113] F. Locatelli, C. Manzoni, A. Cavalli, and S. Di Filippo, "Can convective therapies improve dialysis outcomes?," *Current Opinion in Nephrology and Hypertension*, vol. 18, (no. 6), pp. 476-480, 2009.

[114] P.J. Blankestijn, I. Ledebo, and B. Canaud, "Hemodiafiltration: clinical evidence and remaining questions," *Kidney International*, vol. 77, (no. 7), pp. 581-587, 2010.

[115] V. Wizemann, C. Lotz, F. Techert, and S. Uthoff, "On-line haemodiafiltration versus low-flux haemodialysis. A prospective randomized study," *Nephrology Dialysis Transplantation*, vol. 15, (no. suppl 1), pp. 43-48, 2000.

[116] S. Eloot, W. Van Biesen, A. Dhondt, H. Van de Wynkele, G. Glorieux, P. Verdonck, and R. Vanholder, "Impact of hemodialysis duration on the removal of uremic retention solutes," *Kidney International*, vol. 73, (no. 6), pp. 765-770, 2007.

[117] M. Kalousová, J.T. Kielstein, M. Hodková, T. Zima, S. Dusilová-Sulková, J. Martens-Lobenhoffer, and S.M. Bode-Boger, "No Benefit of Hemodiafiltration over Hemodialysis in Lowering Elevated Levels of Asymmetric Dimethylarginine in ESRD Patients," *Blood Purification*, vol. 24, pp. 439-444, 2006.

[118] P.L. Painter, J.N. Nelson-Worel, M. Hill, D. Thornbery, W. Shelp, A. Harrington, and A. Weinstein, "Effects of exercise training during hemodialysis," *Nephron*, vol. 43, (no. 2), pp. 87-92, 1986.

[119] C.D. Giannaki, I. Stefanidis, C. Karatzaferi, N. Liakos, V. Roka, I. Ntente, and G.K. Sakkas, "The Effect of Prolonged Intradialytic Exercise in Hemodialysis Efficiency Indices," *ASAIO Journal*, vol. 57, (no. 3), pp. 213-218, 2011.

[120] S. Farese, R. Budmiger, F. Aregger, I. Bergmann, F. Frey, and D. Uehlinger, "Effect of transcutaneous electrical muscle stimulation and passive cycling movements on blood pressure and removal of urea and phosphate during hemodialysis," *American Journal of Kidney Diseases*, vol. 52, (no. 4), pp. 745-752, 2008.

[121] M. De Moura Reboredo, D.M.N. Henrique, R. De Souza Faria, A. Chaoubah, M.G. Bastos, and R.B. De Paula, "Exercise training during hemodialysis reduces blood pressure and increases physical functioning and quality of life," *Artificial Organs*, vol. 34, (no. 7), pp. 586-593, 2010.

[122] A.P. Goldberg, E. Geltman, J. Gavin III, R. Carney, J. Hagberg, J. Delmez, A. Naumovich, M. Oldfield, and H. Harter, "Exercise training reduces coronary risk and effectively rehabilitates hemodialysis patients," *Nephron*, vol. 42, (no. 4), pp. 311-316, 2008.

[123] B.W. Miller, C.L. Cress, M.E. Johnson, D.H. Nichols, and M.A. Schnitzler, "Exercise during hemodialysis decreases the use of antihypertensive medications," *American Journal of Kidney Diseases*, vol. 39, (no. 4), pp. 828-833, 2002.

[124] P.N. Bennett, L. Breugelmans, R. Barnard, M. Agius, D. Chan, D. Fraser, L. McNeill, and L. Potter, "Sustaining a hemodialysis exercise program: a review," *Seminars in Dialysis*, vol. 23, (no. 1), pp. 62-73, 2010.

[125] A.M. Kaufman, A.T. Morris, V.A. Lavarias, Y. Wang, J.F. Leung, M.B. Glabman, S.A. Yusuf, A.L. Levoci, H.D. Polaschegg, and N.W. Levin, "Effects of controlled blood cooling on hemodynamic stability and urea kinetics during high-efficiency hemodialysis," *Journal of the American Society of Nephrology*, vol. 9, (no. 5), pp. 877-883, 1998.

[126] R. Duchesne, J.D. Klein, J.B. Velotta, J.J. Doran, P. Rouillard, B.R. Roberts, A.A. McDonough, and J.M. Sands, "UT-A urea transporter protein in heart increased abundance during uremia, hypertension, and heart failure," *Circulation research*, vol. 89, (no. 2), pp. 139-145, 2001.

[127] C. Matwichuk, S. Taylor, C. Shmon, P. Kass, and G. Shelton, "Changes in rectal temperature and hematologic, biochemical, blood gas, and acid-base values in healthy Labrador Retrievers before and after strenuous exercise," *American journal of veterinary research*, vol. 60, (no. 1), pp. 88-92, 1999.

[128] "ATS Statement: Guidelines for the Six-Minute Walk Test," *American Journal of Respiratory and Critical Care Medicine*, vol. 166, (no. 1), pp. 111-117, 2002.

[129] S.S. Fitts and M.R. Guthrie, "Six-minute walk by people with chronic renal failure: assessment of effort by perceived exertion," *American journal of physical medicine & rehabilitation*, vol. 74, (no. 1), pp. 54-58, 1995.

[130] I. Ledebo and P.J. Blankestijn, "Haemodiafiltration-optimal efficiency and safety," *NDT Plus*, vol. 3, (no. 1), pp. 8-16, 2009.

[131] W.R. Witkowski and J.J. Allen, "Approximation of parameter uncertainty in nonlinear optimization-based parameter-estimation schemes," *AIAA Journal*, vol. 31, (no. 5), pp. 947-950, 1993.

[132] A. Yang, E. Martin, G. Montague, and J. Morris, "Optimal experimental design for the precision of a subset of model parameters in process development," in Computer Aided Chemical Engineering, vol. 21, W. Marquardt and C. Pantelides eds.: Elsevier, 2006, pp. 563-568.

[133] M. Fujiwara, Z.K. Nagy, J.W. Chew, and R.D. Braatz, "First-principles and direct design approaches for the control of pharmaceutical crystallization," *Journal of Process Control*, vol. 15, (no. 5), pp. 493-504, 2005.

[134] P. Felix Oliver Lindner and B. Hitzmann, "Experimental design for optimal parameter estimation of an enzyme kinetic process based on the analysis of the Fisher information matrix," *Journal of Theoretical Biology*, vol. 238, (no. 1), pp. 111-123, 2006.

[135] J.R. Banga and E. Balsa-Canto, "Parameter estimation and optimal experimental design," in Essays in Biochemistry: Systems Biology, vol. 45, *Essays in Biochemistry*, 2008, pp. 195-209.

[136] K.H. Cho, S.Y. Shin, W. Kolch, and O. Wolkenhauer, "Experimental Design in Systems Biology, Based on Parameter Sensitivity Analysis Using a Monte Carlo Method: A Case Study for the TNFα-Mediated NF-κ B Signal Transduction Pathway," *Simulation*, vol. 79, (no. 12), pp. 726-739, 2003.

[137] D. Telen, F. Logist, E. Van Derlinden, I. Tack, and J. Van Impe, "Optimal experiment design for dynamic bioprocesses: A multi-objective approach," *Chemical Engineering Science*, vol. 78, pp. 82-97, 2012.

[138] K. Bernaerts, K.J. Versyck, and J.F. Van Impe, "On the design of optimal dynamic experiments for parameter estimation of a Ratkowsky-type growth kinetics at suboptimal temperatures," *International Journal of Food Microbiology*, vol. 54, (no. 1-2), pp. 27-38, 2000.

[139] E. Balsa-Canto, M. Rodriguez-Fernandez, and J.R. Banga, "Optimal design of dynamic experiments for improved estimation of kinetic parameters of thermal degradation," *Journal of Food Engineering*, vol. 82, (no. 2), pp. 178-188, 2007.

[140] G. Franceschini and S. Macchietto, "Model-based design of experiments for parameter precision: State of the art," *Chemical Engineering Science*, vol. 63, (no. 19), pp. 4846-4872, 2008.

[141] Y. Zhang and T.F. Edgar, "PCA Combined Model-Based Design of Experiments (DOE) Criteria for Differential and Algebraic System Parameter Estimation," *Industrial & Engineering Chemistry Research*, vol. 47, (no. 20), pp. 7772-7783, 2008.

[142] F. Galvanin, S. Macchietto, and F. Bezzo, "Model-Based Design of Parallel Experiments," *Industrial & Engineering Chemistry Research*, vol. 46, (no. 3), pp. 871-882, 2007.

[143] A.K. Agarwal and M.L. Brisk, "Sequential experimental design for precise parameter estimation. 2. Design criteria," *Industrial & Engineering Chemistry Process Design and Development*, vol. 24, (no. 1), pp. 207-210, 1985.

[144] G. Franceschini and S. Macchietto, "Novel anticorrelation criteria for model-based experiment design: Theory and formulations," *AIChE Journal*, vol. 54, (no. 4), pp. 1009-1024, 2008.

[145] D.J. Pritchard and D.W. Bacon, "Prospects for reducing correlations among parameter estimates in kinetic models," *Chemical Engineering Science*, vol. 33, (no. 11), pp. 1539-1543, 1978.

[146] M. Rodriguez-Fernandez, P. Mendes, and J.R. Banga, "A hybrid approach for efficient and robust parameter estimation in biochemical pathways," *Biosystems*, vol. 83, (no. 2), pp. 248-265, 2006.

[147] A.K. Agarwal and M.L. Brisk, "Sequential experimental design for precise parameter estimation. 1. Use of reparameterization," *Industrial & Engineering Chemistry Process Design and Development*, vol. 24, (no. 1), pp. 203-207, 1985.

[148] S.P. Asprey and S. Macchietto, "Designing robust optimal dynamic experiments," *Journal of Process Control*, vol. 12, (no. 4), pp. 545-556, 2002.

[149] G. Franceschini and S. Macchietto, "Anti-Correlation Approach to Model-Based Experiment Design: Application to a Biodiesel Production Process," *Industrial & Engineering Chemistry Research*, vol. 47, (no. 7), pp. 2331-2348, 2008.

[150] G. Franceschini and S. Macchietto, "Novel anticorrelation criteria for design of experiments: Algorithm and application," *AIChE Journal*, vol. 54, (no. 12), pp. 3221-3238, 2008.

[151] S.P. Asprey and Y. Naka, "Mathematical Problems in Fitting Kinetic Models - Some New Perspectives," *Journal of Chemical Engineering of Japan*, vol. 32, (no. 3), pp. 328-337, 1999.

[152] K.A.P. McLean and K.B. McAuley, "Mathematical modelling of chemical processes—obtaining the best model predictions and parameter estimates using identifiability and estimability procedures," *The Canadian Journal of Chemical Engineering*, vol. 90, (no. 2), pp. 351–366, 2012.

[153] J.V. Beck and K.J. Arnold, *Parameter estimation in engineering and science*: Wiley New York, 1977.

[154] V.G. Dovi, A.P. Reverberi, and L. Acevedo-Duarte, "New procedure for optimal design of sequential experiments in kinetic models," *Industrial & Engineering Chemistry Research*, vol. 33, (no. 1), pp. 62-68, 1994.

[155] S. Issanchou, P. Cognet, and M. Cabassud, "Precise parameter estimation for chemical batch reactions in heterogeneous medium," *Chemical Engineering Science*, vol. 58, (no. 9), pp. 1805-1813, 2003.

[156] S. Lin, "NGPM -- A NSGA-II Program in Matlab v1.4," in, http://www.mathworks.com/matlabcentral/fileexchange/31166-ngpm-a-nsga-ii-program-in-matlab-v1-4, [Dec 2012].

[157] J.R. Banga, K.J. Versyck, and J.F. Van Impe, "Computation of optimal identification experiments for nonlinear dynamic process models: a stochastic global optimization approach," *Industrial & Engineering Chemistry Research*, vol. 41, (no. 10), pp. 2425-2430, 2002.

[158] K. Deb, *Multi-objective optimization using evolutionary algorithms*: Wiley, 2001.

[159] J. Thibault, "Net Flow and Rough Sets: Two Methods for Ranking the Pareto Domain," in Multi-objective optimization: techniques and applications in chemical engineering, vol. 1, G. P. Rangaiah ed.: World Scientific, 2008.

[160] N.P. Balakrishnan, G.P. Rangaiah, and L. Samavedham, "Review and analysis of blood glucose (BG) models for type 1 diabetic patients," *Industrial & Engineering Chemistry Research*, vol. 50, (no. 21), pp. 12041-12066, 2011.

[161] S.M. Lynch and B.W. Bequette, "Model predictive control of blood glucose in type I diabetics using subcutaneous glucose measurements," in Book Model predictive control of blood glucose in type I diabetics using subcutaneous glucose measurements, vol. 5, *Series Model predictive control of blood glucose in type I*

diabetics using subcutaneous glucose measurements, Editor ed.^eds., City: IEEE, 2002, pp. 4039-4043.

[162] F. Galvanin, M. Barolo, F. Bezzo, and S. Macchietto, "A backoff strategy for model-based experiment design under parametric uncertainty," *AIChE Journal*, vol. 56, (no. 8), pp. 2088-2102, 2010.

[163] R. Hovorka, V. Canonico, L.J. Chassin, U. Haueter, M. Massi-Benedetti, M.O. Federici, T.R. Pieber, H.C. Schaller, L. Schaupp, and T. Vering, "Nonlinear model predictive control of glucose concentration in subjects with type 1 diabetes," *Physiological measurement*, vol. 25, (no. 4), pp. 905-920, 2004.

[164] DirecNet, "The Effect of Basal Insulin During Exercise on the Development of Hypoglycemia in Children with Type 1 Diabetes," in, http://direcnet.jaeb.org, 2005, [Nov-2012 2012].

[165] G. Nucci and C. Cobelli, "Models of subcutaneous insulin kinetics. A critical review," *Computer methods and programs in biomedicine*, vol. 62, (no. 3), pp. 249-257, 2000.

[166] C.L. Chen and H.W. Tsai, "Model-based insulin therapy scheduling: A mixed-integer nonlinear dynamic optimization approach," *Industrial & Engineering Chemistry Research*, vol. 48, (no. 18), pp. 8595-8604, 2009.

[167] F. Galvanin, M. Barolo, S. Macchietto, and F. Bezzo, "Optimal design of clinical tests for the identification of physiological models of type 1 diabetes mellitus," *Industrial & Engineering Chemistry Research*, vol. 48, (no. 4), pp. 1989-2002, 2009.

[168] "Blood Sugar Level Ranges," in, 2012, http://www.diabetes.co.uk/diabetes_care/blood-sugar-level-ranges.html [Dec 2012 2012].

[169] G. Franceschini and S. Macchietto, "The Choice of Sensitivity Metrics in Model-Based Design of Optimal Experiments," in Book The Choice of Sensitivity Metrics in Model-Based Design of Optimal Experiments, *Series The Choice of Sensitivity Metrics in Model-Based Design of Optimal Experiments*, Editor ed.^eds., City, 2006.

[170] M. Nihtilä and J. Virkkunen, "Practical identifiability of growth and substrate consumption models," *Biotechnology and Bioengineering*, vol. 19, (no. 12), pp. 1831-1850, 1977.

[171] S.P. Asprey and S. Macchietto, "Statistical tools for optimal dynamic model building," *Computers & Chemical Engineering*, vol. 24, (no. 2-7), pp. 1261-1267, 2000.

[172] J.T. Daugirdas, "Second generation logarithmic estimates of single-pool variable volume Kt/V: an analysis of error," *Journal of the American Society of Nephrology*, vol. 4, (no. 5), pp. 1205-1213, 1993.

[173] V. Maheshwari, L. Samavedham, and G. Rangaiah, "A Regional Blood Flow Model for β2-Microglobulin Kinetics and for Simulating Intra-dialytic Exercise

Effect," *Annals of Biomedical Engineering*, vol. 39, (no. 12), pp. 2879-2890, 2011.

[174] D. Liberati, S. Biasioli, R. Foroni, F. Rudello, and F. Turkheimer, "New compartmental model approach to dialysis," *Med. Biol. Eng. Comput.*, vol. 31, (no. 2), pp. 171-179, 1993.

[175] R. Popovich, D. Hlavinka, J. Bomar, J. Moncrief, and J. Decherd, "The consequences of physiological resistances on metabolite removal from the patient-artificial kidney system," *ASAIO Journal*, vol. 21, pp. 108-116, 1975.

[176] D. Schneditz, " Article Recommendations on: A regional blood flow model for β2-microglobulin kinetics and for simulating intra-dialytic exercise effect.," in, F1000 Prime: FACULTY of 1000, 2012, [cited 27 Feb 2012].

[177] V. Maheshwari, L. Samavedham, G.P. Rangaiah, Y. Loy, L.L. Hsi, S. Sethi, and T.L. Leong, "Comparison of toxin removal outcomes in online hemodiafiltration and intra-dialytic exercise in high-flux hemodialysis: A prospective randomized open-label clinical study protocol," *BMC nephrology*, vol. 13, (no. 1), pp. 156, 2012.

[178] V. Maheshwari, G.P. Rangaiah, and L. Samavedham, "Multiobjective Framework for Model-based Design of Experiments to Improve Parameter Precision and Minimize Parameter Correlation," *Industrial & Engineering Chemistry Research*, vol. 52, (no. 24), pp. 8289-8304, 2013.

[179] E.L. Penne, N.C. van der Weerd, M.A. van den Dorpel, M.P. Grooteman, R. Lévesque, M.J. Nubé, M.L. Bots, P.J. Blankestijn, and P.M. ter Wee, "Short-term effects of online hemodiafiltration on phosphate control: a result from the randomized controlled Convective Transport Study (CONTRAST)," *American Journal of Kidney Diseases*, vol. 55, (no. 1), pp. 77-87, 2010.

[180] S. Ouzouni, E. Kouidi, A. Sioulis, D. Grekas, and A. Deligiannis, "Effects of intradialytic exercise training on health-related quality of life indices in haemodialysis patients," *Clinical rehabilitation*, vol. 23, (no. 1), pp. 53-63, 2009.

[181] N.M. Selby and C.W. McIntyre, "A systematic review of the clinical effects of reducing dialysate fluid temperature," *Nephrology Dialysis Transplantation*, vol. 21, (no. 7), pp. 1883-1898, 2006.

[182] A.W. Yu, T.S. Ing, R.I. Zabaneh, and J.T. Daugirdas, "Effect of dialysate temperature on central hemodynamics and urea kinetics," *Kidney International*, vol. 48, (no. 1), pp. 237-243, 1995.

[183] L.J. Chesterton, N.M. Selby, J.O. Burton, and C.W. McIntyre, "Cool dialysate reduces asymptomatic intradialytic hypotension and increases baroreflex variability," *Hemodialysis International*, vol. 13, (no. 2), pp. 189-196, 2009.